A CONTINUING INVESTIGATION INTO THE STRESS FIELD AROUND TWO PARALLEL EDGE CRACKS IN A FINITE BODY

A Thesis

by

JUSTIN PATRICK GILMAN

Submitted to the Office of Graduate Studies of
Texas A&M University
in partial fulfillment of the requirements for the degree of

MASTER OF SCIENCE

December 2004

Major Subject: Mechanical Engineering

A CONTINUING INVESTIGATION INTO THE STRESS FIELD AROUND TWO PARALLEL EDGE CRACKS IN A FINITE BODY

A Thesis

by

JUSTIN PATRICK GILMAN

Submitted to Texas A&M University
in partial fulfillment of the requirements
for the degree of

MASTER OF SCIENCE

Approved as to style and content by:

Ravinder Chona (Co-Chair of Committee)	Harry A. Hogan (Co-Chair of Committee)
Junuthula N. Reddy (Member)	Gary T. Fry (Member)
Dennis O'Neal (Head of Department)	

December 2004

Major Subject: Mechanical Engineering

ABSTRACT

A Continuing Investigation into the Stress Field around Two Parallel Edge Cracks in a Finite Body. (December 2004)

Justin Patrick Gilman, B.S., Mississippi State University

Co-Chairs of Advisory Committee: Dr. Ravinder Chona
Dr. Harry Hogan

The goal of this research was to extend the investigation into a method to represent and analyze the stress field around two parallel edge cracks in a finite body. The Westergaard-Schwarz method combined with the local collocation method was used to analyze different cases of two parallel edge cracks in a finite body. Using this method a determination of when two parallel edge cracks could be analyzed as isolated single edge cracks was determined

Numerical experimentation was conducted using ABAQUS. It was used to obtain the coordinate and stress information required in the local collocation method. The numerical models were created by maintaining one crack at a fixed length while varying the length of the second crack as well as the separation distance of the two cracks. The results obtained through the local collocation method were compared with the finite element obtained J-Integrals to verify the accuracy of the results.

The results obtained in the analysis showed that the major factor in determining when the second crack's stress field has to be considered was the crack separation distance. It was found that a reduction in the second crack's length did not have a significant effect on overall stress intensity factors of the fixed crack. A larger change in the opening mode stress intensity factor can be seen by varying the crack separation distance. As well as seeing a steady reduction in shear mode stress intensity factors as the crack separation was increased. The results showed that after a certain crack separation distance the two cracks could be analyzed separately without introducing significant error into the stress field calculations.

DEDICATION

To all the friends at A&M who made my time here very special……

ACKNOWLEDGEMENTS

I would like to express my great appreciation to my parents Dennis and Pat Gilman for their never-ending support and guidance. Thanks to my good friends Nick and Lea Mueschke without whose support I would have never graduated. A special thanks goes to Kim Moses, who helped with me with the unending paper work required throughout my time at Texas A&M. I would also like to thank Amanda Parker and Tabitha Nickelson for their friendship and help gathering the materials that I need to finish my research.

Thanks Sharon Garner for never getting annoyed with me with all the endless calls for help with Patran and Abaqus. Thanks to Dr. Burger for the help and ideas when I got so fixated on the small things that I forgot to look at the overall picture. I would also like to thank Mahesh Jalan with whom I had endless great conversations while sharing the lab.

Finally I would like to thank Dr. Chona for giving me the idea for my research as well as his advice and guidance during my time here.

TABLE OF CONTENTS

CHAPTER Page

LIST OF FIGURES

FIGURE Page

FIGURE Page

LIST OF TABLES

CHAPTER I
INTRODUCTION

Over the years there has been comprehensive analysis of stress fields for single edge cracks for example the configuration shown Figure 1.1. However, analysis of multiple edge cracks in a finite body has been limited because it is a significantly more complicated problem. An analysis of the stress field for multiple cracks in a finite geometry was developed by Hardin[1] with the combined Westergaard-Schwarz approach based on the local collocation method developed by Chona[2,3]. Fully established guidelines for the application of this method to varying situations were not developed. One of the main goals of this study is to expand on Hardin's work and establish guidelines for the application of the Westergaard-Schwarz approach to multiple, parallel cracks in a finite body by exploring a greater range of situations than Hardin studied.

Previous Work

The majority of the published works on multiple-crack scenarios, such as those by Tada, Paris, and Irwin[4,5], involve periodic cracks in infinite and semi-infinite bodies (Figure 1.2). Also, Freese[6] has investigated unequal periodic cracks in a semi-infinite body (Figure 1.3). Ukadgaonker and Naik[7] did work on the interaction effect of two arbitrarily oriented cracks in an infinite plate. Two recent studies on multiple cracks in finite bodies were conducted by Hardin[1] and Keener[8]. This study is largely based on their efforts. They used a method of local collocation developed by Sanford[9,10]

This thesis follows the style and format of *International Journal of Fracture Mechanics.*

and Chona[2,3] for single-ended cracks in finite bodies. Both Hardin's and Keener's studies used the local collocation method in conjunction with the Westergaard-Schwarz method to develop numerical representations of the stress field surrounding a pair of parallel edge cracks. In Hardin's study the focus was on the stress field. Keener took Hardin's work a step further and developed a displacement field representation for the parallel edge crack configuration.

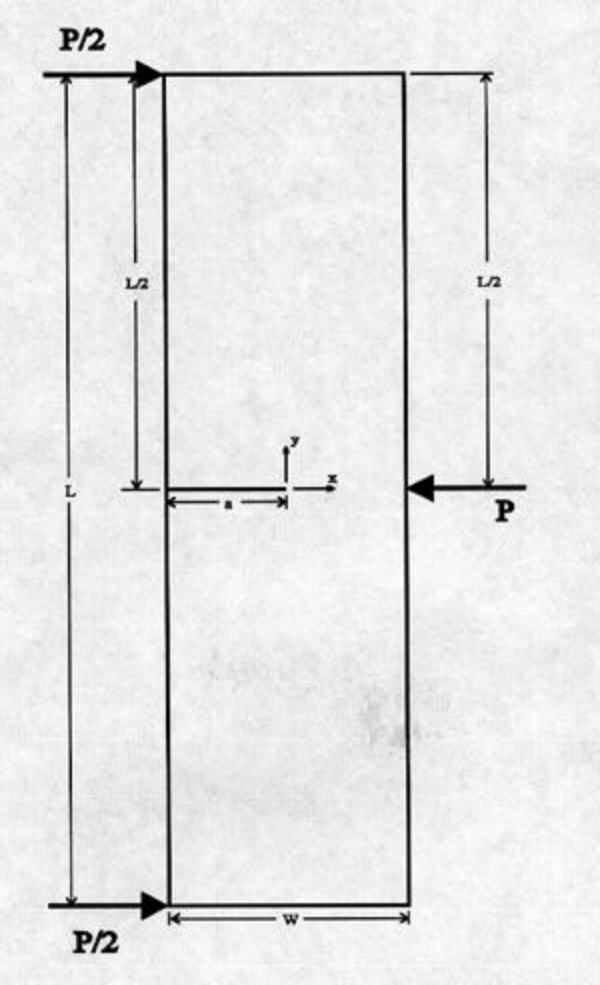

Figure 1.1 – A Three Point Bending Member with a Single Edge Crack

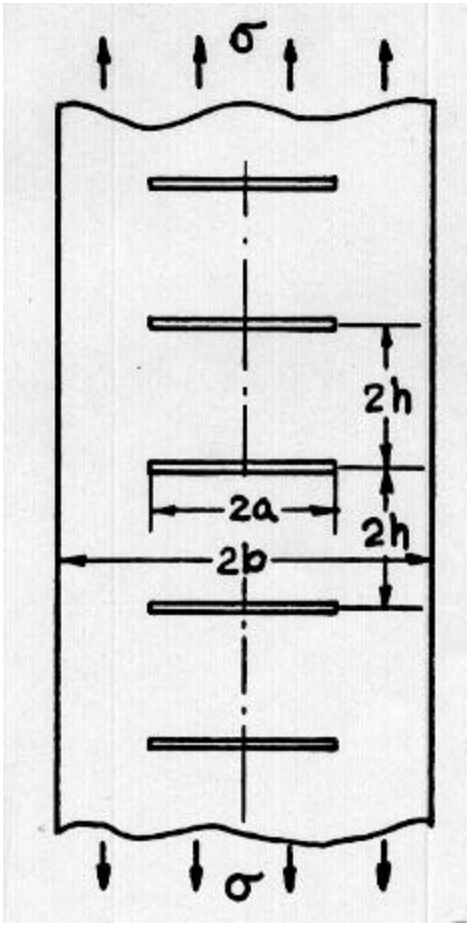

Figure 1.2 – An Example of a Repeating Crack Configuration Located in a Semi-Infinite Body[4]

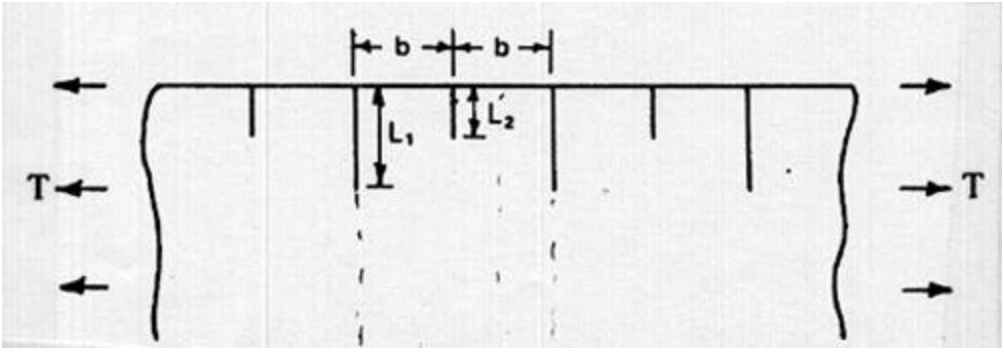

Figure 1.3 – Evenly Spaced edge of Cracks of Unequal Length in a Semi-Infinite Body[6,7]

CHAPTER II
FULL FIELD REPRESENTATION OF THE STRESSES SURROUNDING A PAIR OF PARALLEL EDGE CRACKS

Overview of Methodology

The combined Westergaard-Schwarz method was developed by Patrick Hardin by combining the generalized Westergaard equations[11] and the Schwarz alternating method[7] for understanding the stress fields surrounding a pair of parallel edge cracks (Figure 2.1). The generalized Westergaard equations had previously proven to be very effective for the analysis of stress fields associated with single-ended edge cracks in finite geometries. However, even in the simplest multiple crack scenario, where only two edge cracks may be present, the situation becomes much more complicated than in the simple crack case. For example, application of the generalized Westergaard equations to a multiple crack scenario utilizing simple superposition results in a violation of the usual traction-free crack surface boundary condition. Also mere, superposition of the field associated with the second crack on that associated with the first crack fails to account for the effects of the presence of the second crack on the field associated with the first crack and vice versa. Both of these deficiencies show the need for a method to account for the interaction effects associated with the multiple crack scenario. The Schwarz alternating method is a convenient approach for this case. It allows a body to be treated as an elasticity problem with multiply-connected elastic regions, thus reducing its complexity. It is shown by Hardin[1] that a combination of the two methods, i.e., the generalized Westergaard and the Schwarz alternating method, applied to the multiple parallel edge crack scenario, can develop a complete and useful representation of the stress field around the two cracks.

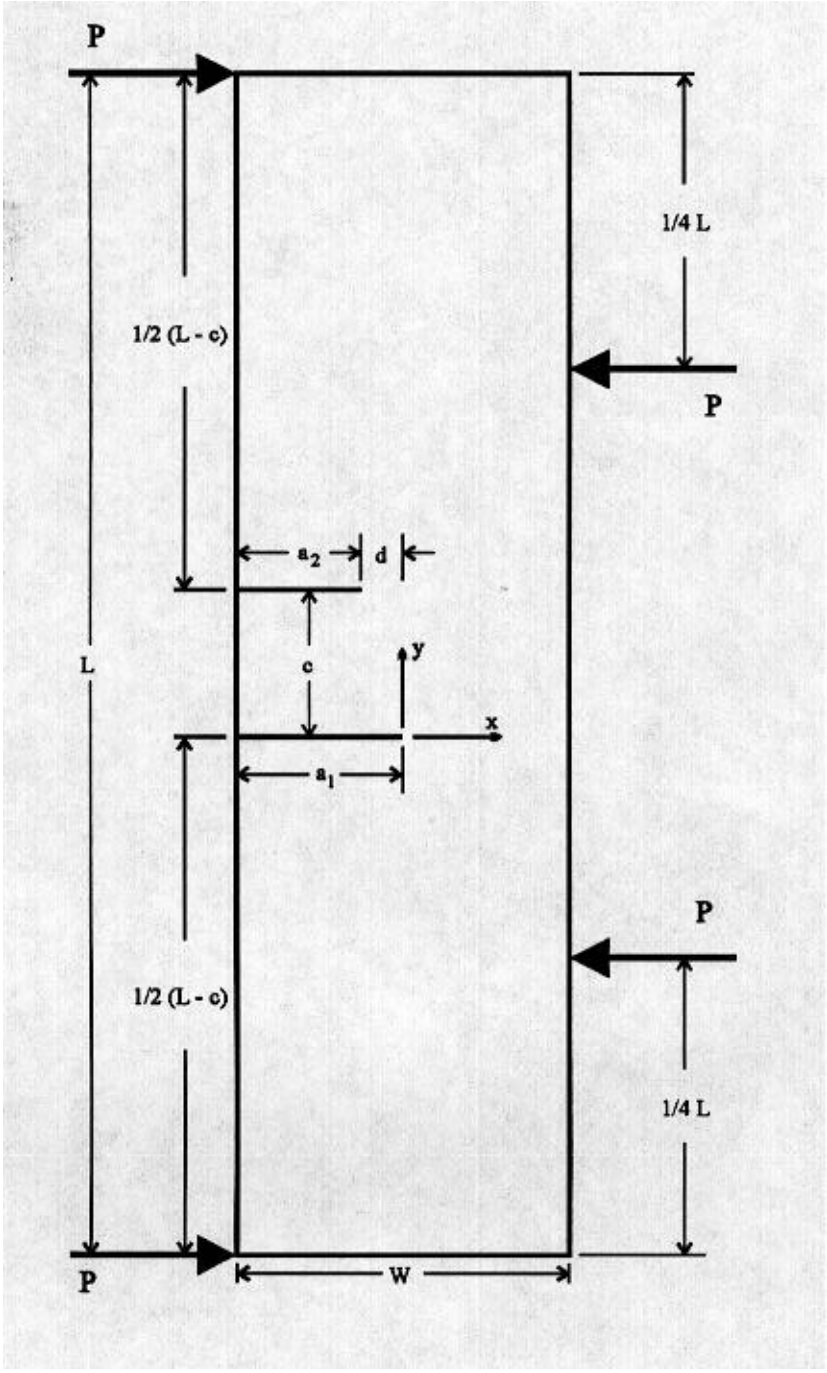

Figure 2.1 - Two Parallel Edge Cracks in a Four Point Bending Member[1,8]

Combined Westergaard-Schwarz Approach

The combination of these methods incorporates several advantages. First, the Westergaard equations, which have the ability to model stress fields over regions of any size, account for the effects of finite boundaries and far-field loading. Second, the Schwarz alternating method ensures that the proper boundary conditions are achieved, as well as accounting for interaction between the fields associated with each of the two individual cracks.

The procedure for applying the combined method for the case of two, traction-free, single-ended cracks is as follows:

1) Using the generalized Westergaard equations, calculate the stress field for the first crack using the loading conditions for the entire body, ignoring the second crack. This creates the stress field that would exist for a single isolated crack.

2) Specify the location of the second crack and determine the tractions along the faces of the second crack predicted by the stress field attached to the tip of first crack.

3) Apply the negative of the stresses as determined in step (2) along the faces of the second crack. This will produce the traction-free crack faces required for crack 2.

4) For the second crack, repeat the first three steps to determine the isolated crack-tip stress field for the second crack; the tractions along the faces of the first crack that are produced by the crack-tip stress field of the second crack;

and the traction removal stresses that must be added to satisfy the boundary conditions on the faces of the first crack.

5) Collect the four stress fields from the steps (1) through (4) to obtain an overall stress field for the multiple-cracked body.

Generalized Westergaard Equations

The generalized Westergaard equations were modified from the original equations proposed by H.M. Westergaard[11]. They have the same ability to model the stress fields around crack-tips as well as to account for aspects like the constant stress field parallel to the crack faces and the effects of far field loading and finite boundaries. The final form of the generalized Westergaard equations follows from two Airy stress functions, which include opening mode (subscript I) and shear mode (subscript II) loading:

$$F_I = Re\overline{\overline{Z_I}}(z) + yIm\overline{Z_I}(z) + yIm\overline{Y_I}(z) \tag{2.1}$$

$$F_{II} = Re\overline{\overline{Y_{II}}}(z) + yIm\overline{Y_{II}}(z) + yIm\overline{Z_{II}}(z) \tag{2.2}$$

where:

$$Z_I' = \frac{d}{dz}Z_I = \frac{d^2}{dz^2}\overline{Z}_I = \frac{d^3}{dz^3}\overline{\overline{Z}}_I \tag{2.3a}$$

$$Z_{II}' = \frac{d}{dz}Z_{II} = \frac{d^2}{dz^2}\overline{Z}_{II} = \frac{d^3}{dz^3}\overline{\overline{Z}}_{II} \tag{2.3b}$$

$$Y_I' = \frac{d}{dz}Y_I = \frac{d^2}{dz^2}\overline{Y}_I = \frac{d^3}{dz^3}\overline{\overline{Y}}_I \tag{2.4a}$$

$$Y_{II}' = \frac{d}{dz}Y_{II} = \frac{d^2}{dz^2}\overline{Y}_{II} = \frac{d^3}{dz^3}\overline{\overline{Y}}_{II} \tag{2.4b}$$

Choices for the complex stress function (Z_I, Z_{II}, Y_I, Y_{II}) that are appropriate to the geometry and loading of interest allow equation (2.1) and (2.2) to be applied to a wide variety of problems of interest. For single-ended crack with traction free crack faces, suitable choices for Z_I, Z_{II}, Y_I, and Y_{II} are:

$$Z_I(z) = \sum_{n=0}^{n=\infty} A_n z^{n-\frac{1}{2}} \quad (2.5a) \qquad Z_{II}(z) = \sum_{n=0}^{n=\infty} -i C_n z^{n-\frac{1}{2}} \quad (2.5b)$$

$$Y_I(z) = \sum_{m=0}^{m=\infty} B_m z^m \quad (2.6a) \qquad Y_{II}(z) = \sum_{m=0}^{m=\infty} -i D_m z^m \quad (2.6b)$$

where $z = x + iy$, $i^2 = -1$. These functions yield the final stress functions seen below.

$$\sigma_{xx} = Re\, Z_I - yImZ_I' - yImY_I' + 2Re\, Y_I + Re\, Y_{II} - yImY_{II}' - yImZ_{II}' + 2Re\, Z_{II} \quad (2.7)$$

$$\sigma_{yy} = Re\, Z_I + yImZ_I' + yImY_I' + Re\, Y_{II} + yImY_{II}' + yImZ_{II}' \quad (2.8)$$

$$\tau_{xy} = -yReZ_I' - yReY_I' - Im\, Y_I - yReY_{II}' - yReZ_{II}' - Im\, Z_{II} \quad (2.9)$$

These stress field equations are based upon certain assumptions. First, the material is assumed to be linear-elastic and isotropic. The Airy stress functions of equations 2.5 and 2.6 assume that the origin of the coordinate system is located at the crack-tip with the negative branch of the x-axis coincident with the crack plane. The crack surfaces are treated as traction-free surfaces. This assumption, however, does not take into account the presence of a second crack in the body. In equations 2.5 and their derivatives an inverse square root singularity exists at the crack-tip.

Crack Tip Stress Fields

The crack-tip stress fields for each individual crack are required for the combined Westergaard-Schwarz Method. The Airy stress functions for the first crack are denoted

by the superscript (1) and those for the second crack by the superscript (2). The stress function for the first crack in opening mode loading is as follows.

$$F_I^{(1)} = Re\overline{\overline{Z}}_I^{(1)} + yIm\overline{Z}_I^{(1)} + yIm\overline{Y}_I^{(1)} \qquad 2.10$$

where:

$$Z_I^{'(1)} = \frac{d}{dz}Z_I^{(1)} = \frac{d^2}{dz^2}\overline{Z}_I^{(1)} = \frac{d^3}{dz^3}\overline{\overline{Z}}_I^{(1)} \qquad 2.11a$$

$$Y_I^{'(1)} = \frac{d}{dz}Y_I^{(1)} = \frac{d^2}{dz^2}\overline{Y}_I^{(1)} = \frac{d^3}{dz^3}\overline{\overline{Y}}_I^{(1)} \qquad 2.11b$$

The functions, $Z_I^{'(1)}$ and $Y_I^{'(1)}$, have the form

$$Z_I^{(1)} = \sum_{n=0}^{n=\infty} A_n^{(1)} z^{n-\frac{1}{2}} \qquad 2.12a$$

$$Y_I^{(1)} = \sum_{m=0}^{m=\infty} B_m^{(1)} z^m \qquad 2.12b$$

where $z = x + iy$, $i^2 = -1$. The Airy stress function for the first crack in shear loading is as follows.

$$F_{II}^{(1)} = Re\overline{\overline{Y}}_{II}^{(1)} + yIm\overline{Y}_{II}^{(1)} + yIm\overline{Z}_{II}(z)^{(1)} \qquad 2.13$$

where:

$$Z_{II}^{'(1)} = \frac{d}{dz}Z_{II}^{(1)} = \frac{d^2}{dz^2}\overline{Z}_{II}^{(1)} = \frac{d^3}{dz^3}\overline{\overline{Z}}_{II}^{(1)} \qquad 2.14a$$

$$Y_{II}^{'(1)} = \frac{d}{dz}Y_{II}^{(1)} = \frac{d^2}{dz^2}\overline{Y}_{II}^{(1)} = \frac{d^3}{dz^3}\overline{\overline{Y}}_{II}^{(1)} \qquad 2.14b$$

The functions, $Z_{II}^{'(1)}$ and $Y_{II}^{'(1)}$, have the form

$$Z_{II}^{(1)} = \sum_{n=0}^{n=\infty} - iC_n^{(1)} z^{n-\frac{1}{2}} \qquad 2.15a$$

$$Y_{II}^{(1)} = \sum_{m=0}^{m=\infty} - iD_m^{(1)} z^m \qquad 2.15b$$

where $z = x + iy,\ i^2 = 1$.

The in-plane cartesian stress components for the crack-tip stress field associated with the first crack tip that result from equations 2.10 through 2.15 are as follows:

$$\begin{aligned} s_{xx}^{(1)} &= Re\, Z_I - yImZ_I^{'(1)} - yImY_I^{'(1)} + 2Re\, Y_I^{(1)} \\ &+ Re\, Y_{II}^{(1)} - yImY_{II}^{'(1)} - yImZ_{II}^{'(1)} + 2Re\, Z_{II}^{(1)} \end{aligned} \qquad 2.16a$$

$$s_{yy}^{(1)} = Re\, Z_I^{(1)} + yImZ_I^{'(1)} + yImY_I^{'(1)} + Re\, Y_{II}^{(1)} + yImY_{II}^{'(1)} + yImZ_{II}^{'(1)} \qquad 2.16b$$

$$t_{xy}^{(1)} = -yReZ_I^{'(1)} - yReY_I^{'(1)} - Im\, Y_I^{(1)} - yReY_{II}^{'(1)} - yReZ_{II}^{'(1)} - Im\, Z_{II}^{(1)} \qquad 2.16c$$

The stress field equations for the second crack are determined in the same manner, as those for the first crack but after a suitable coordinate transformation that recognizes that the second crack-tip is located at coordinate (-d,c) relative to the front crack-tip. The coordinate transformation is as follows with (2) denoting application to the second crack.

$$z^{(2)} = z^{(1)} + d - ic = (x+d) + i(y-c) \qquad 2.17$$

The Airy stress function for the second crack in opening mode loading is

$$F_I^{(2)} = Re\overline{\overline{Z}}_I^{(2)}(z + d - ic) + yIm\overline{Z}_I^{(2)}(z+d-ic) + yIm\overline{Y}_I^{(2)}(z+d-ic) \qquad 2.18$$

where:

$$Z_I^{'(2)} = \frac{d}{dz} Z_I^{(2)} = \frac{d^2}{dz^2}\overline{Z}_I^{(2)} = \frac{d^3}{dz^3}\overline{\overline{Z}}_I^{(2)} \qquad 2.19a$$

$$Y_I^{'(2)} = \frac{d}{dz} Y_I^{(2)} = \frac{d^2}{dz^2}\overline{Y}_I^{(2)} = \frac{d^3}{dz^3}\overline{\overline{Y}}_I^{(2)} \qquad 2.19b$$

The functions, $Z_{I'}^{(2)}$ and $Y_{I'}^{(2)}$, have the form

$$Z_I^{(2)}(z+d-ic) = \sum_{n=0}^{n=\infty} A_n^{(2)}(z+d-ic)^{n-\frac{1}{2}} \qquad 2.20a$$

$$Y_I^{(2)}(z+d-ic) = \sum_{m=0}^{m=\infty} B_m^{(2)}(z+d-ic)^m \qquad 2.20b$$

where z = x + iy, $i^2 = 1$.

The Airy stress function for the second crack in shear loading is as follows:

$$F_{II}^{(2)} = Re\overline{\overline{Y_{II}}}^{(2)}(z+d-ic) + yIm\overline{Y_{II}}^{(2)}(z+d-ic) + yIm\overline{Z_{II}}(z)^{(2)}(z+d-ic) \qquad 2.21$$

where:

$$Z_{II}^{'(2)} = \frac{d}{dz}Z_{II}^{(2)} = \frac{d^2}{dz^2}\overline{Z}_{II}^{(2)} = \frac{d^3}{dz^3}\overline{\overline{Z}}_{II}^{(2)} \qquad 2.22a$$

$$Y_{II}^{'(2)} = \frac{d}{dz}Y_{II}^{(2)} = \frac{d^2}{dz^2}\overline{Y}_{II}^{(2)} = \frac{d^3}{dz^3}\overline{\overline{Y}}_{II}^{(2)} \qquad 2.22b$$

The functions, $Z_{II}^{'(1)}$ and $Y_{II}^{'(1)}$, have the form

$$Z_{II}^{(2)}(z+d-ic) = \sum_{n=0}^{n=\infty} -iC_n^{(2)}(z+d-ic)^{n-\frac{1}{2}} \qquad 2.23a$$

$$Y_{II}^{(2)}(z+d-ic) = \sum_{m=0}^{m=\infty} -iD_m^{(2)}(z+d-ic)^m \qquad 2.23b$$

where z = x + iy, $i^2 = 1$.

The in-plane cartesian stress components for the second crack tip stress field are produced from equation 2.18 through 2.23 and are as follows:

$$\begin{aligned} s_{xx}^{(2)} &= Re\,Z_I - yImZ_I^{'(2)} - yImY_I^{'(2)} + 2Re\,Y_I^{(2)} \\ &+ Re\,Y_{II}^{(2)} - yImY_{II}^{'(2)} - yImZ_{II}^{'(2)} + 2Re\,Z_{II}^{(2)} \end{aligned} \qquad 2.24a$$

$$s_{yy}^{(2)} = Re\,Z_I^{(2)} + yImZ_I^{'(2)} + yImY_I^{'(2)} + Re\,Y_{II}^{(2)} + yImY_{II}^{'(2)} + yImZ_{II}^{'(2)} \qquad 2.24b$$

$$t_{xy}^{(2)} = -yReZ_I^{'(2)} - yReY_I^{'(2)} - ImY_I^{(2)} - yReY_{II}^{'(2)} - yReZ_{II}^{'(2)} - ImZ_{II}^{(2)} \qquad 2.24c$$

Crack Face Traction Removal

In order to obtain the traction-free crack faces for each of cracks 1 and 2, the stress fields produced along the faces of each crack by the crack-tip field of the other crack must be determined. Generalized Westergaard equations were again used to determine the unwanted tractions along the crack faces. A Westergaard function for loading applied along a crack face was found but a direct application was not possible because the function found is not for a traction load but for a point load. To account for the lack of Westergaard equations for traction loading along a crack face, the face was divided into regions. Integrating the load over the length of each region then provides a good approximation of the actual traction load on that region (see Figure 2.2). Adding each region's traction value will then produce the total effect of the traction along the face so that it can be used to create a traction-free face required by the boundary conditions.

The Airy stress function for opening mode traction removal along the first crack face is seen below.

$$F_{I,2}^{(1)} = \mathrm{Re}\,\overline{\overline{Z}}_{I,2}^{(1)}(z, s_{yy}^{(2)}, h_1) + y\,\mathrm{Im}\,\overline{Z}_{I,2}^{1}(z, s_{yy}^{(2)}, h_1) \qquad 2.25$$

where:

$$Z_{I,2}^{1'} = \frac{d}{dz} Z_{I,2}^{(1)} = \frac{d^2}{dz^2} \overline{Z}_{I,2}^{(1)} = \frac{d^3}{dz^3} \overline{\overline{Z}}_{I,2}^{(1)} \qquad 2.26$$

The Westergaard function $Z_{I,2}^{1}$ and $Z_{I,2}^{1'}$ are derived in Appendix A of reference 1; the final equation is seen below.

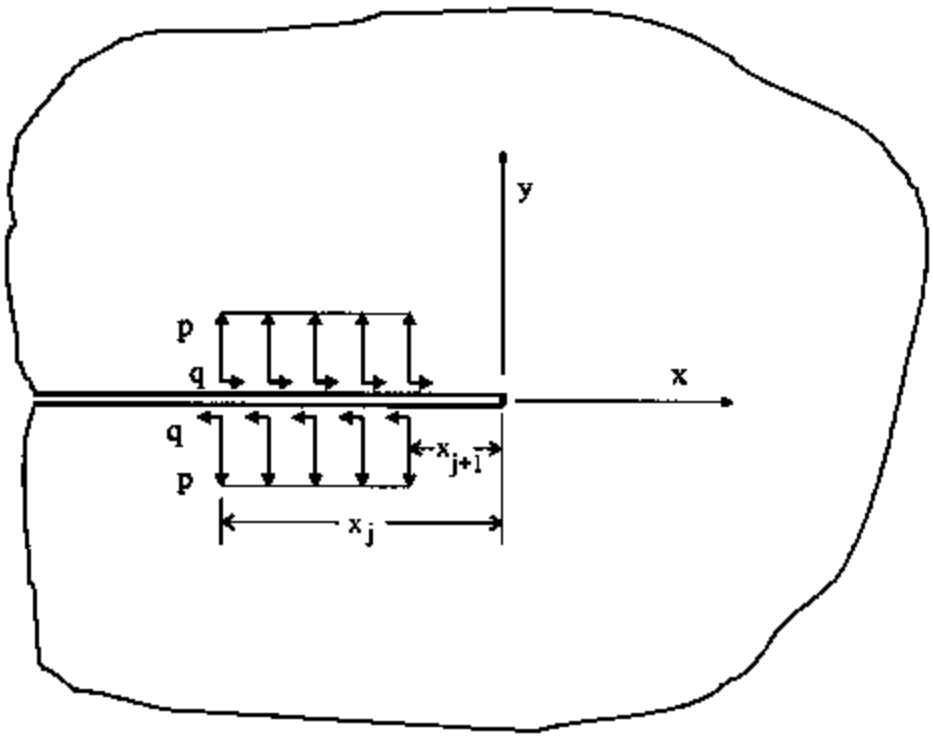

$$p = s_{yy}(x,0)$$
$$q = t_{xy}(x,0)$$

$$Z_I = \int_{x_j}^{x_{J+1}} \left(\frac{s_{yy}}{p} \frac{1}{z-x} \sqrt{\frac{-x}{z}} \right) dx \qquad Z_{II} = \int_{x_j}^{x_{J+1}} \left(\frac{t_{xy}}{p} \frac{1}{z-x} \sqrt{\frac{-x}{z}} \right) dx$$

$$K_I = \int_{x_j}^{x_{j+1}} \left(\frac{s_{yy}\sqrt{2}}{\sqrt{-x \quad p}} \right) dx \qquad K_{II} = \int_{x_j}^{x_{J+1}} \left(\frac{t_{xy}\sqrt{2}}{\sqrt{-x \quad p}} \right)$$

Figure 2.2 – Westergaard Stress Functions and Resulting Stress Intensity Factors for a Crack with Applied Tractions Along Its Faces[1]

$$Z^{1}_{I,2} = \frac{2}{p}\sum_{j=1}^{h_1}[s^{(2)}_{yy}(\frac{x_{j+1}+x_j}{2},c)][-\sqrt{\frac{-x_{j+1}}{z-d-ic}}+\tan^{-1}\sqrt{\frac{-x_{j+1}}{z-d-ic}}+\sqrt{\frac{-x_j}{z-d-ic}}-\tan^{-1}\sqrt{\frac{-x_j}{z-d-ic}}] \quad 2.27a$$

$$Z^{1'}_{I,2} = \frac{1}{p(z-d-ic)^{3/2}}\sum_{j=1}^{h_1}[s^{(2)}_{yy}(\frac{x_{j+1}+x_j}{2},c)][\frac{-x^{3/2}_{j+1}}{(z-d-ic-x_{j+1})}-\frac{-x^{3/2}_{j}}{(z-d-ic-x_j)}] \quad 2.27b$$

where:

h_1 = Number of divisions along the first crack

a_1 = Length of first crack

$x_1 = -a_1$

$x_{j+1} = x_j + dx$

$dx = a_1 / h_1$

The Airy stress function for the shear mode traction removal for the first crack is

$$F^{(1)}_{II,2} = (y-c)\,\mathrm{Im}\,\overline{Z^{1}_{II,2}}(z) \quad 2.28$$

where:

$$Z^{1'}_{II,2} = \frac{d}{dz}Z_{II,2}{}^{(1)} = \frac{d^2}{dz^2}\overline{Z}_{II,2}{}^{(1)} = \frac{d^3}{dz^3}\overline{\overline{Z}}_{II,2}{}^{(1)} \quad 2.29$$

The Westergaard function $Z^{2}_{II,1}$ and $Z^{2'}_{II,1}$ are derived in Appendix A of reference 1; the final equation is seen below.

$$Z^{1'}_{II,2}(z,t^{1}_{xy},h_2) = -iZ^{1}_{I,2}(z,t^{1}_{xy},h_2) \quad 2.30a$$

$$Z^{1'}_{II,2}(z,t^{1}_{xy},h_2) = -iZ^{1'}_{I,2}(z,t^{1}_{xy},h_2) \quad 2.30b$$

Using the equations 2.25 through 2.30 for opening and shear mode traction removal for the second crack resulted in the in-plane cartesian stress components that are listed below.

$$s^{1}_{xx,2} = \mathrm{Re}\, Z^{1}_{I,2} - y\,\mathrm{Im}\, Z^{1'}_{I,2} - y\,\mathrm{Im}\, Z^{1'}_{II,2} + 2\,\mathrm{Re}\, Z^{1}_{II,2} \qquad 2.31a$$

$$s^{1}_{yy,2} = \mathrm{Re}\, Z^{1}_{I,2} + y\,\mathrm{Im}\, Z^{1'}_{I,2} + y\,\mathrm{Im}\, Z^{1'}_{II,2} \qquad 2.31b$$

$$t^{1}_{xxy,2} = -y\,\mathrm{Re}\, Z^{1'}_{I,2} - y\,\mathrm{Re}\, Z^{1'}_{II,2} - \mathrm{Im}\, Z^{1}_{II,2} \qquad 2.31c$$

As seen below the equations for traction removal are determined the same way as the first crack. The Airy stress function for opening mode traction removal along the second crack face is.

$$F^{(2)}_{I,1} = \mathrm{Re}\,\overline{\overline{Z^{(2)}_{I,1}}}(z - d - ic, s^{(1)}_{yy}, h_2) + y\,\mathrm{Im}\,\overline{Z^{2}_{I,1}}(z - d - ic, s^{(1)}_{yy}, h_2) \qquad 2.32$$

where:

$$Z^{2'}_{I,1} = \frac{d}{dz} Z_{I,1}{}^{(2)} = \frac{d^2}{dz^2}\overline{Z}_{I,1}{}^{(2)} = \frac{d^3}{dz^3}\overline{\overline{Z}}_{I,1}{}^{(2)} \qquad 2.33$$

The Westergaard function $Z^{2}_{I,1}$ and $Z^{2'}_{I,1}$ are derived in Appendix A of reference 1; the final equation is seen below.

$$Z^{2}_{I,1} = \frac{2}{p}\sum_{j=1}^{h_2}[s^{(1)}_{yy}(\frac{x_{j+1} + x_j}{2}, c)][-\sqrt{\frac{-x_{j+1}}{z - d - ic}} + \tan^{-1}\sqrt{\frac{-x_{j+1}}{z - d - ic}} + \sqrt{\frac{-x_j}{z - d - ic}} - \tan^{-1}\sqrt{\frac{-x_j}{z - d - ic}} \qquad 2.34a$$

- 2.34b

where:

h_2 = Number of divisions along the second crack

a_2 = length of second crack

$x_1 = -a_2$

$x_{j+1} = x_j + dx$

$dx = a_2 / h_2$

The Airy stress function for the shear mode traction removal on the first crack is

$$F^{(2)}_{II,1} = (y-c)\,\mathrm{Im}\,\overline{Z^{2}_{II,1}}(z-d-ic, t^{1}_{xy}, h_2) \qquad 2.35$$

where:

$$Z^{2'}_{II,1} = \frac{d}{dz} Z_{II,1}{}^{(2)} = \frac{d^2}{dz^2}\overline{Z}_{II,1}{}^{(2)} = \frac{d^3}{dz^3}\overline{\overline{Z}}_{II,1}{}^{(2)} \qquad 2.36$$

The Westergaard function $Z^{2}_{II,1}$ and $Z^{2'}_{II,1}$ are derived in Appendix A of reference 1; the final equation is seen below.

$$Z^{2'}_{II,1}(z-d-ic, t^{1}_{xy}, h_2) = -iZ^{2}_{I,1}(z-d-ic, t^{1}_{xy}, h_2) \qquad 2.37a$$

$$Z^{2'}_{II,1}(z-d-ic, t^{1}_{xy}, h_2) = -iZ^{2'}_{I,1}(z-d-ic, t^{1}_{xy}, h_2) \qquad 2.37b$$

Using the equations for opening and shear mode traction removal on the second crack, as seen in equations 2.32 through 2.37, the in-plane cartesian stress components are found to be

$$s^{2}_{xx,1} = \mathrm{Re}\,Z^{2}_{I,1} - (y-c)\,\mathrm{Im}\,Z^{2'}_{I,1} - (y-c)\,\mathrm{Im}\,Z^{2'}_{II,1} + 2\,\mathrm{Re}\,Z^{2}_{II,1} \qquad 2.38a$$

$$s^{2}_{yy,1} = \mathrm{Re}\,Z_{I,1} + (y+c)\,\mathrm{Im}\,Z^{2'}_{I1} + (y-c)\,\mathrm{Im}\,Z^{2'}_{II,1} \qquad 2.38b$$

$$t^{2}_{xy,1} = -(y-c)\,\mathrm{Re}\,Z^{2}_{I,1} - (y-c)\,\mathrm{Re}\,Z^{2'}_{II,1} - \mathrm{Im}\,Z^{2}_{II,1} \qquad 2.38c$$

Overall Stress Field

As stated in step 5 of the combined Westergaard-Schwarz method, the overall stress field equations are obtained by superposing the traction removal equations, 2.31 and 2.38, and the crack-tip equations, 2.16 and 2.24. The overall in-plane cartesian stress components are found to be

$$\begin{aligned}
s_{xx} &= s_{xx}^{1} + s_{xx,2}^{1} + s_{xx}^{2} + s_{xx,1}^{2} \\
&= \operatorname{Re} Z_I^1 - y \operatorname{Im} Z_I^{1'} - y \operatorname{Im} Y_I^{1'} + 2 \operatorname{Re} Y_I^1 + \operatorname{Re} Y_{II}^1 - y \operatorname{Im} Y_{II}^{1'} - y \operatorname{Im} Z_{II}^{1'} \\
&\quad + 2 \operatorname{Re} Z_{II}^1 + \operatorname{Re} Z_I^2 - (y-c) \operatorname{Im} Z_I^{2'} - (y-c) \operatorname{Im} Y_I^{2'} + 2 \operatorname{Re} Y_I^2 + \operatorname{Re} Y_{II}^2 \\
&\quad - (y-c) \operatorname{Im} Y_{II}^{2'} - (y-c) \operatorname{Im} Z_{II}^{2'} + 2 \operatorname{Re} Z_{II}^2 + \operatorname{Re} Z_{I,2}^1 - y \operatorname{Im} Z_{I,2}^1 - y \operatorname{Im} Z_{II,2}^{1'} \\
&\quad + 2 \operatorname{Re} Z_{II,2}^1 + \operatorname{Re} Z_{I,1}^2 - (y-c) \operatorname{Im} Z_{I,1}^{2'} - (y-c) \operatorname{Im} Z_{II,1}^{2'} + 2 \operatorname{Re} Z_{II,1}^2
\end{aligned} \tag{2.39a}$$

$$\begin{aligned}
s_{yy} &= s_{yy}^{1} + s_{yy,2}^{1} + s_{yy}^{2} + s_{yy,1}^{2} \\
&= \operatorname{Re} Z_I^1 + y \operatorname{Im} Z_I^{1'} + y \operatorname{Im} Y_I^{1'} + \operatorname{Re} Y_{II}^1 + y \operatorname{Im} Y_{II}^{1'} + y \operatorname{Im} Z_{II}^{1'} \\
&\quad + \operatorname{Re} Z_I^2 + (y-c) \operatorname{Im} Z_I^{2'} + (y-c) \operatorname{Im} Y_1^{2'} + \operatorname{Re} Y_{II}^2 + (y-c) \operatorname{Im} Y_{II}^{2'} \\
&\quad + (y-c) \operatorname{Im} Z_{II}^{2'} + \operatorname{Re} Z_{I,2}^1 + y \operatorname{Im} Z_{I,2}^{1'} + y \operatorname{Im} Z_{II,2}^{1'} + \operatorname{Re} Z_{I,1}^2 \\
&\quad + (y-c) \operatorname{Im} Z_{I,1}^2 + (y-c) \operatorname{Im} Z_{II,1}^2
\end{aligned} \tag{2.39b}$$

$$\begin{aligned}
t_{xy} &= t_{xy}^{1} + t_{xy,2}^{1} + t_{xy}^{2} + t_{xy,1}^{2} \\
&= -y \operatorname{Re} Z_I^{1'} - y \operatorname{Re} Y_I^{1'} - \operatorname{Im} Y_I^1 - y \operatorname{Re} Y_{II}^{1'} - y \operatorname{Re} Z_{II}^{1'} - \operatorname{Im} Z_{II} \\
&\quad - (y-c) \operatorname{Re} Z_I^{2'} - (y-c) \operatorname{Re} Y_I^{2'} - \operatorname{Im} Y_I^2 - (y-c) \operatorname{Re} Y_{II}^{2'} \\
&\quad - (y-c) \operatorname{Re} Z_{II}^{2'} - \operatorname{Im} Z_{II}^{2'} - y \operatorname{Re} Z_{I,2}^1 - y \operatorname{Re} Z_{II,2}^{1'} - \operatorname{Im} Z_{II,2}^1 \\
&\quad - (y-c) \operatorname{Re} Z_{I,1}^{2'} - (y-c) \operatorname{Re} Z_{II,1}^{2'} - \operatorname{Im} Z_{II,1}^2
\end{aligned} \tag{2.39c}$$

CHAPTER III
STRESS FIELD PARAMETERS

Photoelastic isochromatic fringe experiments performed by Moran[12] and Hardin[1] indicated that data could be extracted from a region shown in Figure 3.1 and analyzed using local collocation method to find the stress field parameters around each of the two cracks. The data extracted from the region was stored in the form (x, y, N) where x and y are point coordinates of a point in the field, and N is the photoelastic fringe order at that point. However, data was not taken from the region very close to the crack-tip because of the tri-axial stress state, which is in violation of the plane stress assumption normally made for the photoelastic experimentation. Data from numerical experimentation such as a finite element model was converted from stress data to isochromatic fringe data using equations 3.1 and 3.2.

The maximum, in-plane, shear stress in terms of in-plane cartesian stress components is given by:

$$t_{\max} = \left[\left(\frac{s_{yy} - s_{xx}}{2} \right)^2 + t_{xy}^2 \right]^{\frac{1}{2}} \qquad 3.1$$

The governing stress optical equation for isochromatic fringe patterns then relates the stress components to the photoelastic fringe order value through:

$$2t_{\max} = \frac{Nf_s}{t} \qquad 3.2$$

where:

N = Photoelastic fringe order

f_s = Fringe sensitivity of the birefringent model material

t = thickness of specimen

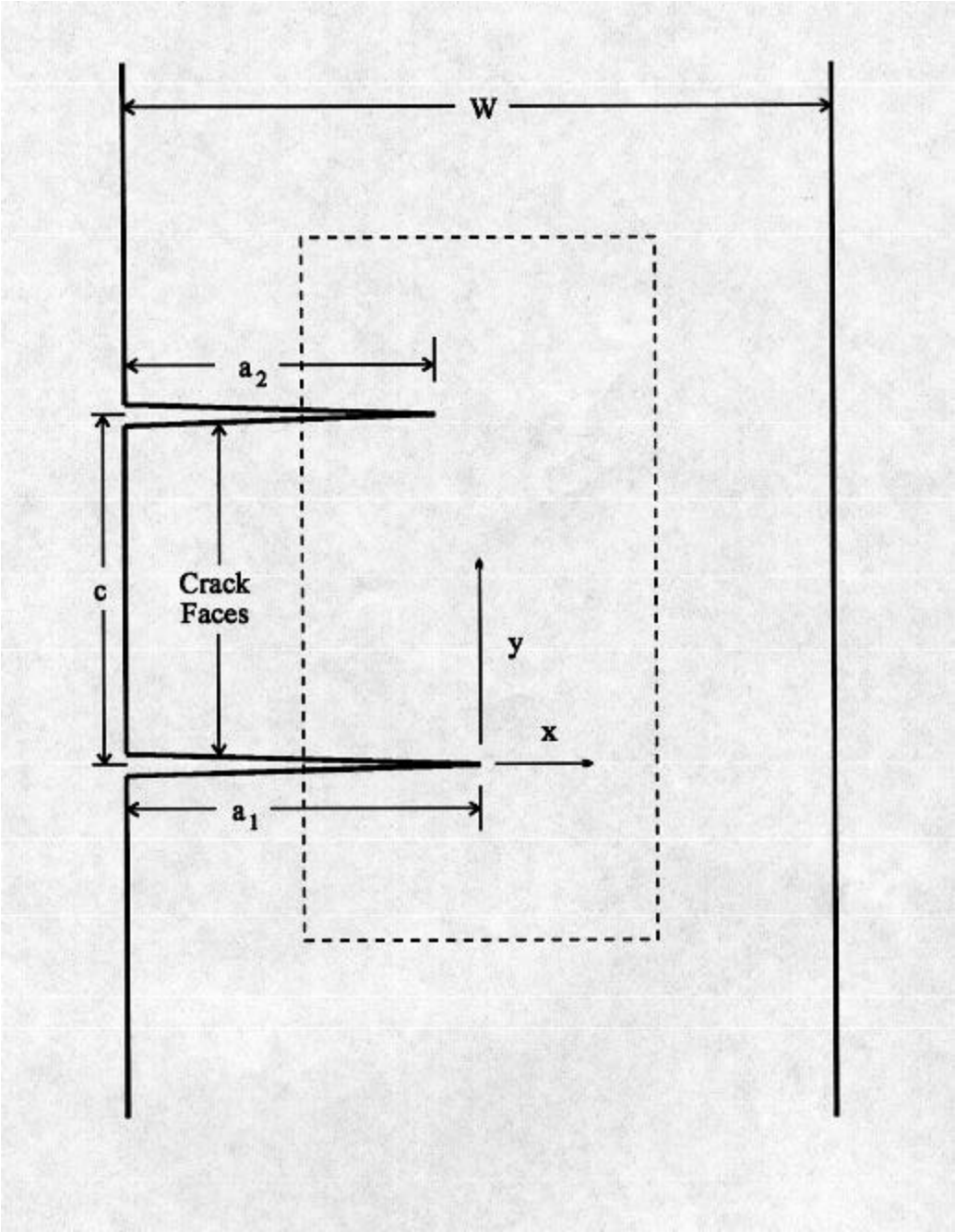

Figure 3.1 – Data Extraction Region of Two Parallel Edge Cracks in a Four Point Bending

Local Collocation

The local collocation method developed by Sanford[9.10] and Chona[3,4] is an over-deterministic method utilizing an iterative process based on the Newton-Raphson Method. The full field stress equations utilize the infinite series coefficients in equations 2.39 in combination with equation 3.1 and 3.2. The best fit for the unknown coefficients is determined in a non-linear, least squares sense in the local region. A combination of equations 3.1 and 3.2 are required to use the Newton-Raphson method and minimize the derivation at each point from:

$$g_k = \left[\left(\frac{s_{yy} - s_{xx}}{2}\right)_k^2 + t_{xy\,k}^2\right]^{\frac{1}{2}} + \frac{N_k f_s}{2t} = 0 \qquad 3.3$$

where k is the subscript that denotes the function at a coordinate and fringe order value. The resulting system of equations can be represented in the matrix form:

$$[N] = [G][C] \qquad 3.4$$

where:

$[N]$ = Elements of Fringe Order

$[G]$ = Known Stress Functions

$[C]$ = Unknown Coefficients

Further details about the procedure of the local collocation method can be found in Appendix B of Reference 3.

Stress Intensity Factors and J-Integrals

One way to determine the accuracy of the results is through a comparison of the Stress Intensity Factors (SIF's) and J-Integrals found through the Westergaard-Schwarz Method with the finite element analysis. In determining the SIF's with the local collocation method, the stress field at the crack-tip as well as the traction removal stress field has to be taken into account. This is accomplished in the same manner as the stresses in the Westergaard-Schwarz Method through a simple superposition of stress values. This means that the SIF for the crack-tip is superposed with the SIF for the traction removal stress.

K = K from the crack-tip stress field + K from the traction removal stress field 3.5

The calculations start with the basic equation for the stress intensity factors for opening mode loading

$$K_I = \lim_{x\to 0, y=0} s_{yy}\sqrt{2px} \tag{3.6}$$

as well as shear mode loading.

$$K_{II} = \lim_{x\to 0, y=0} t_{xy}\sqrt{2px} \tag{3.7}$$

Using these basic equations and superposing the crack tip stress field with the traction removal stress field, the opening mode stress intensity factor for the first crack is:

$$K_I^1 = A_0^1\sqrt{2p} + 2\sqrt{\frac{2}{p}}\sum_{j=1}^{h_1} s_{yy}^2\left(\frac{x_{j+1}+x_j}{2},0\right)\left[-\sqrt{-x_{j+1}}+\sqrt{-x_j}\right] \tag{3.8}$$

and for shear mode loading it is:

$$K_{II}^{1} = C_0^1\sqrt{2p} + 2\sqrt{\frac{2}{p}}\sum_{j=1}^{h_1} t_{xy}^{2}\left(\frac{x_{j+1}+x_j}{2},0\right)\left[-\sqrt{-x_{j+1}}+\sqrt{-x_j}\right] \qquad 3.9$$

The stress intensity factors for the second crack are determined in the same manner as the for first crack. For opening mode loading:

$$K_{I}^{2} = A_0^2\sqrt{2p} + 2\sqrt{\frac{2}{p}}\sum_{j=1}^{h_2} s_{yy}^{1}\left(\frac{x_{j+1}+x_j}{2},0\right)\left[-\sqrt{-x_{j+1}}+\sqrt{-x_j}\right] \qquad 3.10$$

and for shear mode loading:

$$K_{II}^{2} = C_0^2\sqrt{2p} + 2\sqrt{\frac{2}{p}}\sum_{j=1}^{h_2} t_{xy}^{1}\left(\frac{x_{j+1}+x_j}{2},0\right)\left[-\sqrt{-x_{j+1}}+\sqrt{-x_j}\right] \qquad 3.11$$

The exact method by which the stress intensity factor equations are determined can be seen in Appendix A of Reference 1.

In accordance with Hardin[1] and Keener's[8] work, the J-Integrals obtained from the finite element program ABAQUS and the local collocation method were compared to verify the accuracy of the results obtained. The J-Integral comparison was used because of the ability of the J-Integral to account for both opening and shear mode stress intensity factors. The J-Integral from the Westergaard-Schwarz method was determined using the equation below with the SIF's calculated using the coefficients from the stress-field solution.

$$J^{r} = \frac{\left(K_I^r\right)^2 + \left(K_{II}^r\right)^2}{E} \qquad 3.12$$

where:

r = Crack number

K_I = Open mode Stress Intensity Factor

K_{II} = Shear Mode Stress Intensity Factor

E = Modulus of Elasticity of Specimen

The finite element J-Integral value was determined in the ABAQUS using the CONTOUR INTEGRAL function. This function required the number of contours calculated to be input into the function. In this finite element analysis it was found that after six contours the J-Integral value did not change.

CHAPTER IV
NUMERICAL EXPERIMENTATION

Since Hardin[1] and Keener[8] showed that finite element data accurately compared to the data extracted from photoelastic experimentation, this study exclusively used numerically determined stress fields. Several issues had to be taken into account before a local collocation stress field analysis could be made. Since the purpose of this study was a continuation of previous research, a decision about which aspects that would be carried to the current study had to be made. Whether to reuse the finite element model design was the first issue to consider. It was decided that the basic design of the four point bending member would be used because this produces a predominantly opening mode stress on the cracks. A few modifications of the original specimen had to be made since this study would explore a greater separation between the parallel edge cracks. Increasing the distance between loading was needed to maintain an open mode stress state. The regions of fine mesh were also increased to accommodate the different models studied.

Finite Element Experimentation

The finite element models were created to extract data to study the shielding and interaction effects of parallel edge cracks in a four point bending specimen. The use of finite element models over physical experimentation was chosen because of the ease with which the numerous computer generated models could be run, as well as the ability to rapidly make changes to the model without much downtime. The finite element models were built using PATRAN 2004 and analyzed using ABAQUS 6.4. Both programs were accessed using the supercomputers at the Texas A&M University Supercomputing Facility. In the beginning, Hardin's models were replicated so that the correctness of the procedures being followed could be made fairly easily. An example of Hardin's model dimensions and properties is given in Table 4.1 and Table 4.2.

Table 4.1 - Dimension of Numerical Model 1 Used by Hardin[1]

Model	1.1	1.2	1.3	1.4
First Crack Length, a_1 (in)	1.00	1.00	1.00	1.00
Second Crack Length, a_2 (in)	0.5	0.75	1.00	1.25
Separation, c (in)	0.50	0.50	0.50	0.50
Width, W (in)	2.00	2.00	2.00	2.00
a_2/a_1	0.50	0.75	1.00	1.25
c/a_1	0.50	0.50	0.50	0.50
a_1/W	0.50	0.50	0.50	0.50
a_2/W	0.25	0.375	0.5	0.625

Table 4.2 - Information about Numerical Model Used by Hardin[1]

Material	Steel
Applied Bending Moment, M (lb-in)	1000
Thickness of Specimen, t (in)	1.0
Length of Specimen, L (in)	8.0
Modulus of Elasticity, E (psi)	30×10^6
Poisson ratio, ν	0.30

Eight basic models were constructed starting with the three that Hardin created. The parameters varied were the separation of the cracks as well as the ratio of the two crack lengths. The eight crack separation distances that were initially constructed were 0.5 in, 0.75 in, 1.00 in, 1.25 in, 1.50 in, 1.75 in, and 2.00 in. The models were created using 8-node quadrilateral elements with full integration. The cracks were created by eliminating all coinciding nodes in the model except for nodes required to simulate the two cracks. The length of crack 1 was kept fixed. The length was of the second crack was then varied by eliminating the coinciding nodes at the tip until the desired length was achieved. In Tables 4.3 through 4.10 the model dimension variations are presented. The material properties of the specimen simulated in the finite element analysis can be seen in Table 4.11.

Table 4.3 - Dimension of Numerical Model 1

Model	1.1	1.2	1.3
First Crack Length, a_1 (in)	1.00	1.00	1.00
Second Crack Length, a_2 (in)	0.5	0.75	1.00
Separation, c (in)	0.50	0.50	0.50
Width, W (in)	2.00	2.00	2.00
a_2/a_1	0.50	0.75	1.00
c/a_1	0.50	0.50	0.50
c/l	0.0625	0.0625	0.0625

Table 4.4 - Dimension of Numerical Model 2

Model	2.1	2.2	2.3
First Crack Length, a_1 (in)	1.00	1.00	1.00
Second Crack Length, a_2 (in)	0.5	0.75	1.00
Separation, c (in)	0.75	0.75	0.75
Width, W (in)	2.00	2.00	2.00
a_2/a_1	0.50	0.75	1.00
c/a_1	0.75	0.75	0.75
c/l	0.09375	0.09375	0.09375

Table 4.5 - Dimension of Numerical Model 3

Model	3.1	3.2	3.3
First Crack Length, a_1 (in)	1.00	1.00	1.00
Second Crack Length, a_2 (in)	0.5	0.75	1.00
Separation, c (in)	1.00	1.00	1.00
Width, W (in)	2.00	2.00	2.00
a_2/a_1	0.50	0.75	1.00
c/a_1	1.00	1.00	1.00
c/l	0.125	0.125	0.125

Table 4.6 - Dimension of Numerical Model 4

Model	4.1	4.2	4.3
First Crack Length, a_1 (in)	1.00	1.00	1.00
Second Crack Length, a_2 (in)	0.50	0.75	1.00
Separation, c (in)	1.25	1.25	1.25
Width, W (in)	2.00	2.00	2.00
a_2/a_1	0.50	0.75	1.00
c/a_1	1.25	1.25	1.25
c/l	0.15625	0.15625	0.15625

Table 4.7 - Dimension of Numerical Model 5

Model	5.1	5.2	5.3
First Crack Length, a_1 (in)	1.00	1.00	1.00
Second Crack Length, a_2 (in)	0.5	0.75	1.00
Separation, c (in)	1.50	1.50	1.50
Width, W (in)	2.00	2.00	2.00
a_2/a_1	0.50	0.75	1.00
c/a_1	1.50	1.50	1.50
c/l	0.1875	0.1875	0.1875

Table 4.8 - Dimension of Numerical Model 6

Model	6.1	6.2	6.3
First Crack Length, a_1 (in)	1.00	1.00	1.00
Second Crack Length, a_2 (in)	0.5	0.75	1.00
Separation, c (in)	1.75	1.75	1.75
Width, W (in)	2.00	2.00	2.00
a_2/a_1	0.50	0.75	1.00
c/a_1	1.75	1.75	1.75
c/l	0.21875	0.21875	0.21875

Table 4.9 - Dimension of Numerical Model 7

Model	7.1	7.2	7.3
First Crack Length, a_1 (in)	1.00	1.00	1.00
Second Crack Length, a_2 (in)	1.25	1.25	1.25
Separation, c (in)	2.00	2.00	2.00
Width, W (in)	2.00	2.00	2.00
a_2/a_1	0.50	0.75	1.00
c/a_1	2.00	2.00	2.00
c/l	0.25	0.25	0.25

Table 4.10 - Information about Numerical Model

Material	Steel
Applied Bending Moment, M (lb-in)	1000
Thickness of Specimen, t (in)	1.0
Length of Specimen, L (in)	8.0
Modulus of Elasticity, E (psi)	30×10^6
Poisson ratio, ν	0.30

Seen in Figures 4.1 and 4.2 are examples of the mesh that was created for the numerical experimentation. The same mesh was used for all the models with only slight variations due to crack separation.

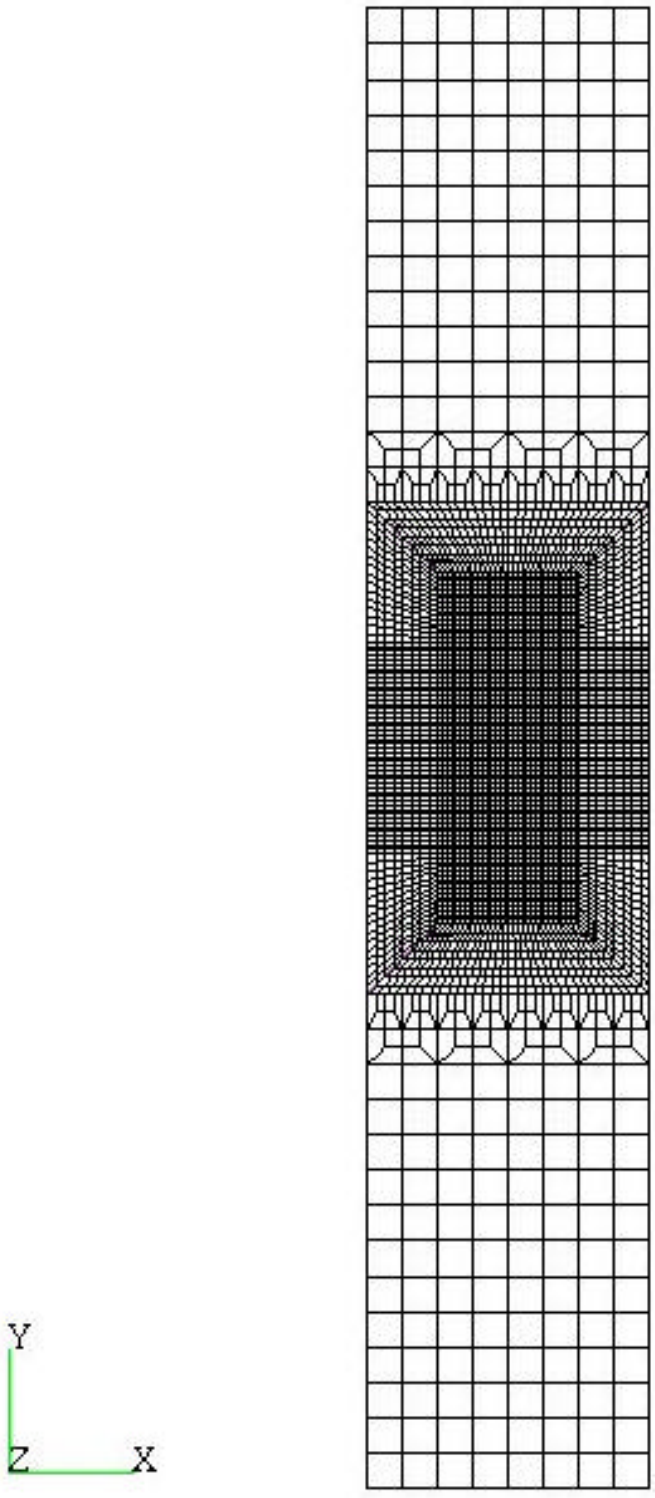

Figure 4.1: Mesh Created for Numerical Model

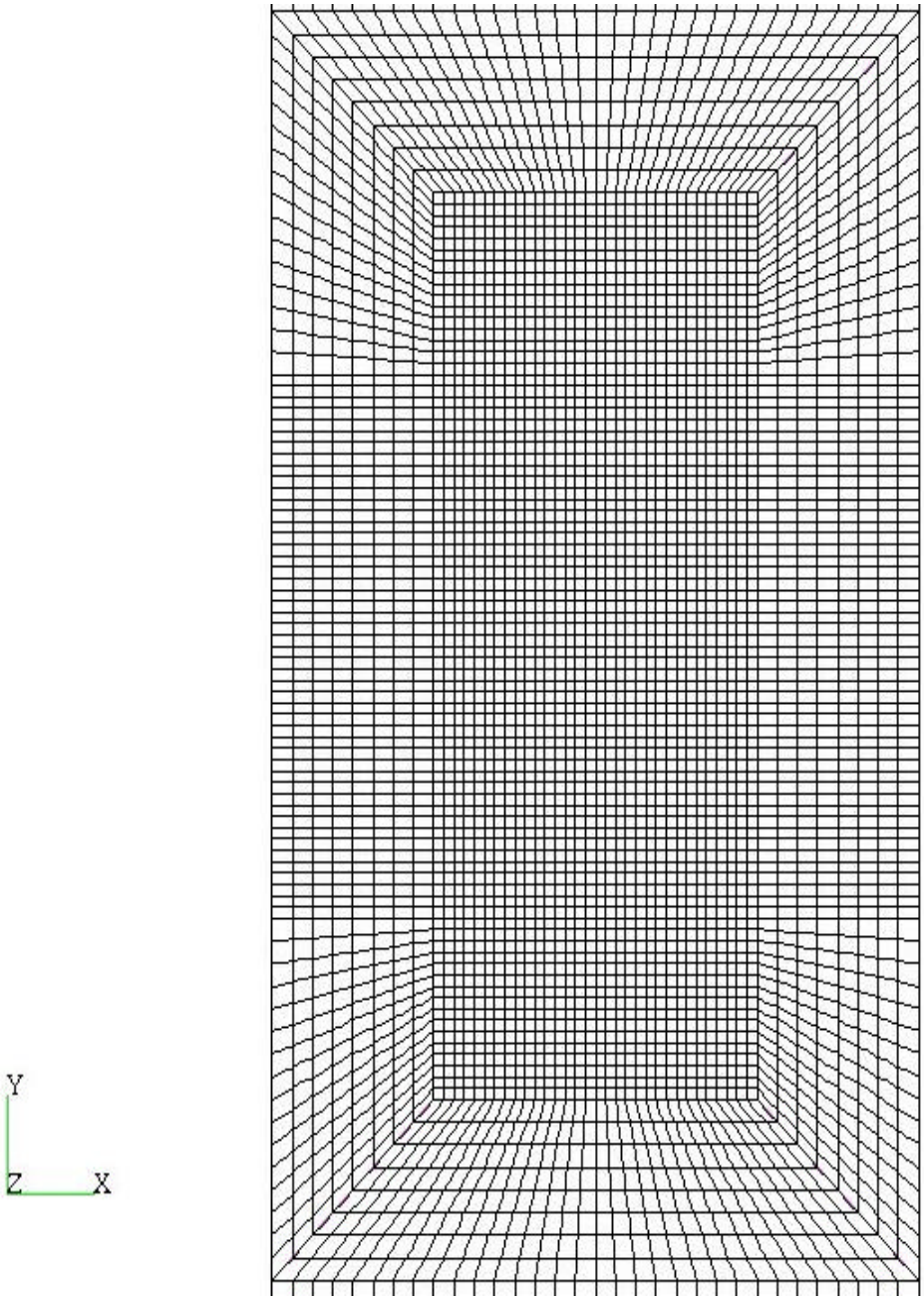

Figure 4.2: Mesh Created for Numerical Model (Zoom in on Crack Interaction Region)

CHAPTER V
RESULTS AND DISCUSSION

In this study the results for the stress field analysis were determined from data gathered from finite element models using a local collocation method to determine the coefficients in the Westergaard series stress functions shown in equations 2.5 and 2.6. The coefficients were then used to calculate the crack-tip parameters that form the basis for the investigation into the effects of interacting cracks. The original programs used for this analysis are presented in Appendix E of Reference 1; the modified versions used here as well as other programs develop can be viewed in Appendix A.

The quality and consistency of the results was checked using several different methods consistent with Hardin and Keener's evaluations. Several of these error checks were built into the local collocation program labeled as ERROR, DELTA N (FRG), and DELTA N (PCT), which can also be used to determine the appropriate number of coefficients to accurately represent the stress field over the region of data acquisition. The ERROR computed in the program was a sum of the squares of the difference between the fringe order value calculated from the local collocation method and the fringe order value at the same location from the finite element analysis. Mathematically, this measure is given by:

$$error = \sum_{i=1}^{n} (N^{i}_{input} - N^{i}_{calcualted})^{2} \qquad 5.1$$

where:

N_{input} = Input fringe order value at a given location

$N_{calculated}$ = Calculated fringe order value at the same location

n = number of data points

The next parameter, DELTA N (FRG), was used to establish the appropriate number of coefficients for modeling the stress field, over the data acquisition region, and is expressed as:

$$\Delta N = \frac{1}{n}\sum_{i=1}^{n} abs(N_{input} - N_{calculated}) \qquad 5.2$$

This provides a measure of the average difference in the fringe order values input into the local collocation program, and the fringe order values calculated using the coefficients from the analysis. When this parameter stabilizes, and converges to some small number, the order of the model was felt to be accurate. DELTA N (FRG) was the first indicator of the appropriate number of coefficients to be retained in the stress field representation by showing that retaining additional coefficients would not significantly change the accuracy of the series representation. This value was used in conjunction with converging leading coefficients (A_0,C_0) to determine where the truncation of the Westergaard series should occur in the analysis.

The final check built into the local collocation program was the DELTA N (PCT). This value, shown below, represents the ratio of DELTA N (FRG) calculated from equation 5.2 to the average input fringe order value.

$$\Delta N(Percent) = 100 * \frac{\Delta N}{N_{avg}} \qquad 5.3$$

where:

ΔN = Average Fringe Order Difference

N_{avg} = Average Input Fringe Order

By using a combination of the parameter values discussed above, estimates could be obtained of how well the calculated coefficients had captured and represented the stress field over the data acquisition region.

In accordance with Hardin[1] and Keener's[8] procedures, the calculated J-Integral was used as an additional comparison tool. Individually determined K_I and K_{II} cannot be determined from the finite element analysis program. Hence, the finite element analysis only gives the J-Integral along various contours enveloping each crack tip. Thus, the

only way of comparing the local collocation results to the finite element analysis directly is by looking at the J-Integral values from the finite element analysis and J-Integral values from the local collocation using equation 3.12. Also since the results obtained by Hardin[1] were available, a comparison with the results found in this study was made as another way to verify the validity of the data.

Preliminary Issues

The application of the local collocation approach to the scenarios of interest was demonstrated previously. Several issues arose as the present study progressed. The additional cases to be studied here required changes in the design of the finite element models. To maintain a predominantly opening mode situation, the point loads applied to the specimen must be significantly far from the cracks. Analyzing the four point bending members used by Hardin[1] and Keener[8] as well as advice from outside sources, it was decided that a minimum distance of 1 inch from the nearest crack to the point load had to be maintained as well as maintaining the distances between top and bottom point load used in the previous research. The area of very fine mesh also had to be increased to account for the greater crack plane separations to be studied.

The second issue that arose was that the increased separation between the two parallel cracks also created a larger area from which to gather data. A study was therefore conducted on whether the same number of randomly sampled points used in Hardin's study could be used with an increase in data acquisition region. The study consisted of varying the number of samples taken from a region of fixed size and analyzing the effects it had on the leading coefficients (A_0,C_0). The results are given in Appendix C. The conclusion of the study was that increasing or decreasing the number of points even over a larger sampling area did not significantly increase the stability of the leading coefficients. Therefore, the number of sampling points taken from the finite element generated stress field was not changed from the value used in previous research (229 Points).

A measure for determining interaction of the two cracks was needed to achieve the objectives of the present study. It was decided that an opening mode stress intensity factor determined by an estimating equation presented in Reference 5 for a single crack in a finite specimen under four point bending. The opening mode stress intensity factors for 1.0 inch, 0.75 inch, and 0.5 inch long single cracks were calculated, see Appendix C, and used to determine when each individual crack could have been analyzed without having to account for the second crack.

Lastly since the finite element analysis program produces J-Integral values for several different contours. The appropriate J-Integral value had to be determined from all the different contour values. It was seen that after the sixth contour the J-Integral value would remain the same through the higher contours.

Numerical Experiments

The stress intensity factors were computed for each case using the coefficients determined from the local collocation program. In Tables 5.1 through 5.7 the stress intensity factor values as well as the J-Integral values found through ABAQUS and the local collocation program are presented. Included in the tables is a percent difference value between the J-Integral calculated from the local collocation values of K_I and K_{II} and the J-Integral provided by ABAQUS. This percent difference was calculated from:

$$\%diff = 100 \cdot Abs\left[\frac{J^c_{FEM} - J^c_{Calc}}{J^c_{FEM} + J^c_{Calc}}\right] \qquad 5.4$$

where:

c = Number of the Crack

J_{FEM} = J-Integral provided by ABAQUS

J_{Calc} = J-Integral calculated using equation 3.12

As a second verification, a comparison between the J-Integrals obtained by Hardin and the J-Integrals obtained in this for the cases where the geometry studied was the same as a case that Hardin had previously examined.

Results

Each model was given a model number in the form A.B. Starting at 1 the first number increments for each for value of separation distance ratio analyzed in the study. The second number represents the models crack length ratio. An example of the identification method would be the model with .5 separation ratio and a crack length ratio would be Model 1.1.

In viewing the tables below some trends can be seen. First as expected the opening mode stress intensity factor for the symmetrical models (A.3) are approximately equal. This result was expected since the two cracks are of equal length. Also in each table it is seen that as the crack ratio decreases the opening mode stress intensity factor for crack 1 increases. Inversely the opening mode stress intensity factor for crack 2 decreases. Since the specimen is in a predominantly opening mode state the J-Integral for both cracks follow the trends of it respective opening mode stress intensity factor.

Table 5.1 - Results of Numerical Model 1

Model	1.1	1.2	1.3
$K_I^1\,(psi-in^{1/2})$	4037	3908	3225
$K_I^2\,(psi-in^{1/2})$	1039	1833	3248
$K_{II}^1\,(psi-in^{1/2})$	145	461	457
$K_{II}^2\,(psi-in^{1/2})$	-415	-667	-549
$J_{FEM}^1\,(psi-in)$	0.539	0.507	0.396
$J_{Calc}^1\,(psi-in)$	0.544	0.516	0.354
$J_{FEM}^2\,(psi-in)$	0.024	0.104	0.396
$J_{Calc}^2\,(psi-in)$	0.042	0.127	0.362
% Diff[1]	0.42	0.87	5.71
% Diff[2]	26.39	9.93	4.57

K – Stress Intensity Factor

Superscript – Crack Number

Subscript – Opening (I) or Shear Mode (II)

J – J-Integral

Superscript – Crack Number

Subscript – Finite Element Analysis (FEM)

Local Collocation (Calc)

Model Number (A.B)

A – Crack Separation Case

(1: 0.5 in; 2: 0.75 in; …..N: max value)

B – Crack Length Ratio Case

(1: a2/a1 = 0.50; 2: a2/a1 = 0.75; 3: a2/a1 = 1.0)

% Diff – Percent Difference Between J_{FEM} and J_{CALC} Values

Superscript – Crack Number

Table 5.2 - Results of Numerical Model 2

Model	2.1	2.2	2.3
$K_I^1\,(psi-in^{1/2})$	4115	3853	3488
$K_I^2\,(psi-in^{1/2})$	1588	2278	3517
$K_{II}^1\,(psi-in^{1/2})$	191	591	233
$K_{II}^2\,(psi-in^{1/2})$	-672	-400	-396
$J_{FEM}^1\,(psi-in)$	0.536	0.507	0.447
$J_{Calc}^1\,(psi-in)$	0.566	0.506	0.407
$J_{FEM}^2\,(psi-in)$	0.054	0.161	0.447
$J_{Calc}^2\,(psi-in)$	0.099	0.178	0.417
% Diff[1]	2.73	0.09	4.69
% Diff[2]	29.38	5.05	3.46

K – Stress Intensity Factor

Superscript – Crack Number

Subscript – Opening (I) or Shear Mode (II)

J – J-Integral

Superscript – Crack Number

Subscript – Finite Element Analysis (FEM)

Local Collocation (Calc)

Model Number (A.B)

A – Crack Separation Case

(1: 0.5 in; 2: 0.75 in; …..N: max value)

B – Crack Length Ratio Case

(1: a2/a1 = 0.50; 2: a2/a1 = 0.75; 3: a2/a1 = 1.0)

% Diff – Percent Difference Between J_{FEM} and J_{CALC} Values

Superscript – Crack Number

Table 5.3 - Results of Numerical Model 3

Model	3.1	3.2	3.3
$K_I^1\,(psi-in^{1/2})$	4061	3855	3629
$K_I^2\,(psi-in^{1/2})$	1323	2422	3721
$K_{II}^1\,(psi-in^{1/2})$	467	256	67
$K_{II}^2\,(psi-in^{1/2})$	-114	-365	-345
$J_{FEM}^1\,(psi-in)$	0.536	0.517	0.486
$J_{Calc}^1\,(psi-in)$	0.557	0.498	0.439
$J_{FEM}^2\,(psi-in)$	0.082	0.202	0.486
$J_{Calc}^2\,(psi-in)$	0.059	0.200	0.465
% Diff[1]	1.95	1.89	5.03
% Diff[2]	16.50	0.38	2.13

K – Stress Intensity Factor

Superscript – Crack Number

Subscript – Opening (I) or Shear Mode (II)

J – J-Integral

Superscript – Crack Number

Subscript – Finite Element Analysis (FEM)

Local Collocation (Calc)

Model Number (A.B)

A – Crack Separation Case

(1: 0.5 in; 2: 0.75 in; …..N: max value)

B – Crack Length Ratio Case

(1: a2/a1 = 0.50; 2: a2/a1 = 0.75; 3: a2/a1 = 1.0)

% Diff – Percent Difference Between J_{FEM} and J_{CALC} Values

Superscript – Crack Number

Table 5.4 - Results of Numerical Model 4

Model	4.1	4.2	4.3
$K_I^1\,(psi-in^{1/2})$	3991	3979	3863
$K_I^2\,(psi-in^{1/2})$	1598	2595	3876
$K_{II}^1\,(psi-in^{1/2})$	577	597	147
$K_{II}^2\,(psi-in^{1/2})$	-137	-288	-276
$J_{FEM}^1\,(psi-in)$	0.538	0.527	0.512
$J_{Calc}^1\,(psi-in)$	0.542	0.540	0.498
$J_{FEM}^2\,(psi-in)$	0.105	0.229	0.512
$J_{Calc}^2\,(psi-in)$	0.086	0.227	0.503
% Diff^1	0.33	1.15	1.38
% Diff^2	9.93	0.50	0.86

K – Stress Intensity Factor

Superscript – Crack Number

Subscript – Opening (I) or Shear Mode (II)

J – J-Integral

Superscript – Crack Number

Subscript – Finite Element Analysis (FEM)

Local Collocation (Calc)

Model Number (A.B)

A – Crack Separation Case

(1: 0.5 in; 2: 0.75 in; …..N: max value)

B – Crack Length Ratio Case

(1: a2/a1 = 0.50; 2: a2/a1 = 0.75; 3: a2/a1 = 1.0)

% Diff – Percent Difference Between J_{FEM} and J_{CALC} Values

Superscript – Crack Number

Table 5.5 - Results of Numerical Model 5

Model	**5.1**	**5.2**	**5.3**
$K_I^1\,(psi-in^{1/2})$	4066	3973	3967
$K_I^2\,(psi-in^{1/2})$	1881	2692	4019
$K_{II}^1\,(psi-in^{1/2})$	314	78	47
$K_{II}^2\,(psi-in^{1/2})$	-182	-273	-218
$J_{FEM}^1\,(psi-in)$	0.542	0.536	0.529
$J_{Calc}^1\,(psi-in)$	0.554	0.526	0.525
$J_{FEM}^2\,(psi-in)$	0.122	0.248	0.529
$J_{Calc}^2\,(psi-in)$	0.119	0.244	0.540
% Diff[1]	1.13	0.92	0.43
% Diff[2]	1.04	0.89	1.02

K – Stress Intensity Factor

Superscript – Crack Number

Subscript – Opening (I) or Shear Mode (II)

J – J-Integral

Superscript – Crack Number

Subscript – Finite Element Analysis (FEM)

Local Collocation (Calc)

Model Number (A.B)

A – Crack Separation Case

(1: 0.5 in; 2: 0.75 in; …..N: max value)

B – Crack Length Ratio Case

(1: a2/a1 = 0.50; 2: a2/a1 = 0.75; 3: a2/a1 = 1.0)

% Diff – Percent Difference Between J_{FEM} and J_{CALC} Values

Superscript – Crack Number

Table 5.6 - Results of Numerical Model 6

Model	**6.1**	**6.2**	**6.3**
$K_I^1\,(psi-in^{1/2})$	4055	4020	3979
$K_I^2\,(psi-in^{1/2})$	1841	2687	4046
$K_{II}^1\,(psi-in^{1/2})$	132	95	23
$K_{II}^2\,(psi-in^{1/2})$	-362	-353	-195
$J_{FEM}^1\,(psi-in)$	0.545	0.543	0.540
$J_{Calc}^1\,(psi-in)$	0.549	0.539	0.528
$J_{FEM}^2\,(psi-in)$	0.133	0.261	0.540
$J_{Calc}^2\,(psi-in)$	0.117	0.245	0.547
% Diff^1	0.30	0.34	1.12
% Diff^2	6.29	3.14	0.66

K – Stress Intensity Factor

Superscript – Crack Number

Subscript – Opening (I) or Shear Mode (II)

J – J-Integral

Superscript – Crack Number

Subscript – Finite Element Analysis (FEM)

Local Collocation (Calc)

Model Number (A.B)

A – Crack Separation Case

(1: 0.5 in; 2: 0.75 in; …..N: max value)

B – Crack Length Ratio Case

(1: a2/a1 = 0.50; 2: a2/a1 = 0.75; 3: a2/a1 = 1.0)

% Diff – Percent Difference Between J_{FEM} and J_{CALC} Values

Superscript – Crack Number

Table 5.7 - Results of Numerical Model 7

Model	7.1	7.2	7.3
$K_I^1\,(psi-in^{1/2})$	4168	4032	3992
$K_I^2\,(psi-in^{1/2})$	1917	2630	4077
$K_{II}^1\,(psi-in^{1/2})$	197	108	79
$K_{II}^2\,(psi-in^{1/2})$	-214	-488	-180
$J_{FEM}^1\,(psi-in)$	0.545	0.544	0.543
$J_{Calc}^1\,(psi-in)$	0.580	0.542	0.532
$J_{FEM}^2\,(psi-in)$	0.139	0.266	0.543
$J_{Calc}^2\,(psi-in)$	0.124	0.238	0.555
% Diff[1]	3.17	0.11	1.04
% Diff[2]	5.61	5.48	1.13

K – Stress Intensity Factor

Superscript – Crack Number

Subscript – Opening (I) or Shear Mode (II)

J – J-Integral

Superscript – Crack Number

Subscript – Finite Element Analysis (FEM)

Local Collocation (Calc)

Model Number (A.B)

A – Crack Separation Case

(1: 0.5 in; 2: 0.75 in; …..N: max value)

B – Crack Length Ratio Case

(1: a2/a1 = 0.50; 2: a2/a1 = 0.75; 3: a2/a1 = 1.0)

% Diff – Percent Difference Between J_{FEM} and J_{CALC} Values

Superscript – Crack Numb er

The results from the previous tables are presented graphically in Figures 5.1 through 5.25. They are presented using three non-dimensionalized values so that greater understanding and application can be obtained from both the stress intensity factors and the J-Integral. The first non-dimensionalized value is a percent difference between the local collocation determined stress intensity factor and the simple crack in pure opening mode loading stress intensity factor. The second non-dimensionalized is the ratio of the local collocation determined opening mode stress intensity factor to the pure opening mode simple crack stress intensity factor. The last non-dimensionalized value is a ratio of the shear mode stress intensity factor to the opening mode stress intensity factor determined from local collocation. In the nondimensionalized figures two independent parameters are presented; the ratio of crack separation to the first crack's length (c/a_1), and the ratio of the second crack's length to the first crack's length (a_2/a_1).

Figure 5.1 presents the percent difference of the calculated opening mode stress intensity factor and the estimated open mode stress intensity factor versus the ratio of crack separation to fixed crack length (c/a_1). In Figure 5.2 the ratio of local collocation determined opening mode stress intensity factors to a simple crack in pure opening mode versus ratio of crack separation to fixed crack length is presented. Figure 5.3 shows the ratio of shear mode stress intensity factor to the calculated open mode stress intensity factor versus the ratio of crack separation to fixed crack length. Figures 5.4 and 5.5 show the percent difference of the mixed mode determined J-Integral and the pure open mode determined J-Integral for both calculated and finite element determined values for each crack. Including the finite element determined J-Integral values in the figures was used to check the accuracy of the calculated values.

As expected at a certain crack separation distance analyzing the two interacting parallel edge cracks as two individual simple cracks will not create a significant error in the results as first seen in Figure 5.1 where the percent difference of the stress intensity factors from the local collocation method and the simple crack in pure opening mode. The percent difference value for all the crack length ratios becomes increasing small as the crack separation distance is increased. At a crack separation ratio of 1.5 the percent

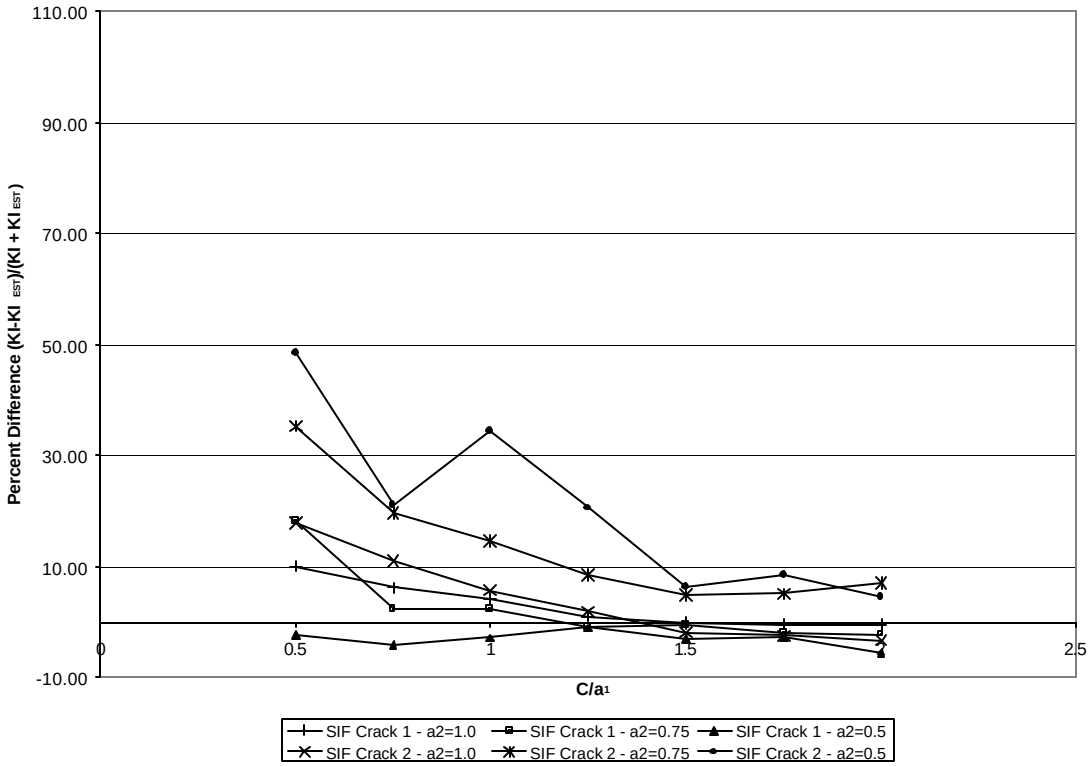

Figure 5.1 - Open Mode Stress Intensity Factor Percent Difference vs. Ratio of Crack Separation to Crack 1

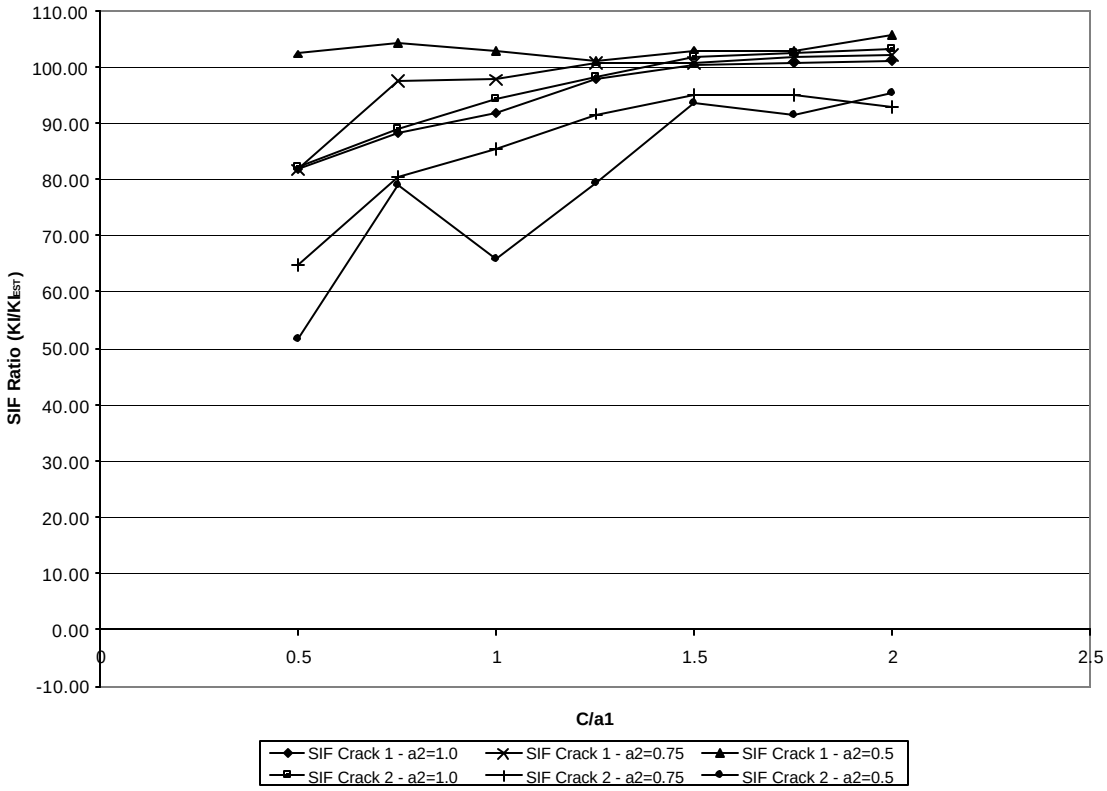

Figure 5.2 – Open Mode Stress Intensity Factor Ratio vs. the Ratio of Crack Separation to Crack 1

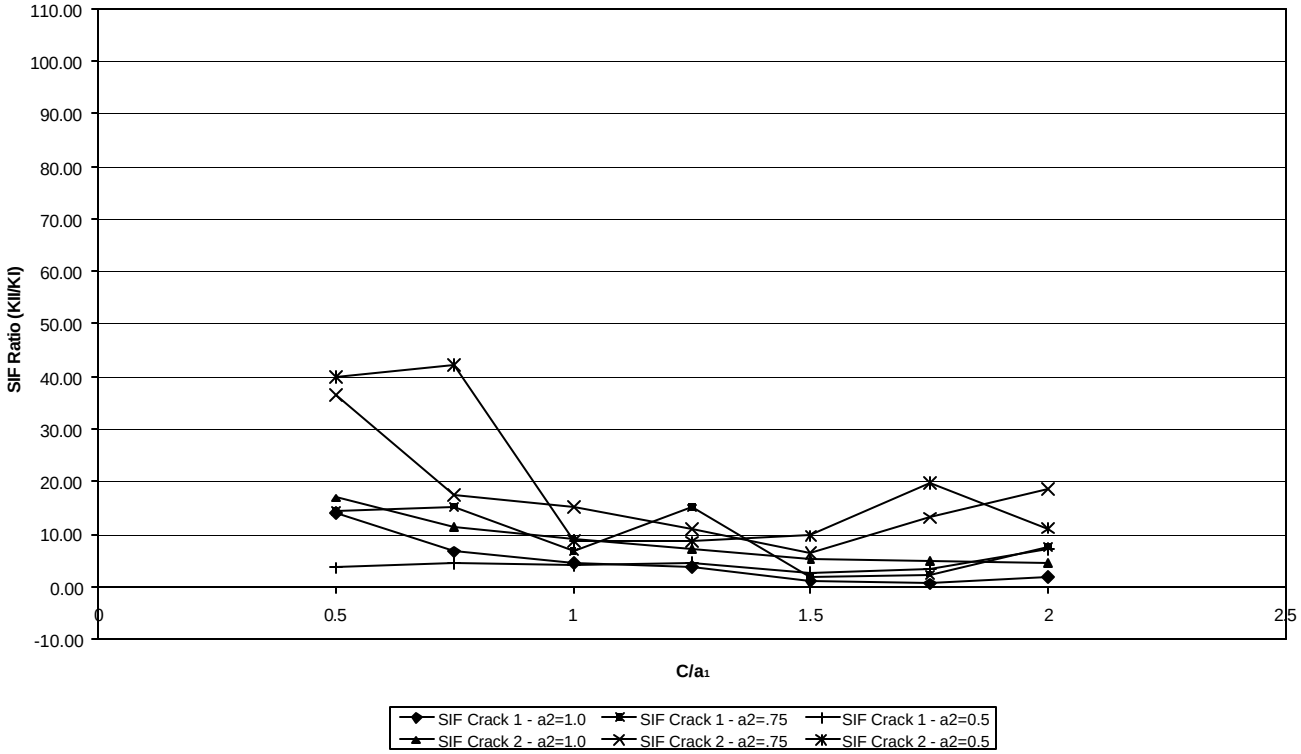

Figure 5.3 - Shear Mode Stress Intensity Factor Ratio vs. the Ratio of Crack Separation to Crack 1

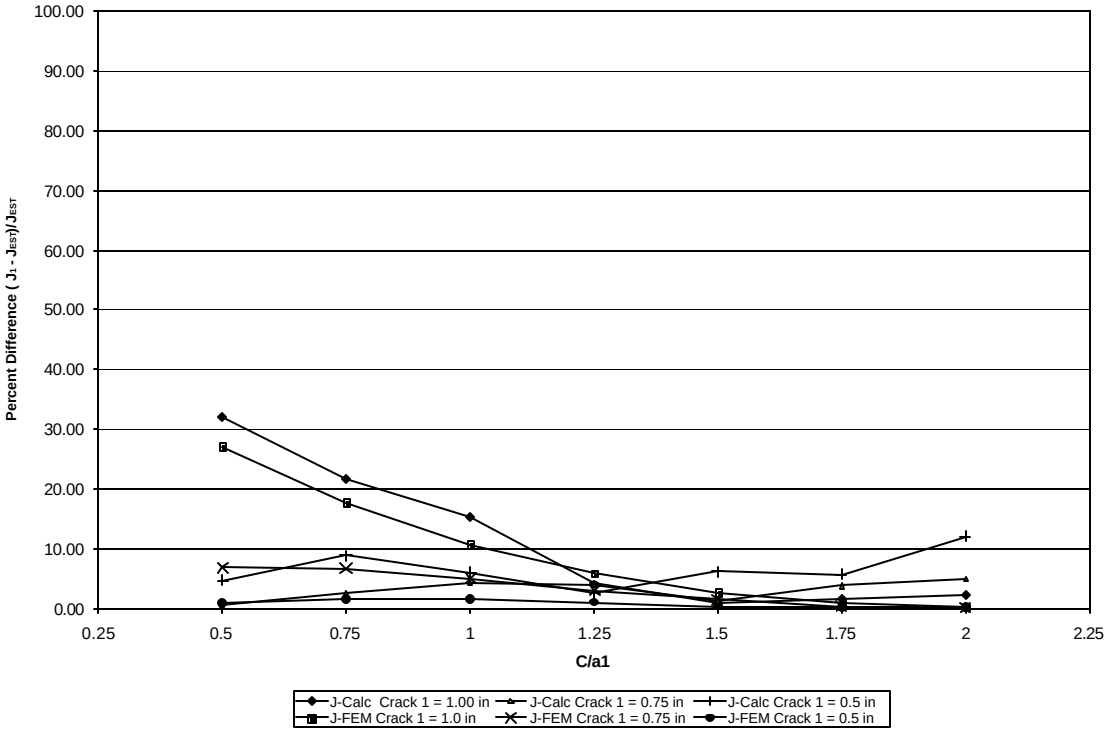

Figure 5.4 – J-Integral Percent Difference vs. Ratio of Crack Separation for Crack 1

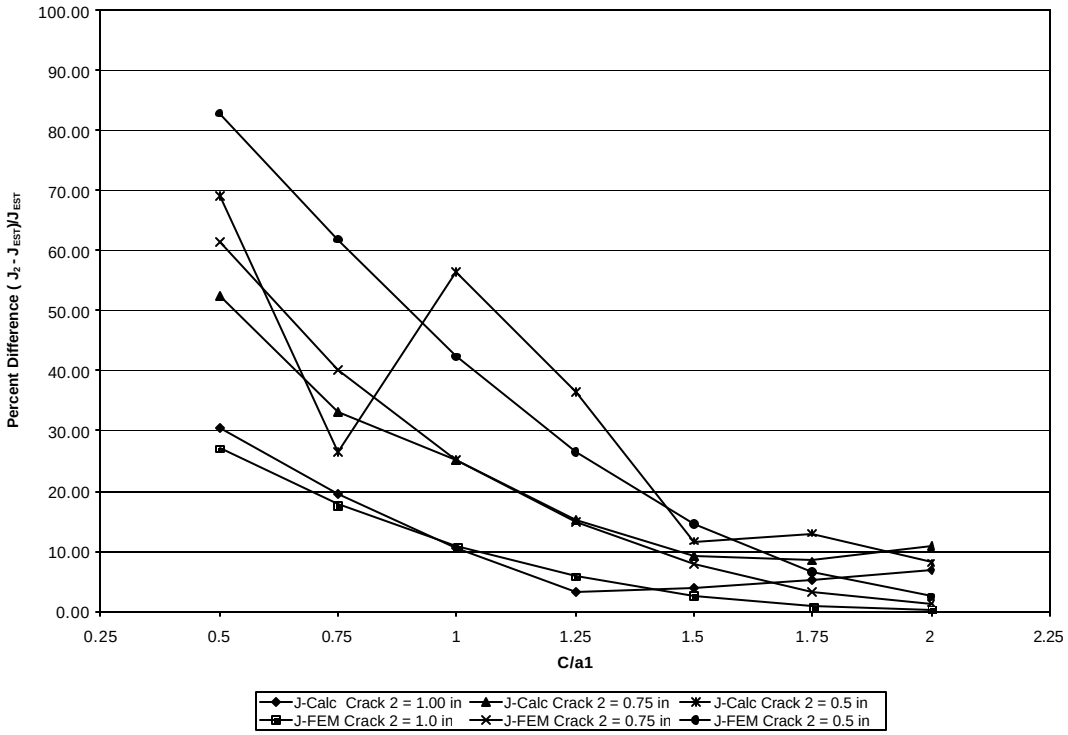

Figure 5.5 – J-Integral Percent Difference vs. Ratio of Crack Separation for Crack 2

difference for all the crack length ratios becomes less than 10 percent. This means that the value obtained through the simple crack analysis to obtain stress intensity factors when used on cracks that have a separation ratio of 1.5 or greater will have an acceptably low error value. A result seen in all the crack separation ratio figures is a slight increase in percent difference and stress intensity factor ratio at the largest crack separation ratio. This is thought to be caused be the closeness of the cracks to the loading points in the member, which would cause an increase in the shear stress in the stress field. In the figure the percent difference values of the first crack are all low compared to the values for the second crack except for the symmetrical case. This is expected where the second cracks length is reduced the first crack has the dominant stress field and would be decreasingly influenced by the second crack, as the crack separation was increase. The same trend can be seen in Figure 5.2 with the shear mode ratio values. The stress intensity factor ratio for the second crack is low in comparison with that of the first crack. In both Figure 5.1 and 5.2 all values start to converge as the crack separation ratios increase. As the local collocation determined stress intensity factor more closely equal to the simple crack stress intensity factor the stress intensity factor ratio presented in Figure 5.2 will become increasing close to 1.

Conclusions for the shear mode values presented in Figure 5.3 are not quite as obvious as in the opening mode. Both figures have the same trends even though the ratios are being compared to different independent variables. The stress intensity factor ratios for the first crack are always less than 20 percent meaning that the first crack is always in a predominantly opening mode stress. This value becomes close to zero signaling the lack of influence of shear mode in the stress field around the first crack. The results for the second crack are very much different than that of the first crack. The stress intensity factor ratio for the second crack starts out high and as the crack separation ratios increase the stress intensity factor ratios decrease. The ratios increase slightly at the highest crack separation because of the closeness of the cracks to the loading points on the member. From the tables it can be seen that the opening mode stress intensity values for the second cracks of 0.5 inch and 0.75 inch length are very

small therefore any increase in the shear mode stress intensity factor will increase the stress intensity factor ratios substantially.

Using J-Integral values from equation 3.12, ABAQUS, and a simple crack in pure open mode the percent differences are show in Figure 5.5 and 5.6. In Figure 5.5 the percent difference is that of the J-Integral value using equation 3.12 and the J-Integral value from the simple crack in pure opening mode as well as the J-Integral values obtained from using ABAQUS and the J-Integral value from the simple crack in pure opening mode are shown. The same trends can be seen in Figure 5.5 and 5.6 that were seen in Figure 5.1 this is because the open mode stress intensity factors are much larger than that of the shear stress intensity factors therefore the opening mode stress intensity factor is the driving value in equation 3.12. This again shows that as the crack separation ratio increases the difference between the local collocation determined values and the simple crack in pure opening mode values becomes very small.

The second independent variable explored in this research was the ratio of second crack's length to the first crack's length (a_2/a_1) seen in Figures 5.6 through 5.26. Three graphs are presented for each crack separation are Opening Mode Percent Difference, Shear Mode Ratio, and J-Integral Percent Difference.

For the first test case of .5-inch separation the open mode stress intensity percent difference demonstrates the influence the cracks have on one another can be seen. In Figure 5.6 the percent difference between the local collocation opening mode stress intensity factor and the simple crack in pure bending stress intensity factor is small when the second crack is .5 inches. This shows how little influence the second crack has on the first crack when the second crack is small in comparison. The opening mode percent difference then increases, as the length of the second crack is made larger. The opposite is true for the second crack as the ratio of crack lengths is increased the percent difference between the local collocation opening mode stress intensity factor and the simple crack in pure bending stress intensity factor becomes smaller. The same trends see in Figure 5.6 are produced in Figure 5.9 with the shear mode stress intensity factors. In Figure 5.8 the J-Integral percent difference for the local collocation and finite element

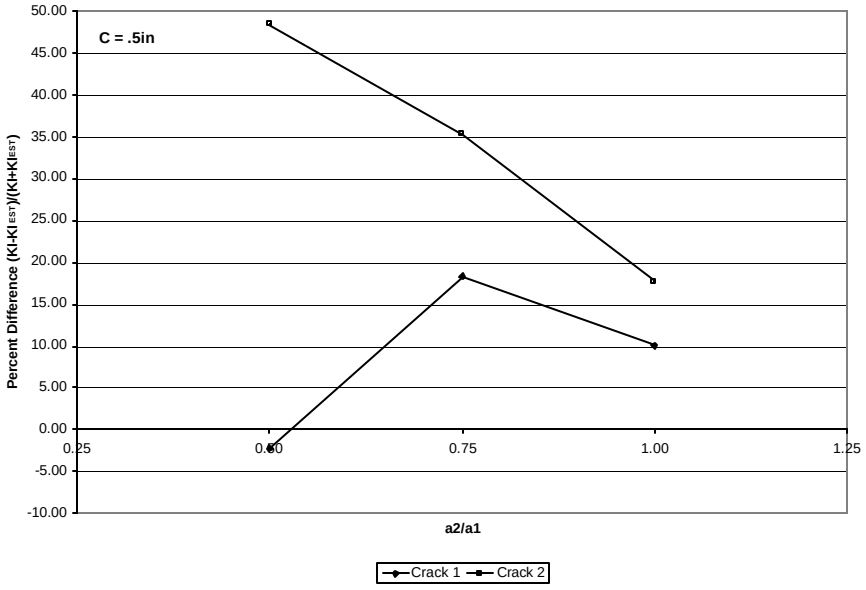

Figure 5.6 - Open Mode Stress Intensity Factor Percent Difference vs. Ratio of Crack Lengths for Numeric Model 1

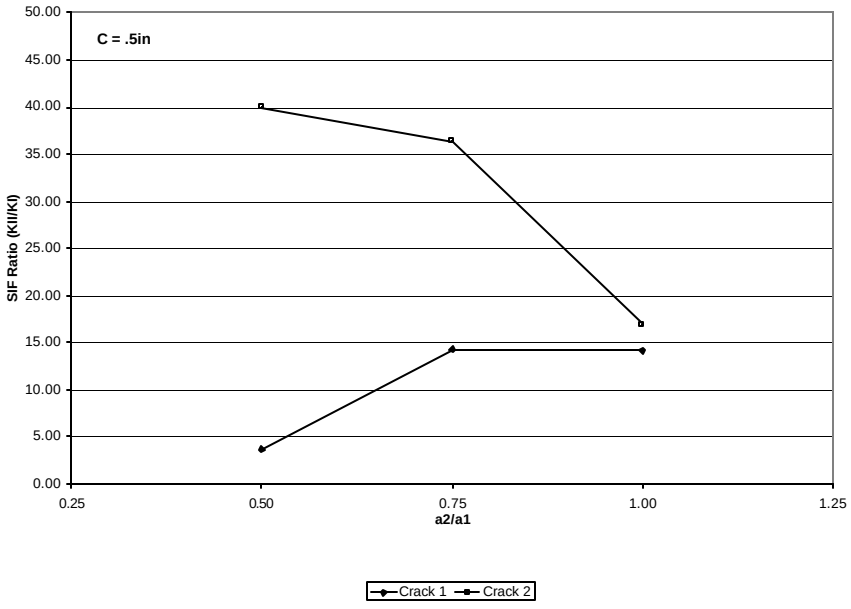

Figure 5.7 - Shear Mode Stress Intensity Factor Percent Difference vs. Ratio of Crack Lengths for Numeric Model 1

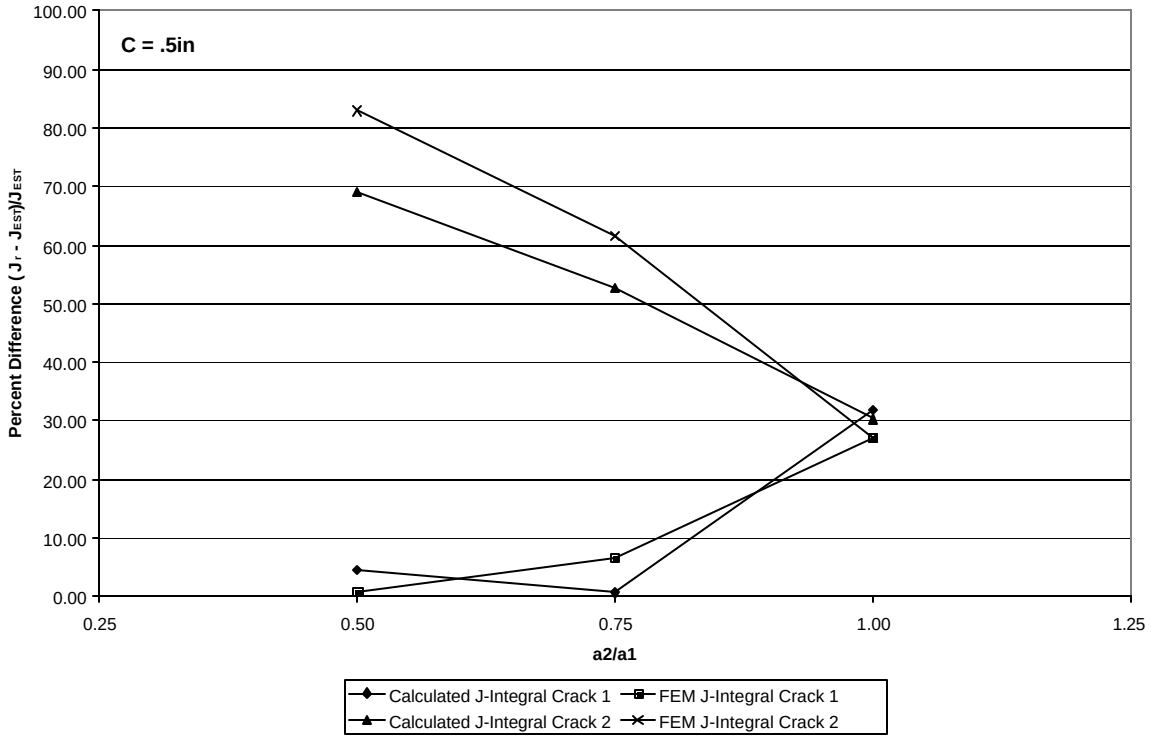

Figure 5.8 - J - Integral Percent Difference vs. Ratio of Crack Lengths for Numeric Model 1

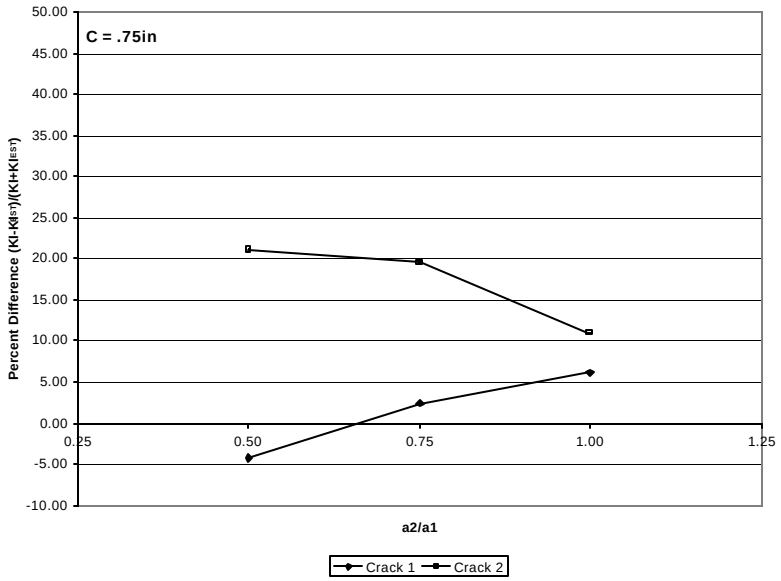

Figure 5.9 - Open Mode Stress Intensity Factor Percent Difference vs. Ratio of Crack Lengths for Numeric Model 2

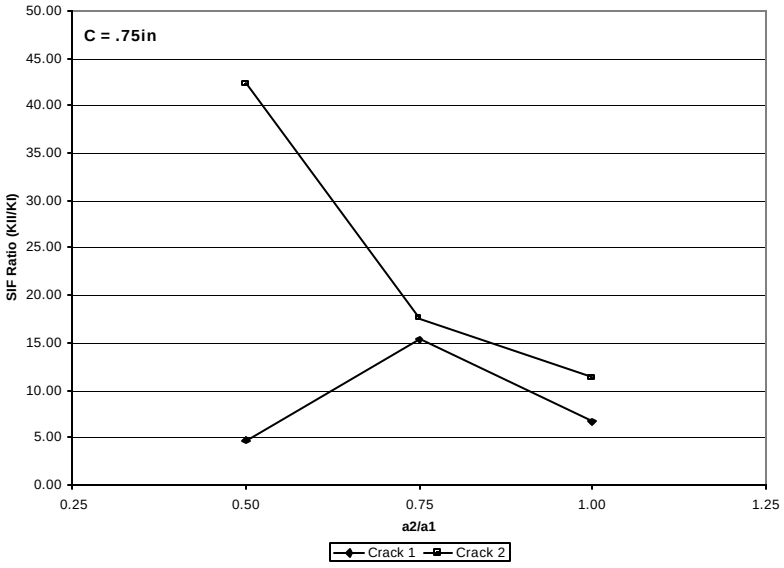

Figure 5.10 - Shear Mode Stress Intensity Factor Percent Difference vs. Ratio of Crack Lengths for Numeric Model 2

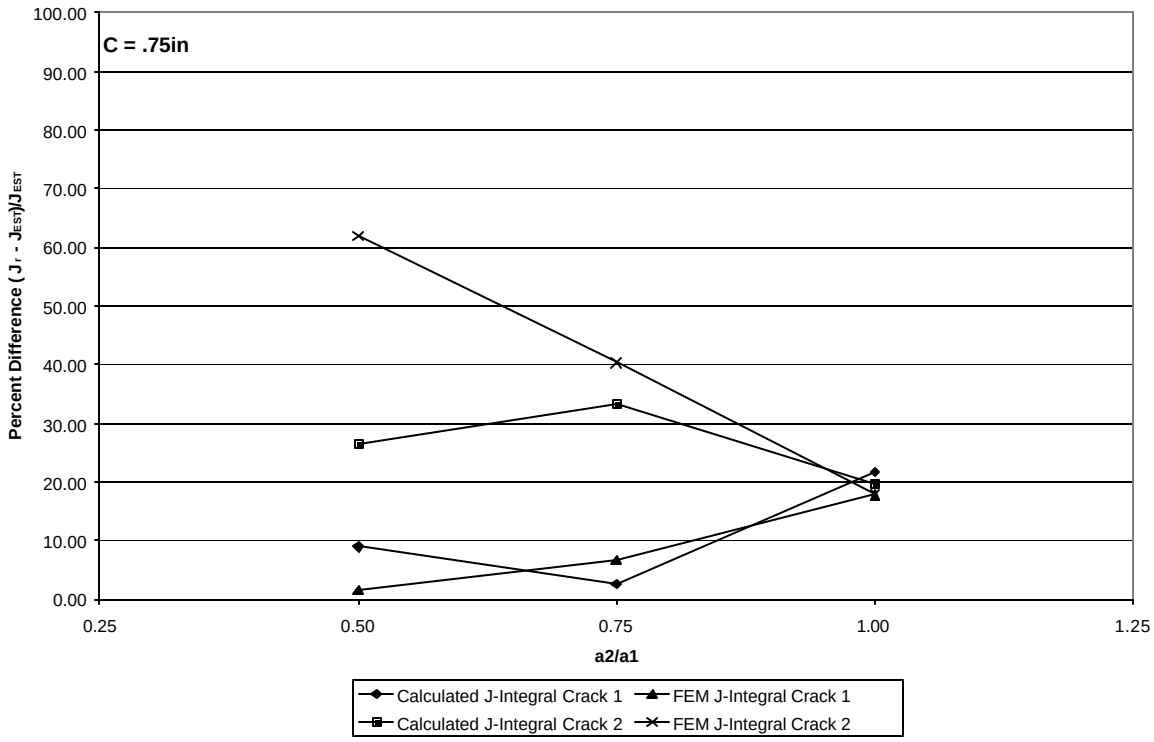

Figure 5.11 - J - Integral Percent Difference vs. Ratio of Crack Lengths for Numeric Model 2

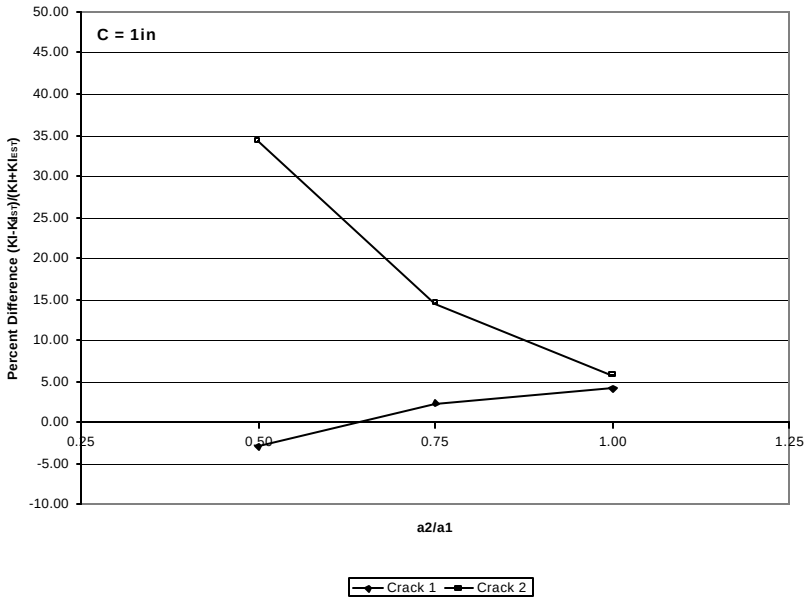

Figure 5.12 - Open Mode Stress Intensity Factor Percent Difference vs. Ratio of Crack Lengths for Numeric Model 3

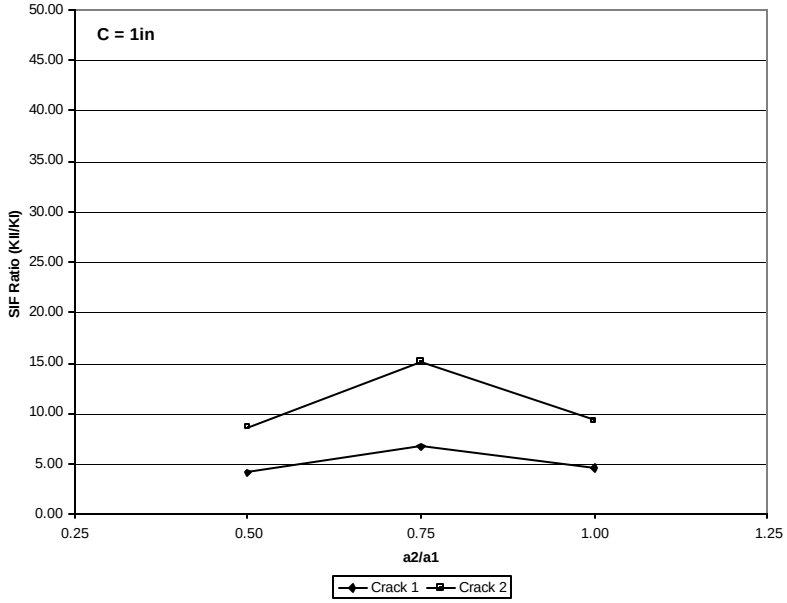

Figure 5.13 – Shear Mode Stress Intensity Factor Percent Difference vs. Ratio of Crack Lengths for Numeric Model 3

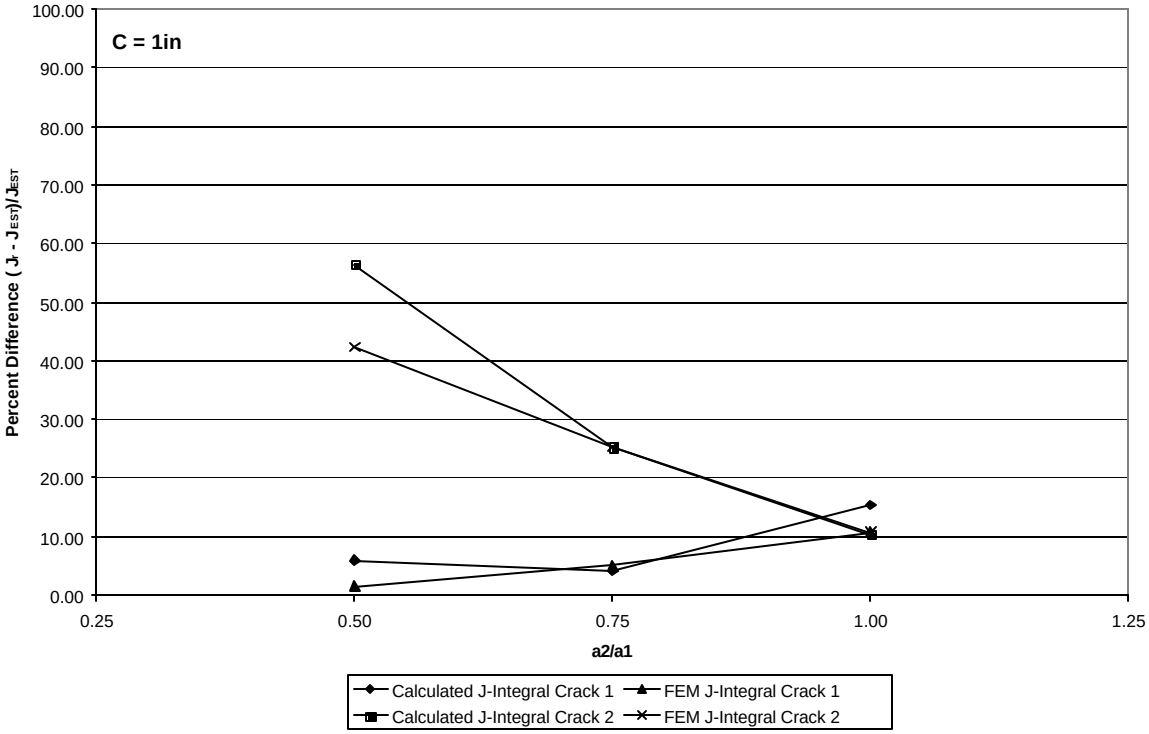

Figure 5.14 - J - Integral Percent Difference vs. Ratio of Crack Lengths for Numeric Model 3

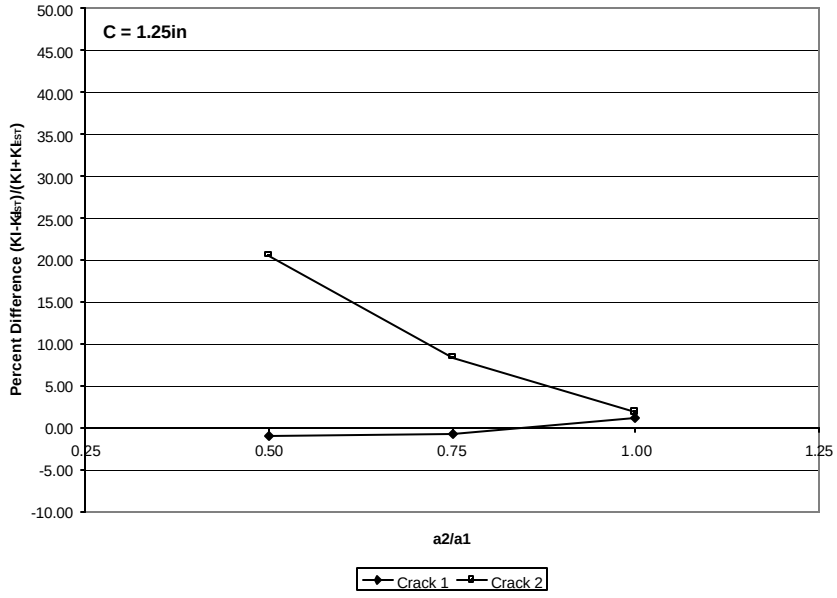

Figure 5.15 - Open Mode Stress Intensity Factor Percent Difference vs. Ratio of Crack Lengths for Numeric Model 4

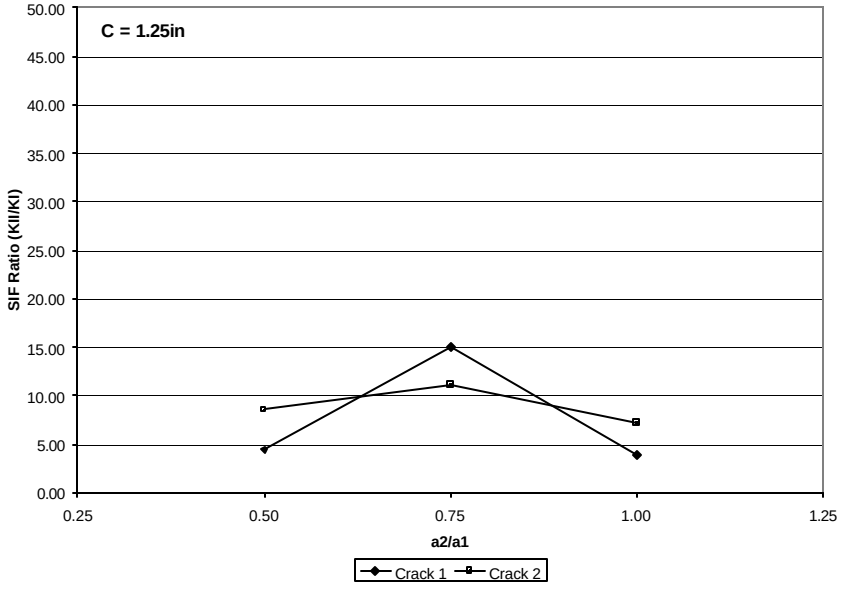

Figure 5.16 - Shear Mode Stress Intensity Factor Percent Difference vs. Ratio of Crack Lengths for Numeric Model 4

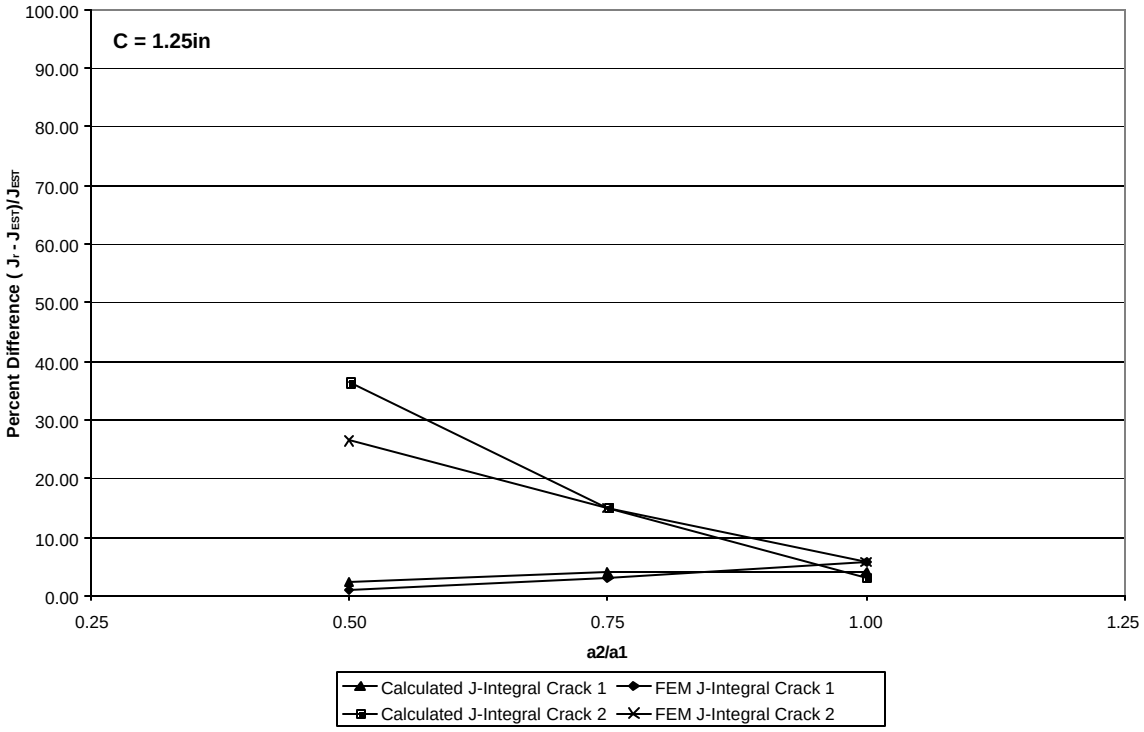

Figure 5.17 - J - Integral Percent Difference vs. Ratio of Crack Lengths for Numeric Model 4

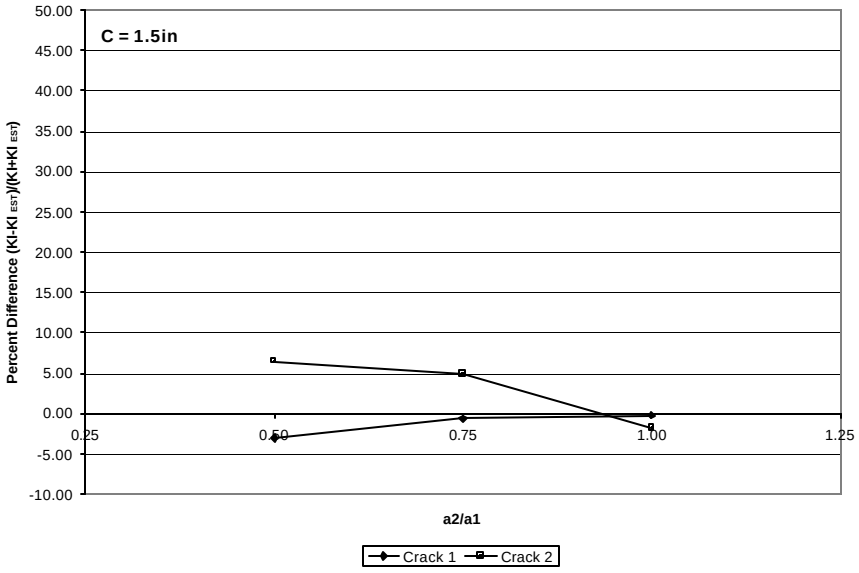

Figure 5.18 - Open Mode Stress Intensity Factor Percent Difference vs. Ratio of Crack Lengths for Numeric Model 5

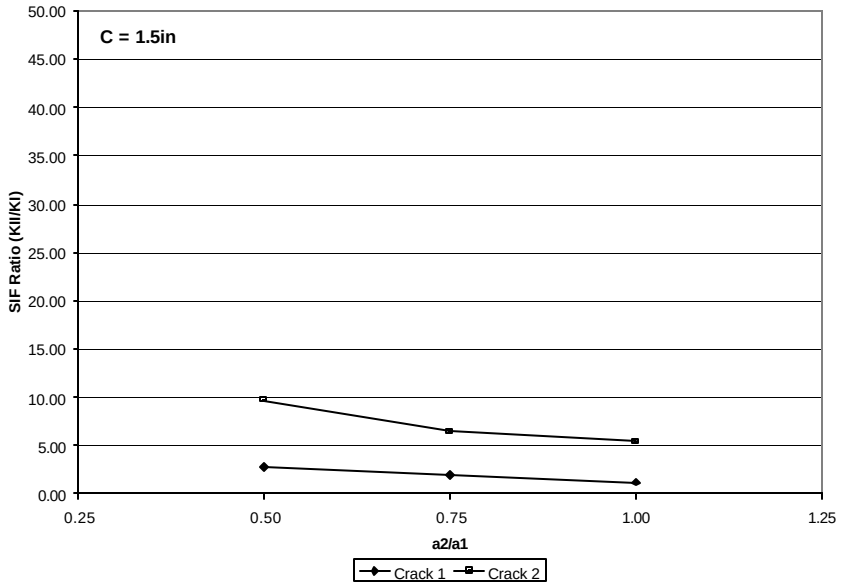

Figure 5.19 - Shear Mode Stress Intensity Factor Percent Difference vs. Ratio of Crack Lengths for Numeric Model 5

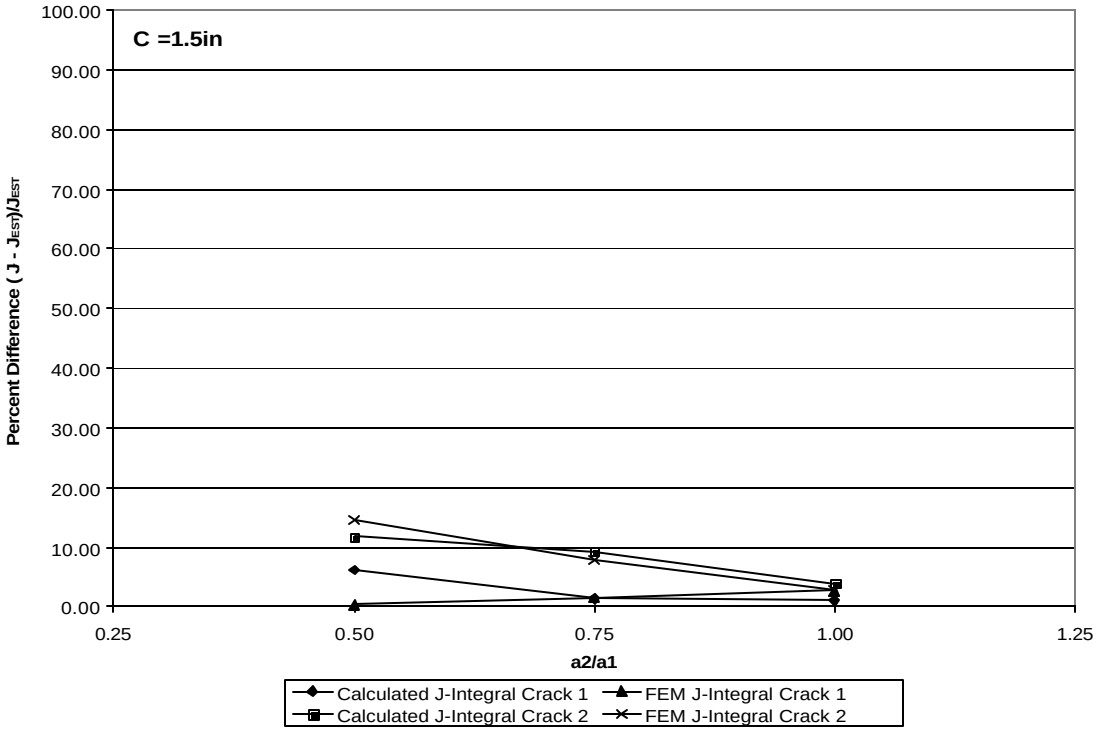

Figure 5.20 - J - Integral Percent Difference vs. Ratio of Crack Lengths for Numeric Model 5

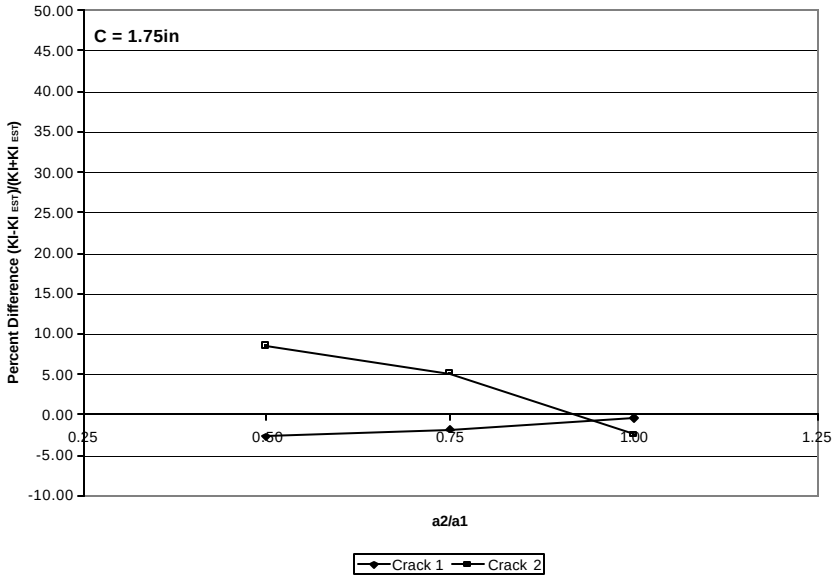

Figure 5.21 - Open Mode Stress Intensity Factor Percent Difference vs. Ratio of Crack Lengths for Numeric Model 6

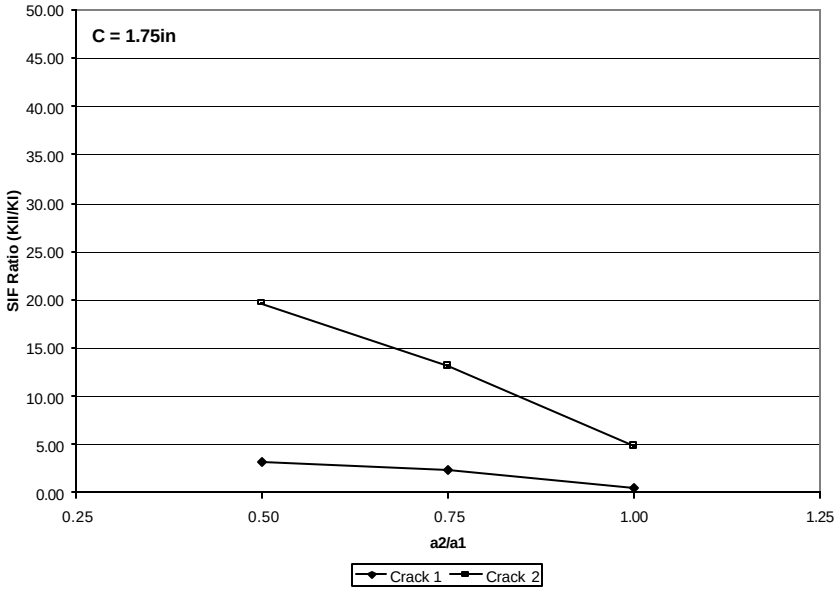

Figure 5.22 - Shear Mode Stress Intensity Factor Percent Difference vs. Ratio of Crack Lengths for Numeric Model 6

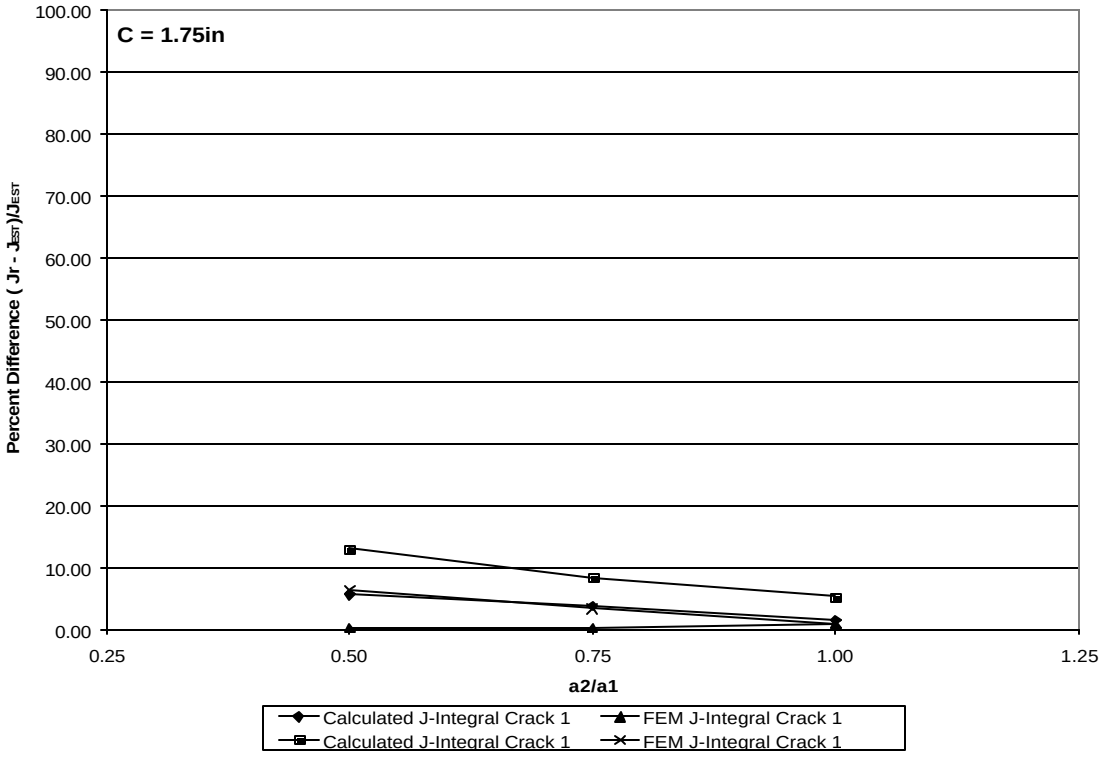

Figure 5.23 - J - Integral Percent Difference vs. Ratio of Crack Lengths for Numeric Model 6

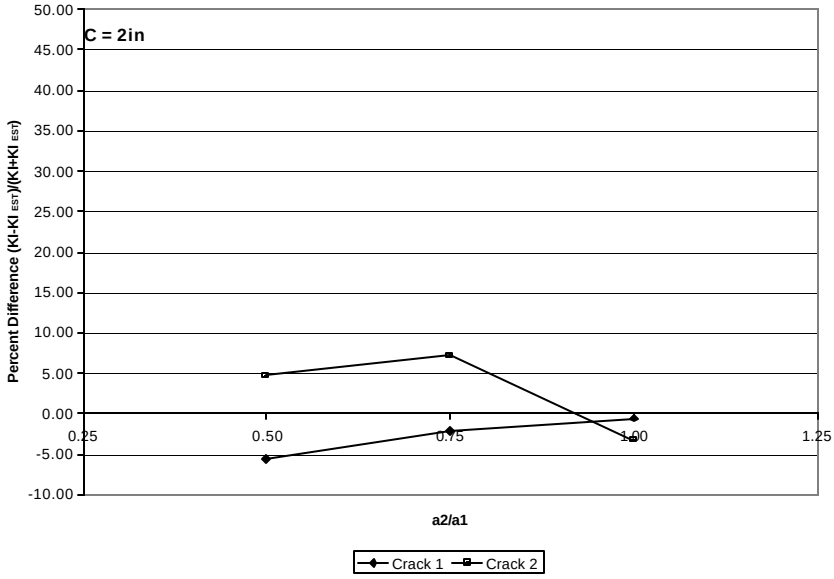

Figure 5.24 - Open Mode Stress Intensity Factor Percent Difference vs. Ratio of Crack Lengths for Numeric Model 7

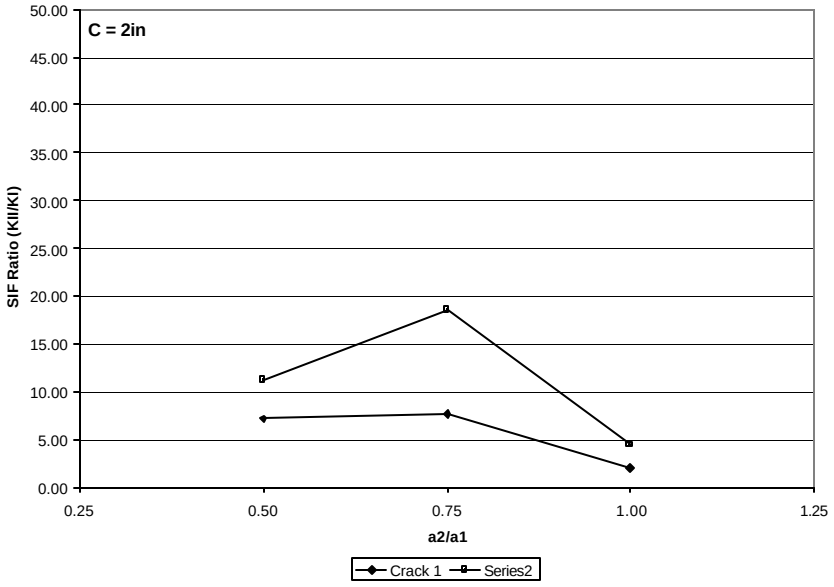

Figure 5.25 - Shear Mode Stress Intensity Factor Percent Difference vs. Ratio of Crack Lengths for Numeric Model 7

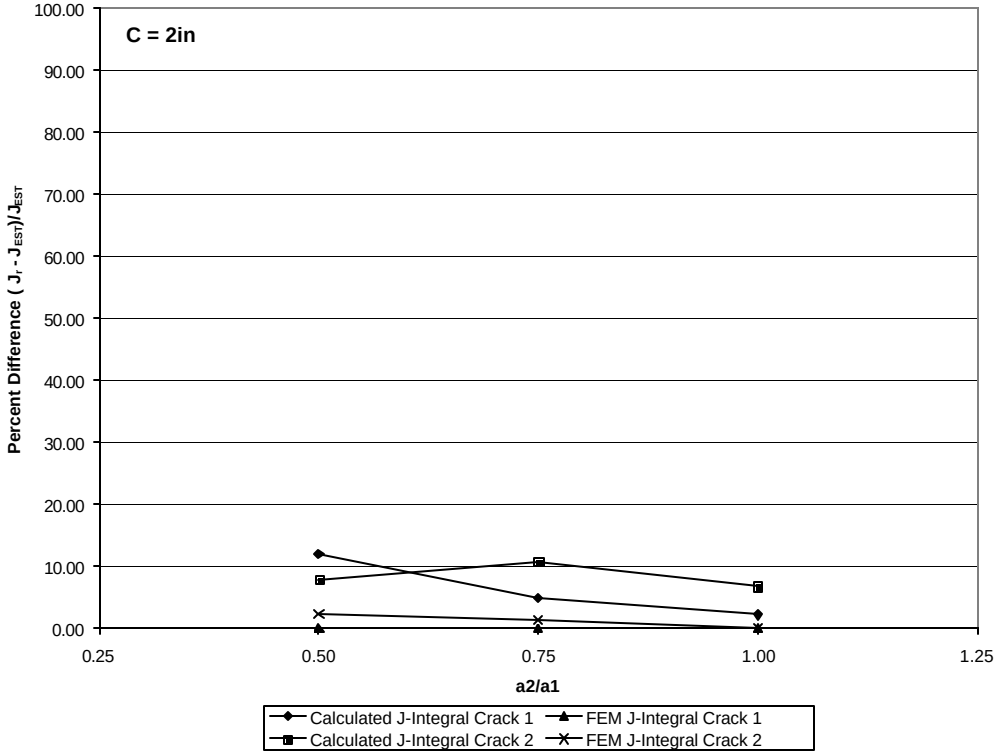

Figure 5.26 - J - Integral Percent Difference vs. Ratio of Crack Lengths for Numeric Model 7

analysis determined values are presented. It is expected that the driving value in equation 3.12 used to calculate the value for the local collocation method was the opening mode stress intensity factor. For this reason Figure 5.7 follows the trends presented in Figure 5.6. The J-Integral from the finite element analysis was included in the figure as another method to check the accuracy of the results obtained through the local collocation method. For the numerical model of .75 inch in plane crack separation, Figures 5.9, 5.10, and 5.11, the values approximately the same as the values presented in figures for .5-inch separation. In model 3 for the 1-inch separation two things are noticeable about the stress intensity factor figures. First there is a large decrease in the percent difference of the second crack as the crack length ratio increases. Second the percent difference values for the first crack stabilized and don't change for the different crack length ratios. The ratio of shear mode stress intensity factor to the opening mode stress intensity factor became less than .15. This shows the start of the decreasing influence that the shear stress has on the overall stress field. Very little difference between Model 3 and Model 4 for the 1.25-inch separation is apparent. The same trends are evident with a slight overall reduction in the all the percent difference values. Model 5, however, shows a more constant percent difference value over the range of crack length ratios for the opening and the shear mode stress intensity factors as well as the J-Integral values. The percent difference values for both cracks in Figure 5.18 show that the local collocation stress intensity values are within 5 percent of the simple crack in pure opening mode stress intensity factor. In Figure 5.19 both cracks shear mode stress intensity factor to opening mode stress intensity factor ratios show how little the shear mode influences the overall stress field at a 1.5 inch in plane crack separation. This follows the conclusions made from the separation ratio figures that after a certain separation distance the cracks have little influence on each other's stress fields. There is a slight increase in shear mode stress intensity factor ratio and percent difference in numerical models 6 and 7. This can be explained by the closeness of the cracks to the load points in the model as well as having to extract data from a more coarse mesh. If the distance from the point loads was increased and the mesh made finer the values would decrease in model 7. The opening

mode percent difference values maintain the same trends as model 5 at a very small almost constant percent difference over the crack length ratios.

CHAPTER VI
CONCLUSIONS AND RECOMMENDATIONS

The primary goal of this research was to determine if and when two parallel edge cracks in a finite geometry can be analyzed as individual cracks. This goal was achieved. Using the combined Westergaard-Schwarz approach models of varying crack length ratio and crack plane separation was studied for the case of two parallel edge cracks. The studied revealed that at a separation of 1.5 inches for all crack length ratios could be analyzed as single cracks in pure bending while introducing very little error into the analysis.

It is recommended that further study into increasing separation ratio and non-parallel cracks to determine if a pure open mode stress field could ever be achieved. It is expected from trends presented in this research that the shear mode stress intensity factor eventually would become very close to zero. Also it is recommended that photoelastic experimentation be conducted so a direct comparison between numerical and experimental results could be conducted for the larger separation ratios. Lastly an investigation in the singularity-dominated zone[3] in a multi-crack model is recommended. The developing of a singularity dominated zone criteria for parallel edge cracks would complete the development of a stress field analysis method for analyzing cases with two parallel edge cracks.

In summary, following conclusion can be drawn based on the results gathered in this study

- All the crack length ratio values greater than a crack length separation ratio(c/a_1) of 1.5 can be analyzed as two individual cracks in pure bending while only introducing a small amount error to the stress field values.
- In separations less than 1.5 the crack length ratio has a substantial effect on the behavior of the stress field values.

.

REFERENCES

1. *Hardin, P., "The Stress Field Around Two Parallel Edge Cracks in a Finite Body," M.S. thesis, Texas A&M University (1993).*

2. *Chona, R, "Non-Singular Stress Effects in Fracture Test Specimens a Photoelastic Study," M.S. thesis, Department of Mechanical Engineering, University of Maryland, College Park (1985).*

3. *Chona, R, "The Stress Field Surrounding the Tip of a Crack Propagating in a Finite Body", Ph.D. dissertation, Department of Mechanical Engineering, University of Maryland, College Park (1987).*

4. *Tada, H., Paris, P. C., and Irwin, G. R, The Stress Analysis of Cracks Handbook, Research Corporation, Hellertown, Pennsylvania (1985).*

5. *Irwin, G.R.,"Discussion of: The Dynamic Stress Distribution Surrounding a Running Crack – A Photoelastic Analysis," S.E.S.A Proceedings,* XVI *(1), 93-96 (1958).*

6. *Freese, C.E., "Periodic Edge Cracks of Unequal Length in a Semi-Infinite Tensile Sheet", International Journal of Fracture Mechanics,* 12 *(1), 125-134 (1976).*

7. *Ukadgaonker V.G. and NAIK, A.P.," Interaction effect of two arbitrarily oriented cracks – Part I", International Journal of Fracture Mechanics, 51, 219-230 (1991).*

8. *Keener, T, "The Displacement Field Characterization of Two Interacting Parallel Edge Cracks in a Finite Body", M.S. thesis, Department of Mechanical Engineering, Texas A&M University (1996).*

9. *Sanford, R.J., "A Critical Re-examination of the Westergaard Method for Solving Opening-Mode Crack Problems," Mechanics Research Communications,* 6*, pp 289-294 (1979).*

10. *Sanford, R. J., and Berger, J. R., "The Numerical Solution of Opening Mode Finite Body Fracture Problems Using Generalized Westergaard Functions," Engineering Fracture Mechanics,* 37*, pp. 461-471 (1990).*

11. *Westergaard, H.M., "Bearing Pressures and Cracks," Journal of Applied Mechanics, Transactions ASME,* 61*, pp. A49-A53 (1939).*

12. *Moran, I., Parallel Interacting Edge Cracks Under Pure Bending, M.S. thesis, Department of Mechanical Engineering, Texas A&M University (1991).*

APPENDIX A
FORTRAN PROGRAMS

The FORTRAN programs during this study are presented here. The programs are modifications of programs presented in Appendix E of Reference 1. Specifics on the programs can be viewed in the comments section of the program.

```
      Program DCIANDIISYM
      CHARACTER*66 PD,YD,ZD
      REAL K5,K6,K7,K9,K10,Z(2000,3),A(32,1),B(32,1),C(2000,32),
     +D(32,32),F(32,1),CT(32,2000),DI(32,32),G(2000,1),H(32,1),
     +M1(40,5),PI,N1,N3,N4,N7,N8,E1,E2,E3,DD,TT,PDD,PTT,
     +TEMP(50),K12,K11
      INTEGER K1,K2,K3,K4,K8,I,J,K,L,L1,I1,I2,I3,I4,I7,I8,I9
      PD='*=========================================================*'
      YD='  ITER. NO.      ERROR     DELTA N (FRGS)       DELTA N (PCT)'


* Progam to compute up to an eight parameter (32 Coefficient) Model
* and output the coefficients of the series solution to the program
* uses the Newton-Raphson Non-linear least squares up to 2000 data
* points may be specified and should be entered in File Named 'DATB'


            Call Zero2(Z,2000,3)
            PI=3.141592654

* Read in parameters from input files
            Open (Unit=12, File='DAT', Status='old')
            Read (12,*) K1,K2,K3,K4,K8,K5,K6,K9,K12,K10,K7,K11
         Close (12)
            Open (Unit=12, File='DATA', Status='old')
            Read (12,100) ZD
            Close (12)

* Create and open output file
            Open (Unit=15, File='Output', Status='New')
            Write (15,100) ZD
            Write (15,*) 'Number of Data Points = ', K1
            Write (15,*) 'Lowest Order Model = ', K2
            Write (15,*) 'Highest Order Model = ', K3
            Write (15,*) 'Max. # of iterations within each model = ', K4
```

```
      Write (15,*) 'Number of divisions along crack faces = ', K8
      Write (15,*) 'Material Fringe Constant = ', K5
      Write (15,*) 'Model Thickness = ', K6
      Write (15,*) 'First Crack Length = ', K9
      Write (15,*) 'Second Crack Length = ', K12
      Write (15,*) 'Crack Seperation = ',K10
      Write (15,*) 'Initial Estimate of K-I-1 = ',K7
      Write (15,*) 'Initial Estimate of K-I-2 = ',K11

*   Make inital guess

      Call ZERO1(Temp, 50)
      Call ZERO2(A,32,1)
      A(1,1)=K7*K6/K5/SQRT(2*PI)
       Do 1, I5=1,32
        TEMP(I5)=A(I5,1)
1      Continue


* Loop once for each order model solution

      Do 7, I=K2,K3
       Call First(PD,YD,ZD,K5,K6,K7,K9,K10,Z,A,B,C,D,F,CT,
     +DI,G,H,M1,PI,N1,N3,N4,N7,N8,E1,E2,E3,DD,TT,PDD,PTT,
     +K1,K4,K8,K12,I,J,L,L1,I1,I2,I3,I4,I7,I8,I9,TEMP,K3)
7     CONTINUE
      CLOSE (15)

100   Format(A66)
      END
* End of Main Program

      Subroutine First(PD,YD,ZD,K5,K6,K7,K9,K10,Z,A,B,C,D,F,CT,
     +DI,G,H,M1,PI,N1,N3,N4,N7,N8,E1,E2,E3,DD,TT,PDD,PTT,
     +K1,K4,K8,K12,I,J,L,L1,I1,I2,I3,I4,I7,I8,I9,TEMP,K3)
```

```
      Character*66 PD,YD,ZD
      Integer K1,K2,K3,K4,K8,I,J,J1,L,L1,I1,I2,I3,I4,I7,I8,I9
      Real K5,K6,K7,K9,K10,PI,N1,N3,N4,N7,N8,E1,E2,E3,DD,TT,
     +PDD,PTT,K12
      Real Z(K1,3),A(I*2-1,1),B(I*2-1,1),C(K1,I*2-1),
     +D(I*2-1,I*2-1),F(I*2-1,1),CT(I*2-1,K1),DI(I*2-1,I*2-1),
     +G(K1,1),H(I*2-1,1),TEMP(50),M1(40,5)

      Do 1, I5=1,32
    A(I5,1)=TEMP(I5)
1     Continue
      Call ZERO1(TEMP,50)
      Open (Unit=12,File='DATB',Status='old')
      Do 3 I111=1,K1
      Read (12,*) Z(I111,1),Z(I111,2),Z(I111,3)
3     Continue
      Close(12)

* Average Fringe Order Calculation
      N1=0.0
      Do 5, L2=1,K1
            N1=N1+Z(L2,3)
5     Continue
      N8=N1/K1


      Write (15,*) PD
      Write (15,*) I, 'Parameter Model -- Parallel Edge Crack Solution'
      Write (15,*) ' ', ZD
      Write (15,*) PD
      Write (15,*)

      Write (15,*) ' Average Input Fringe Order = ',N8
      Write (15,*)
      Write (15,*) YD
```

```
* Loop for number iterations allowed within each model

          Call ZERO2(M1,40,5)
          Do 300, I1=1,K4
        Call ZERO2(C,K1,I*2-1)
           Call ZERO2(CT,I*2-1,K1)
           Call ZERO2(DI,I*2-1,I*2-1)
           Call ZERO2(D,I*2-1,I*2-1)
           Call ZERO2(F,I*2-1,1)
           Call ZERO2(G,K1,1)
           Call ZERO2(H,I*2-1,1)

          E1=0.0
          N3=0.0

                  Do 100, L=1,K1
                    Call DNT(DD,TT,Z(L,1),Z(L,2),K10,K9,A,I,K8,K12)
                    G(L,1)=((Z(L,3)/2)**2-(DD**2)-(TT**2))
                      E1=E1+G(L,1)**2
         N4=2*SQRT(DD**2+TT**2)
                      N3=N3+ABS(Z(L,3)-N4)
          Do 20, L1=1,I*2-1
           Call ZERO2(B,I*2-1,1)
           B(L1,1)=1.0
                  Call DNT(PDD,PTT,Z(L,1),Z(L,2),K10,K9,B,I,K8,K12)
                  C(L,L1)=2*DD*PDD+2*TT*PTT
20          Continue
100               Continue

          N7=N3/K1
          Call TRNSPS(CT,I*2-1,K1,C)
          Call MATMUL(CT,C,D,I*2-1,K1,K1,I*2-1)
          Call INVERSE(DI,I*2-1,D)
          Call MATMUL(CT,G,F,I*2-1,K1,K1,1)
```

```
          Call MATMUL(DI,F,H,I*2-1,I*2-1,I*2-1,1)
          Call ADD(A,I*2-1,1,A,I*2-1,1,H,I*2-1,1)

          M1(I1,1)=I1*1
          M1(I1,2)=E1
          M1(I1,3)=N7
          M1(I1,4)=N7/N8*100
     If (I1 .EQ. 1) Then
          Go To 300
     End If

*Check for error among increasing number of overall iterations

          E3=ABS(1-M1(I1,2)/M1(I1-2,2))
          If (E3 .LE. 0.002) Then
                    Go To 310
                    End If
300       Continue

310     If(I1 .GT. K4) I1=I1-1
          Do 320, I4=1,I1
        Write (15,350) M1(I4,1),M1(I4,2),M1(I4,3),M1(I4,4)
320       Continue
          Write (15,*)
          Write (15,*)
          ABC=0.0
       E5=K5/K6
          Do 330, I7=1,I
            I75=AINT(ABC)
            L=(-1)**I7
            If (I7 .EQ. 1) Then
              Write (15,360) I75,A(1,1)*E5,I9,A(1,1)/A(1,1),I75,
     +      A(2,1)*E5,I75,A(2,1)/A(1,1)
                    Else If (I7 .EQ. 2) Then
              Write (15,370) I75,A(3,1)*E5,I75,A(3,1)/A(1,1),I75,
```

```
     +      0.0,I75,0.0/A(1,1)
              Else
                    If (L .LE. 0) Then
               Write (15,360) I75,A(I7*2-2,1)*E5,I75,A(I7*2-2,1)/A(1,1),
     +      I75,A(I7*2-1,1)*E5,I75,A(I7*2-1,1)/A(1,1)
                    Else
               Write (15,370) I75,A(I7*2-2,1)*E5,I75,A(I7*2-2,1)/A(1,1),
     +      I75,A(I7*2-1,1)*E5,I75,A(I7*2-1,1)/A(1,1)
                    End If
               End If
               ABC=ABC+0.5
330          Continue

                    If(I .EQ. K3)THEN
             CALL PLOTFILE(K3,K5,K6,K8,K9,K10,K12,A,L,I)
                    ENDIF
        Do 345 I5=1,32
             TEMP(I5)=A(I5,1)
345          Continue
             Write (15,*)
             Write (15,*) PD




350    Format (4X,F3.0,6X,F12.3,5X,F7.4,8X,F8.4)
360    Format (1x,'A',I1,'-1 = ',F8.2,'   A',I1,'-1/AO-1 = ',
     +F7.3,5X,'C',I1,'-1 =', F8.2,'   C',I1,'-1/AO-1 = ',F7.3)
370    Format (1X,'B',I1,'-1 = ',F8.2,'   B',I1,'-1/AO-1 =',
     +F7.3,5X,'D',I1,'-1 =', F8.2,'   D',I1,'-1/AO-1 = ',F7.3)

             End
* End of First Subroutine
```

```
      SUBROUTINE PLOTFILE(K3,K5,K6,K8,K9,K10,K12,A,L,I)

       INTEGER P,L,I,K8,K3
       REAL K5,K6,K9,K10,K12,A(I*2-1,1)

       OPEN(UNIT=16,FILE='PLOTDATA',STATUS='NEW')
       WRITE (16,*) K5,K6
       WRITE (16,101) K8,K10,K9,K12
       WRITE (16,102) K3/2,K3/2
      E5=K5/K6
       DO 100,P=1,2
            WRITE(16,*) A(1,1)*E5,A(4,1)*E5,A(8,1)*E5,A(12,1)*E5,
     +A(16,1)*E5
            WRITE(16,*) A(2,1)*E5,A(5,1)*E5,A(9,1)*E5,A(13,1)*E5,
     +A(17,1)*E5
            WRITE(16,*) A(3,1)*E5,A(6,1)*E5,A(10,1)*E5,A(14,1)*E5,
     +A(18,1)*E5
            WRITE(16,*) A(20,1)*E5,A(7,1)*E5,A(11,1)*E5,A(15,1)*E5,
     +A(19,1)*E5
100   CONTINUE
      Close(16)

101   Format(I4,',',F6.3,',',F6.3,',',F6.3)
102   Format(I3,','I3)
      END

*END OF PLOTFILE CREATION SUBROUTINE


      Subroutine ZERO1(MAT,ROW)
       Integer I,ROW
       Real MAT(ROW)
       Do 10, I=1,ROW
         MAT(I)=0.0
10     Continue
```

```
      End

      Subroutine ZERO2(MAT,ROW,COL)
            Integer ROW,COL,I,J
            Real MAT(ROW,COL)
            Do 20, I=1,ROW
              Do 10, J=1,COL
               MAT(I,J)=0.0
10            Continue
20          Continue
      End

      Subroutine MATMUL(MAT1,MAT2,PROD,M,N,P,Q)
            Integer M,N,P,Q,I,J,K
            Real MAT1(M,N),MAT2(P,Q),PROD(M,Q),SUM
              If (N .EQ. P) Then
                    Do 330, I=1,M
                     Do 320, J=1,Q
                            SUM=0.0
                            Do 310, K=1,N
                              SUM=SUM+(MAT1(I,K)*MAT2(K,J))
310                         Continue
                            PROD(I,J)=SUM
320                   Continue
330                 Continue
              Else
         Stop 'Matrices are not Compatible for Multiplication'
              End If
      End

      Subroutine ADD(MAT1,ROW1,COL1,MAT2,ROW2,COL2,MAT3,ROW3,COL3)
        Integer ROW1,COL1,ROW2,COL2,ROW3,COL3,I,J
        Real MAT1(ROW1,COL1),MAT2(ROW2,COL2),MAT3(ROW3,COL3)
            Do 380, I=1,ROW1
             Do 370 J=1,COL1
```

```
                    MAT1(I,J)=MAT2(I,J)+MAT3(I,J)
370                 Continue
380                 Continue
          End

          Subroutine TRNSPS(MAT1,M,N,MAT2)
            Integer M,N,I,J
         Real MAT1(M,N),MAT2(N,M),TERM
                  Do 20, I=1,N
                    Do 10, J=1,M
                          TERM=MAT2(I,J)
                          MAT1(J,I)=TERM
10                  Continue
20                  Continue
          End

          Subroutine INVERSE(MAT1,N,MAT2)
            Integer N,I,J,K,L,PIVOT
            Real MAT1(N,N),MAT2(N,N),MULT,AUG(200,201),TEMP,X(200)
               Do 590, K=1,N
                    Do 510, I=1,N
                     Do 505, J=1,N
                          AUG(I,J)=MAT2(I,J)
505                  Continue
510                 Continue
                    Do 520, L=1,N
                      If(L .EQ. K) Then
                          AUG(L,N+1)=1
                      Else
                          AUG(L,N+1)=0
                      End If
520                 Continue

      Do 570, I=1,N
```

```
* Locate Nonzero Diagonal Entry

            If (AUG(I,I) .EQ. 0) Then
             PIVOT=0
             J=I+1
530          If((PIVOT .EQ. O) .AND. (J .EQ. N)) Then
                    If (AUG(J,I) .NE. 0)Then
                     PIVOT=J
                    EndIF
                    J=J+1
                    GO TO 530
             END IF
             If(PIVOT .EQ. 0) Then
              Print*, J
              Stop 'Matrix is Singular'
             Else
* Interchange Rows I and Pivot
             Do 540, J=1,N+1
                    TEMP=AUG(I,J)
                    AUG(I,J)=AUG(PIVOT,J)
                    AUG(PIVOT,J)=TEMP
540          Continue
             End If
            End If

* Eliminate Ith Unkown from Equations I+1,....,N

            Do 560, J=I+1,N
             MULT=-AUG(J,I)/AUG(I,I)
             Do 550, L=I,N+1
                    AUG(J,L)=AUG(J,L)+MULT*AUG(I,L)
550          Continue
560         Continue
570    Continue
```

```
* Find Solutions

          X(N)=AUG(N,N+1)/AUG(N,N)
          Do 585, J=N-1,1,-1
            X(J)=AUG(J,N+1)
            Do 580, L=J+1,N
                  X(J)=X(J)-AUG(J,L)*X(L)
580       Continue
            X(J)=X(J)/AUG(J,J)
585       Continue

          Do 587, I=1,N
            MAT1(I,K)=X(I)
587       Continue
590   Continue
     End
* End of Inverse Subroutine



     Subroutine DNT(D,T,X,Y,C,AA1,P,K,W,AA2)
       Real X,Y
       Complex z,z1,z2,z3,z4,z5,z6,z7,z8,z9,z10,z11,z12,
    +  zi1,zi1p,yi1,yi1p,zi2,zi2p,yi2,yi2p,zi12,zi12p,zii12,zii12p,
    +  zi21,zi21p,zii21,zii21p,zii1,zii1p,yii1,yii1p,zii2,zii2p,
    + yii2,yii2p,z13,z14,z15,z16,z17,z18
          Real p(32),a1(8),b1(8),c1(8),d1(8),a2(8),b2(8),c2(8),d2(8),
    + aa1,c,D,T,g,aa2,jj
          Integer i,j,n,m,w,k,l

           Do 2, i=1,8
                  a1(i)=0.0
                  b1(i)=0.0
                  c1(i)=0.0
                  d1(i)=0.0
                  a2(i)=0.0
```

```
                b2(i)=0.0
                c2(i)=0.0
                d2(i)=0.0
2       Continue

      n=aint(k/2.0+0.5)
      m=aint(k/2.0)
          jj=1.0

                Do 5, i=1,k
                 j=aint(jj)
                 l=(-1)**i
                 if(i .EQ. 1) Then
                        a1(j)=p(1)
                        a2(j)=p(1)
                        c1(j)=p(2)
                        c2(j)=p(2)
                 Else If(i .EQ. 2) Then
                        b1(j)=p(3)
                        b2(j)=p(3)
                        d1(j)=0.0
                        d2(j)=0.0
                 Else
                  If (l .LE. 0) Then
                         a1(j)=p(i*2-2)
                         a2(j)=p(i*2-2)
                         c1(j)=p(i*2-1)
                         c2(j)=p(i*2-1)
                  Else
                         b1(j)=p(i*2-2)
                         b2(j)=p(i*2-2)
                         d1(j)=p(i*2-1)
                         d2(j)=p(i*2-1)
                  End if
                 End if
```

```
                    jj=jj+0.5
5                   Continue
            g=y-c
            d=aa1-aa2
            z=cmplx(x,y)

            z1=zi1p(z,n,a1)
            z2=zi2p(z,n,a2,c,d)
            z3=yi1p(z,m,b1)
            z4=yi2p(z,m,b2,c,d)
            z5=yi1(z,m,b1)
            z6=yi2(z,m,b2,c,d)
            z7=zi12p(z,aa2,c,d,n,a1,m,b1,w,c1,d1)
            z8=zii12(z,aa2,c,d,n,a1,m,b1,w,c1,d1)
            z9=zii12p(z,aa2,c,d,n,a1,m,b1,w,c1,d1)
            z10=zi21p(z,aa1,c,d,n,a2,m,b2,w,c2,d2)
            z11=zii21(z,aa1,c,d,n,a2,m,b2,w,c2,d2)
            z12=zii21p(z,aa1,c,d,n,a2,m,b2,w,c2,d2)
            z13=yii1p(z,m,d1)
            z14=zii1p(z,n,c1)
            z15=zii1(z,n,c1)
            z16=yii2p(z,m,d2,c,d)
            z17=zii2p(z,n,c2,c,d)
            z18=zii2(z,n,c2,c,d)

* d = (sigmayy-sigmaxx)/2
            d=y*aimag(z1)+y*aimag(z3)-real(z5)+y*aimag(z13)+y*aimag(z14)
     +-real(z15)+g*aimag(z2)+g*aimag(z4)-real(z6)+g*aimag(z16)
     ++g*aimag(z17)-real(z18)+g*aimag(z7)+g*aimag(z9)-real(z8)
     ++y*aimag(z10)+y*aimag(z12)-real(z11)

* d= shear stress
          t=-y*real(z1)-y*real(z3)-aimag(z5)-y*real(z13)-y*real(z14)
     +-aimag(z15)-g*real(z2)-g*real(z4)-aimag(z6)-g*real(z16)
     +-g*real(z17)-aimag(z18)-g*real(z7)-g*real(z9)-aimag(z8)
```

```
     +-y*real(z10)-y*real(z12)-aimag(z11)
           End
* End of DNT Subroutine

           function zi1(z,n,a1)
            Complex zi1,z
            Real a1(8)
            Integer i,n
                  zi1=(0.0,0.0)
            Do 200, i=1,n
                   zi1=zi1+a1(i)*(sqrt(z))**(2*i-3)
200              Continue
           End

           function zi1p(z,n,a1)
            Complex zi1p,z
            Real a1(8)
            Integer i,n
                  zi1p=(0.0,0.0)
                  Do 210, i=1,n
                    zi1p=zi1p+(i-1.5)*a1(i)*(sqrt(z))**(2*i-5)
210               Continue
           End

           function zii1(z,n,c1)
            Complex zii1,z
            Real c1(8)
            Integer i,n
            zii1=(0.0,0.0)
                  Do 200, i=1,n
                    zii1=zii1+c1(i)*(sqrt(z))**(2*i-3)
200               Continue
            zii1=zii1*cmplx(0.0,-1.0)
           end
```

```
      function zii1p(z,n,c1)
        Complex zii1p,z
        Real c1(8)
        Integer i,n
        zii1p=(0.0,0.0)
        Do 200, i=1,n
              zii1p=zii1p+(i-1.5)*c1(i)*(sqrt(z))**(2*i-5)
200     Continue
        zii1p=zii1p*cmplx(0.0,-1.0)
      end


      function yi1(z,m,b1)
        Complex yi1,z
        Real b1(8)
        Integer i,m
        yi1=(0.0,0.0)
          Do 220, i=1,m
              yi1=yi1+b1(i)*z**(i-1)
220       Continue
      End

      function yi1p(z,m,b1)
        Complex yi1p,z
        Real b1(8)
        Integer i,m
        yi1p=(0.0,0.0)
          Do 230, i=1,m
              yi1p=yi1p+(i-1)*b1(i)*z**(i-2)
230       Continue
      End

      function yii1(z,m,d1)
        Complex yii1,z
        Real d1(8)
```

```
      Integer i,m
      yii1=(0.0,0.0)
        Do 220, i=i,m
            yii1=yii1+d1(i)*z**(i-1)
220     Continue
      yii1=yii1*cmplx(0.0,-1.0)
    End

    function yii1p(z,m,d1)
      Complex yii1p,z
      Real d1(8)
      Integer i,m
      yii1p=(0.0,0.0)
     Do 220, i=1,m
          yii1p=yii1p+(i-1)*d1(i)*z**(i-2)
220          Continue
      yii1p=yii1p*cmplx(0.0,-1.0)
    End

    function zi2(z,n,a2,c,d)
      Complex zi2,z,h,zi1
      Real a2(8),c,d
      Integer n
      zi2=(0.0,0.0)
      h=cmplx(d,-c)
      zi2=zi1(z+h,n,a2)
    end

    function zi2p(z,n,a2,c,d)
      Complex zi2p,z,h,g,zi1p
      Real a2(8),c,d
      Integer n
      zi2p=(0.0,0.0)
      h=cmplx(d,-c)
      zi2p=zi1p(z+h,n,a2)
```

```
    end

    function zii2(z,n,c2,c,d)
      Complex zii2,z,h,zii1
      Real c2(8),c,d
      Integer n
      zii2=(0.0,0.0)
      h=cmplx(d,-c)
      zii2=zii1(z+h,n,c2)
    end

    function zii2p(z,n,c2,c,d)
      Complex zii2p,z,h,zii1p
      Real c2(8),c
      Integer n
      zii2p=(0.0,0.0)
      h=cmplx(d,-c)
      zii2p=zii1p(z+h,n,c2)
    end

    function yi2(z,m,b2,c,d)
      Complex yi2,z,h,g,yi1
      Real b2(8),c,d
      Integer m
      yi2=(0.0,0.0)
      h=cmplx(d,-c)
yi2=yi1(z+h,m,b2)
    end

    function yi2p(z,m,b2,c,d)
      Complex yi2p,z,h,yi1p
      Real b2(8),c,d
      Integer m
      yi2p=(0.0,0.0)
      h=cmplx(d,-c)
```

```
      yi2p=yi1p(z+h,m,b2)
        end

        function yii2(z,m,d2,c,d)
          Complex yii2,z,h,g,yii1
          Real d2(8),c,d
          Integer m
          yii2=(0.0,0.0)
          h=cmplx(d,-c)
          yii2=yii1(z+h,m,d2)
        end

        function yii2p(z,m,d2,c,d)
          Complex yii2p,z,h,g,yii1p
          Real d2(8),c,d
          Integer m
          yii2p=(0.0,0.0)
          h=cmplx(d,-c)
          yii2p=yii1p(z+h,m,d2)
        end

        function zi12(z,aa2,c,d,n,a1,m,b1,w,c1,d1)
      Complex zi12,z,h,g,p,zi1,zi1p,yi1p,u,catan,q,yii1,
     +          yii1p,zii1p
          External catan
          Real x1,x2,dx,a1(8),b1(8),c1(8),d1(8),c,d,aa1,pi
          Integer i,n,m,w
          zi12=(0.0,0.0)
          pi=3.1415926536
          dx=aa2/w
          x1=-aa2
          q=z+cmplx(d,-c)
            Do 300, i=1,w
                  x2=x1+dx
                  g=cmplx(-x1/q)
```

```
                p=cmplx(-x2/q)
                h=cmplx((x1+x2)/2,c)
         zi12=zi12+2/pi*(real(zi1(h,n,a1))+c*aimag(zi1p(h,n,a1))
     +     +c*aimag(yi1p(h,m,b1))+real(yii1(h,m,d1))
     +     +c*aimag(yii1p(h,m,d1))+c*aimag(zii1p(h,n,c1)))*(-sqrt(p)
     +     +catan(sqrt(p))+sqrt(g)-catan(sqrt(g)))
                x1=x2
300          Continue
           end

           function zi12p(z,aa2,c,d,n,a1,m,b1,w,c1,d1)
              Complex zi12p,z,g,p,h,q,zi1,zi1p,yi1p,yii1,yii1p,zii1p
              Real a1(8),b1(8),c1(8),d1(8),aa2,c,d,pi,dx,x1,x2
              Integer i,n,m,w
              zi12p=(0.0,0.0)
              pi=3.1415926536
              dx=aa2/w
              x1=-aa2
              q=z+cmplx(d,-c)
                Do 310, i=1,w
                x2=x1+dx
                g=cmplx(-x1)
                p=cmplx(-x2)
                h=cmplx((x1+x2)/2,c)
          zi12p=zi12p+1/(pi*(sqrt(q))**3)*(real(zi1(h,n,a1))
     +    +c*aimag(zi1p(h,n,a1))+c*aimag(yi1p(h,m,b1))
     +    +real(yii1(h,m,d1))+c*aimag(yii1p(h,m,d1))
     +    +c*aimag(zii1p(h,n,c1)))*(sqrt(p)**3/(q+p)-sqrt(g)**3/(q+g))
                x1=x2
310          Continue
           end

           function zii12(z,aa2,c,d,n,a1,m,b1,w,c1,d1)
         Complex zii12,z,h,g,p,zi1p,yi1p,yi1,u,catan,q,yii1p,zii1p,zii1
         External catan
```

```
      Real x1,x2,dx,aa2,c,d,a1(8),b1(8),c1(8),d1(8),pi
      Integer i,n,m,w
       zii12=(0.0,0.0)
       pi=3.1415926536
           dx=aa2/w
           x1=-aa2
           q=z+cmplx(d,-c)
             Do 320, i=1,w
                   x2=x1+dx
                   g=cmplx(-x1/q)
                   p=cmplx(-x2/q)
                   h=cmplx((x1+x2)/2,c)
        zii12=zii12-2/pi*(c*real(zi1p(h,n,a1))+c*real(yi1p(h,m,b1))
     +  +aimag(yi1(h,m,b1))+c*real(yii1p(h,m,d1))
     +  +c*real(zii1p(h,n,c1))+aimag(zii1(h,n,c1)))*(-sqrt(p)
     +  +catan(sqrt(p))+sqrt(g)-catan(sqrt(g)))
                   x1=x2
320          Continue
           zii12=zii12*cmplx(0.0,-1.0)
         end

         function zii12p(z,aa2,c,d,n,a1,m,b1,w,c1,d1)
           Complex zii12p,z,q,g,h,p,zi1p,yi1p,yi1,yii1p,zii1p,zii1
           Real aa2,c,d,a1(8),b1(8),c1(8),d1(8),pi,dx,x1,x2
           Integer i,n,m,w
           zii12p=(0.0,0.0)
           pi=3.1415926536
           dx=aa2/w
           x1=-aa2
           q=z+cmplx(d,-c)
             Do 420, i=1,w
                   x2=x1+dx
                   g=cmplx(-x1)
                   p=cmplx(-x2)
                   h=cmplx((x1+x2)/2,c)
```

```
      zii12p=zii12p-1/(pi*(sqrt(q))**3)*(c*real(zi1p(h,n,a1))
     +    +c*real(yi1p(h,m,b1))+aimag(yi1(h,m,b1))
     +    +c*real(yii1p(h,m,d1))+c*real(zii1p(h,n,c1))
     +    +aimag(zii1(h,n,c1)))*(sqrt(p)**3/(q+p)-sqrt(g)**3/(q+g))
                  x1=x2
420           Continue
              zii12p=zii12p*cmplx(0.0,-1.0)
          end

          function zi21(z,aa1,c,d,n,a2,m,b2,w,c2,d2)
             Complex zi21,z,h,g,zi2,zi2p,yi2p,u,p,catan,yii2,yii2p,zii2p
             Real x1,x2,dx,aa1,c,d,a2(8),b2(8),c2(8),d2(8),pi
             Integer i,n,m,w
             zi21=(0.0,0.0)
             pi=3.1415926536
             dx=aa1/w
             x1=-aa1
               Do 320, i=1,w
                  x2=x1+dx
                  g=cmplx(-x1/z)
                  p=cmplx(-x2/z)
                  h=cmplx((x1+x2)/2,0.0)
     zi21=zi21+2/pi*(real(zi2(h,n,a2,c,d))-c*aimag(zi2p(h,n,a2,c,d))
     +  -c*aimag(yi2p(h,m,b2,c,d))+real(yii2(h,m,d2,c,d))
     +  -c*aimag(yii2p(h,m,d2,c,d))-c*aimag(zii2p(h,n,c2,c,d)))
     +  *(-sqrt(p)+catan(sqrt(p))+sqrt(g)-catan(sqrt(g)))
                  x1=x2
320           Continue
          end

          function zi21p(z,aa1,c,d,n,a2,m,b2,w,c2,d2)
             Complex zi21p,z,g,h,p,zi2,zi2p,yi2p,yii2,yii2p,zii2p
             Real aa1,c,d,a2(8),b2(8),c2(8),d2(8),pi,dx,x1,x2
             Integer i,n,m,w
             zi21p=(0.0,0.0)
```

```
      pi=3.1415926536
           dx=aa1/w
           x1=-aa1
             Do 440, i=1,w
                  x2=x1+dx
                  g=cmplx(-x1)
                  p=cmplx(-x2)
                  h=cmplx((x1+x2)/2,0.0)
                  zi21p=zi21p+1/(pi*(sqrt(z))**3)*(real(zi2(h,n,a2,c,d))
     +      -c*aimag(zi2p(h,n,a2,c,d))-c*aimag(yi2p(h,m,b2,c,d))
     +      +real(yii2(h,m,d2,c,d))-c*aimag(yii2p(h,m,d2,c,d))
     +      -c*aimag(zii2p(h,n,c2,c,d)))*(sqrt(p)**3/(z+p)
     +      -sqrt(g)**3/(z+g))
                  x1=x2
440           Continue
         end

         function zii21(z,aa1,c,d,n,a2,m,b2,w,c2,d2)
           Complex zii21,z,h,g,zi2,yi2,yi2p,u,p,catan,yii2p,zii2p,zii2
           External catan
           Real x1,x2,dx,aa1,c,d,a2(8),b2(8),c2(8),d2(8),pi
           Integer i,n,m,w
           zii21=(0.0,0.0)
           pi=3.1415926536
           dx=aa1/w
           x1=-aa1
             Do 330, i=1,w
                  x2=x1+dx
                  g=cmplx(-x1/z)
                  p=cmplx(-x2/z)
                  h=cmplx((x1+x2)/2,0.0)
          zii21=zii21+2/pi*(c*real(zi2(h,n,a2,c,d))
     +      +c*real(yi2p(h,m,b2,c,d))-aimag(yi2(h,m,b2,c,d))
     +      +c*real(yii2p(h,m,d2,c,d))+c*real(zii2p(h,n,c2,c,d))
     +      -aimag(zii2(h,n,c2,c,d)))*(-sqrt(p)+catan(sqrt(p))
```

```
     +       +sqrt(g)-catan(sqrt(g)))
                    x1=x2
330              Continue
                 zii21=zii21*cmplx(0.0,-1.0)
            end

            function zii21p(z,aa1,c,d,n,a2,m,b2,w,c2,d2)
               Complex zii21p,z,g,h,p,zi2p,yi2p,yi2,yii2p,zii2p,zii2
               Real aa1,c,d,a2(8),b2(8),c2(8),d2(8),dx,x1,x2,pi
               Integer i,n,m,w
               zii21p=(0.0,0.0)
               pi=3.1415926536
               dx=aa1/w
               x1=-aa1
                 Do 460, i=1,w
                    x2=x1+dx
                    g=cmplx(-x1)
                    p=cmplx(-x2)
                    h=cmplx((x1+x2)/2,0.0)
           zii21p=zii21p+1/(pi*(sqrt(z))**3)*(c*real(zi2p(h,n,a2,c,d))
     +       +c*real(yi2p(h,m,b2,c,d))-aimag(yi2(h,m,b2,c,d))
     +       +c*real(yii2p(h,m,d2,c,d))+c*real(zii2p(h,n,c2,c,d))
     +       -aimag(zii2(h,n,c2,c,d)))
     +       *(sqrt(p)**3/(z+p)-sqrt(g)**3/(z+g))
                    x1=x2
460              Continue
                 zii21p=zii21p*cmplx(0.0,-1.0)
       END
* End of Program
```

```
      Program DCIANDII
       CHARACTER*66 PD,YD,ZD
       REAL K5,K6,K7,K9,K10,Z(2000,3),A(40,1),B(40,1),C(2000,40),
     +  D(40,40),F(40,1),CT(32,2000),DI(40,40),G(2000,1),H(40,1),
     +  M1(40,5),PI,N1,N3,N4,N7,N8,E1,E2,E3,DD,TT,PDD,PTT,
     +  TEMP(50),K12,K11
           INTEGER K1,K2,K3,K4,K8,I,J,K,L,L1,I1,I2,I3,I4,I7,I8,I9

       PD= '*=======================================================*'
       YD= ' ITER. NO.     ERROR    DELTA N (FRGS)     DELTA N (PCT)'

* This is a progam to compute up to a ten parameter (40 coefficient) model
* and output the coefficients of the series of solution to the parallel,
* unequal length, edge crack problem.  The program uses the Newton-Raphson,
* non-linear, least-squares technique following the method due to R.J. Sanford.
* Up to 2000 data points may be specified and should be entered in a file
* named 'DATB'

      Call Zero2(Z,2000,3)
      PI=3.141592654

* Read in parameters from input files
           Open (Unit=12, File='DAT', Status='old')
           Read (12,*) K1,K2,K3,K4,K8,K5,K6,K9,K12,K10,K7,K11
       Close (12)
       Open (Unit=12, File='DATA', Status='old')
       Read (12,100) ZD
       Close (12)

* Create and open output file
           Open (Unit=15, File='Output', Status='New')
           Write (15,*) ZD
           Write (15,*) 'Number of Data Points = ', K1
           Write (15,*) 'Lowest Order Model = ', K2
           Write (15,*) 'Highest Order Model = ', K3
```

```
            Write (15,*) 'Max. # of iterations within each model = ', K4
            Write (15,*) 'Number of divisions along crack faces = ', K8
            Write (15,*) 'Material Fringe Constant = ', K5
            Write (15,*) 'Model Thickness = ', K6
            Write (15,*) 'First Crack Length = ', K9
            Write (15,*) 'Second Crack Length = ', K12
            Write (15,*) 'Crack Seperation = ',K10
            Write (15,*) 'Initial Estimate of K-I-1 = ',K7
            Write (15,*) 'Initial Estimate of K-I-2 = ',K11

*    Make inital guess
       Call ZERO1(Temp,50)
            Call ZERO2(A,40,1)
            A(1,1)=K7*K6/K5/SQRT(2*PI)
       A(2,1)=K11*K6/K5/SQRT(2*PI)
             Do 1, I5=1,40
              TEMP(I5)=A(I5,1)
1            Continue


* Loop once for each order model solution

            Do 7, I=K2,K3
       Call First(PD,YD,ZD,K5,K6,K7,K9,K10,Z,A,B,C,D,F,CT,
     +  DI,G,H,M1,PI,N1,N3,N4,N7,N8,E1,E2,E3,DD,TT,PDD,PTT,
     +  K1,K4,K8,K12,I,J,L,L1,I1,I2,I3,I4,I7,I8,I9,TEMP)
7           CONTINUE
            CLOSE (15)
100         FORMAT(A66)
            END

* End of Main Program

* Start of Subroutines
       Subroutine First(PD,YD,ZD,K5,K6,K7,K9,K10,Z,A,B,C,D,F,CT,
```

```
     +  DI,G,H,M1,PI,N1,N3,N4,N7,N8,E1,E2,E3,DD,TT,PDD,PTT,
     +  K1,K4,K8,K12,I,J,L,L1,I1,I2,I3,I4,I7,I8,I9,TEMP)

            Character*66 PD,YD,ZD
            Integer K1,K2,K3,K4,K8,I,J,J1,L,L1,I1,I2,I3,I4,I7,I8,I9
            Real K5,K6,K7,K9,K10,PI,N1,N3,N4,N7,N8,E1,E2,E3,DD,TT,
     +  PDD,PTT,K12
            Real Z(K1,3),A(I*4-3,1),B(I*4-3,1),C(K1,I*4-3),
     +  D(I*4-3,I*4-3),F(I*4-3,1),CT(I*4-3,K1),DI(I*4-3,I*4-3),
     +  G(K1,1),H(I*4-3,1),TEMP(50),M1(40,5),ABC



            Do 1, I5=1,40
          A(I5,1)=TEMP(I5)
1           Continue
            Call ZERO1(TEMP,50)
            Open (Unit=12, File='DATB', Status='old')
            Do 3 I111=1,K1
            Read (12,*) Z(I111,1),Z(I111,2),Z(I111,3)
3           Continue
             N1=0.0
            Do 5, L2=1,K1
             N1=N1+z(L2,3)
5           Continue
            N8=N1/K1
          Close(12)

         Write (15,*) PD
         Write (15,*) I, 'Parameter Model -- Parallel Edge Crack Solution'
         Write (15,*) ' ', ZD
         Write (15,*) PD
         Write (15,*)

            Write (15,*) ' Average Input Fringe Order = ',N8
            Write (15,*)
```

```
          Write (15,*) YD

* Loop for number iterations allowed within each model

          Call ZERO2(M1,40,5)
       Do 300, I1=1,K4
          Call ZERO2(C,K1,I*4-3)
            Call ZERO2(CT,I*4-3,K1)
            Call ZERO2(DI,I*4-3,I*4-3)
            Call ZERO2(D,I*4-3,I*4-3)
            Call ZERO2(F,I*4-3,1)
            Call ZERO2(G,K1,1)
            Call ZERO2(H,I*4-3,1)

          E1=0.0
          N3=0.0

                   Do 100, L=1,K1
         Call DNT(DD,TT,Z(L,1),Z(L,2),K10,K9,A,I,K8,K12)
                    G(L,1)=((Z(L,3)/2)**2-DD**2-TT**2)
                    E1=E1+G(L,1)**2
              N4=2*SQRT(DD**2+TT**2)
                    N3=N3+ABS(Z(L,3)-N4)
                Do 20, L1=1,I*4-3
                Call ZERO2(B,I*4-3,1)
                B(L1,1)=1.0
                Call DNT(PDD,PTT,Z(L,1),Z(L,2),K10,K9,B,I,K8,K12)
                C(L,L1)=2*DD*PDD+2*TT*PTT
20               Continue
100                 Continue

          N7=N3/K1
          Call TRNSPS(CT,I*4-3,K1,C)
          Call MATMUL(CT,C,D,I*4-3,K1,K1,I*4-3)
          Call INVERSE(DI,I*4-3,D)
```

```
          Call MATMUL(CT,G,F,I*4-3,K1,K1,1)
          Call MATMUL(DI,F,H,I*4-3,I*4-3,I*4-3,1)
          Call ADD(A,I*4-3,1,A,I*4-3,1,H,I*4-3,1)

          M1(I1,1)=I1*1
          M1(I1,2)=E1
          M1(I1,3)=N7
          M1(I1,4)=N7/N8*100
      If (I1 .EQ. 1) Then
       Go To 300
      End If

*Check for error among increasing number of overall iterations

          E3=ABS(1-M1(I1,2)/M1(I1-2,2))
          If (E3 .LE. 0.002) Then
                    Go To 310
                    End If
300       Continue

310     If(I1 .GT. K4) I1=I1-1
          Do 320, I4=1,I1
        Write (15,350) M1(I4,1),M1(I4,2),M1(I4,3),M1(I4,4)
320       Continue
          Write (15,*)
          Write (15,*)
          ABC=0.0
       E5=K5/K6
          Do 330, I7=1,I
            I75=AINT(ABC)
            L=(-1)**I7
            If (I7 .EQ. 1) Then
              Write (15,360) I75,A(1,1)*E5,I9,A(1,1)/A(1,1),I75,
     +     A(2,1)*E5,I75,A(2,1)/A(2,1)
              Write (15,365) I75,A(3,1)*E5,I9,A(3,1)/A(1,1),I75,
```

```
     +     A(4,1)*E5,I75,A(4,1)/A(2,1)
                      Else If (I7 .EQ. 2) Then
                 Write (15,370) I75,A(5,1)*E5,I75,A(5,1)/A(1,1),I75,
     +     A(5,1)*E5,I75,A(5,1)/A(2,1)
                       Write (15,375) I75,0.0,I75,0.0/A(1,1),I75,
     +     0.0,I75,0.0/A(2,1)
              Else
           If (L .LE. 0) Then
            Write (15,360) I75,A(I7*4-6,1)*E5,I75,A(I7*4-6,1)/A(1,1),
     +      I75,A(I7*4-5,1)*E5,I75,A(I7*4-5,1)/A(2,1)
            Write (15,365) I75,A(I7*4-4,1)*E5,I75,A(I7*4-4,1)/A(1,1),
     +      I75,A(I7*4-3,1)*E5,I75,A(I7*4-3,1)/A(2,1)
           Else
            Write (15,370) I75,A(I7*4-6,1)*E5,I75,A(I7*4-6,1)/A(1,1),
     +      I75,A(I7*4-5,1)*E5,I75,A(I7*4-5,1)/A(2,1)
            Write (15,375) I75,A(I7*4-4,1)*E5,I75,A(I7*4-4,1)/A(1,1),
     +      I75,A(I7*4-3,1)*E5,I75,A(I7*4-3,1)/A(2,1)
           End If
              End If
              ABC=ABC+0.5
    330       Continue

         Do 345 I5=1,40
              TEMP(I5)=A(I5,1)
    345       Continue
              Write (15,*)
              Write (15,*) PD

    350    Format (4X,F3.0,6X,F12.3,5X,F7.4,8X,F8.4)
    360    Format (1x,'A',I1,'-1 = ',F10.2,'   A',I1,'-1/AO-1 = ',
       +   F10.2,5X,'A',I1,'-2 =', F10.2,'   A',I1,'-2/AO-2 = ',F10.2)
    365    Format (1x,'C',I1,'-1 = ',F10.2,'   C',I1,'-1/AO-1 = ',
       +   F10.2,5X,'C',I1,'-2 =', F10.2,'   C',I1,'-2/AO-2 = ',F10.2)
    370    Format (1x,'B',I1,'-1 = ',F10.2,'   B',I1,'-1/AO-1 = ',
       +   F10.2,5X,'B',I1,'-2 =', F10.2,'   B',I1,'-2/AO-2 = ',F10.2)
```

```
375     Format (1x,'D',I1,'-1 = ',F10.2,'   D',I1,'-1/AO-1 = ',
    +   F10.2,5X,'D',I1,'-2 =', F10.2,'   D',I1,'-2/AO-2 = ',F10.2)

          END


     Subroutine ZERO1(MAT,ROW)
           Integer I,ROW
           Real MAT(ROW)
           Do 10, I=1,ROW
             MAT(I)=0.0
10           Continue
          End

          Subroutine ZERO2(MAT,ROW,COL)
                    Integer ROW,COL,I,J
                    Real MAT(ROW,COL)
                    Do 20, I=1,ROW
                      Do 10, J=1,COL
                        MAT(I,J)=0.0
10                    Continue
20                  Continue
          End

          Subroutine MATMUL(MAT1,MAT2,PROD,M,N,P,Q)
                    Integer M,N,P,Q,I,J,K
                    Real MAT1(M,N),MAT2(P,Q),PROD(M,Q),SUM
                      If (N .EQ. P) Then
                Do 330, I=1,M
                 Do 320, J=1,Q
                  SUM=0.0
                   Do 310, K=1,N
                    SUM=SUM+(MAT1(I,K)*MAT2(K,J))
310                   Continue
                  PROD(I,J)=SUM
```

```
320             Continue
330            Continue
                    Else
          Stop 'Matrices are not Compatible for Multiplication'
                    End If
        End


        Subroutine ADD(MAT1,ROW1,COL1,MAT2,ROW2,COL2,MAT3,ROW3,COL3)
          Integer ROW1,COL1,ROW2,COL2,ROW3,COL3,I,J
          Real MAT1(ROW1,COL1),MAT2(ROW2,COL2),MAT3(ROW3,COL3)
                Do 380, I=1,ROW1
                 Do 370 J=1,COL1
                   MAT1(I,J)=MAT2(I,J)+MAT3(I,J)
370              Continue
380             Continue

    END

        Subroutine TRNSPS(MAT1,M,N,MAT2)
          Integer M,N,I,J
       Real MAT1(M,N),MAT2(N,M),TERM
                Do 20, I=1,N
                  Do 10, J=1,M
                        TERM=MAT2(I,J)
                        MAT1(J,I)=TERM
10                Continue
20              Continue
    END

        Subroutine INVERSE(MAT1,N,MAT2)
          Integer N,I,J,K,L,PIVOT
          Real MAT1(N,N),MAT2(N,N),MULT,AUG(200,201),TEMP,X(200)
         Do 590, K=1,N
                  Do 510, I=1,N
```

```
                    Do 505, J=1,N
                        AUG(I,J)=MAT2(I,J)
505                 Continue
510                 Continue
                    Do 520, L=1,N
                      If(L .EQ. K) Then
                        AUG(L,N+1)=1
                      Else
                        AUG(L,N+1)=0
                END If
520                 Continue

     Do 570, I=1,N

* Locate Nonzero Diagonal Entry


          If (AUG(I,I) .EQ. 0) Then
            PIVOT=0
            J=I+1
530         If((PIVOT .EQ. O) .AND. (J .EQ. N)) Then
                If (AUG(J,I) .NE. 0) PIVOT=J
                J=J+1
                GO TO 530
            END IF
            If(PIVOT .EQ. 0) Then
                Stop 'Matrix is Singular'
            Else
* Interchange Rows I and Pivot
            Do 540, J=1,N+1
                TEMP=AUG(I,J)
                AUG(I,J)=AUG(PIVOT,J)
                AUG(PIVOT,J)=TEMP
540         Continue
        End If
```

```
            End If

* Eliminate Ith Unknown from Equations I+1,...,N
       Do 560, J=I+1,N
        MULT=-AUG(J,I)/AUG(I,I)
        DO 550, L=I,N+1
         AUG(J,L)=AUG(J,L)+MULT*AUG(I,L)
550      CONTINUE
560      CONTINUE
570     CONTINUE

* Find Solutions

            X(N)=AUG(N,N+1)/AUG(N,N)
            Do 585, J=N-1,1,-1
              X(J)=AUG(J,N+1)
              Do 580, L=J+1,N
                      X(J)=X(J)-AUG(J,L)*X(L)
580         Continue
            X(J)=X(J)/AUG(J,J)
585         Continue

            Do 587, I=1,N
              MAT1(I,K)=X(I)
587         Continue
590    Continue
      End
* End of Inverse Subroutine

            Subroutine DNT(D,T,X,Y,C,AA1,P,K,W,AA2)
        REAL X,Y
        Complex z,z1,z2,z3,z4,z5,z6,z7,z8,z9,z10,z11,z12,
     c   zi1,zi1p,yi1,yi1p,zi2,zi2p,yi2,yi2p,zi12,zi12p,zii12,zii12p,
     c   zi21,zi21p,zii21,zii21p,zii1,zii1p,yii1,yii1p,zii2,zii2p,
     c   yii2,yii2p,z13,z14,z15,z16,z17,z18
```

```
      Real p(32),a1(8),b1(8),c1(8),d1(8),a2(8),b2(8),c2(8),d2(8),
     c  aa1,c,d,t,g,aa2,jj
      Integer i,j,n,m,w,k,l



      Do 2, i=1,8
            a1(i)=0.0
            b1(i)=0.0
            c1(i)=0.0
            d1(i)=0.0
            a2(i)=0.0
            b2(i)=0.0
            c2(i)=0.0
            d2(i)=0.0
2     Continue

     n=AINT(k/2.0+0.5)
     m=AINT(k/2.0)
      jj=1.0

            Do 5, i=1,k
             j=aint(jj)
             l=(-1)**i
             if(i .EQ. 1) Then
                  a1(j)=p(1)
                  a2(j)=p(2)
                  c1(j)=p(3)
                  c2(j)=p(4)
              Else If(i .EQ. 2) Then
                  b1(j)=p(5)
                  b2(j)=p(5)
                  d1(j)=0.0
                  d2(j)=0.0
              Else
               If (l .LE. 0) Then
```

```
                    a1(j)=p(i*4-6)
                    a2(j)=p(i*4-5)
                    c1(j)=p(i*4-4)
                    c2(j)=p(i*4-3)
                Else
                    b1(j)=p(i*4-6)
                    b2(j)=p(i*4-5)
                    d1(j)=p(i*4-4)
                    d2(j)=p(i*4-3)
                End if
            End if
            jj=jj+0.5
5           Continue
      g=y-c
      d=aa1-aa2
      z=cmplx(x,y)

        z1=zi1p(z,n,a1)
        z2=zi2p(z,n,a2,c,d)
        z3=yi1p(z,m,b1)
        z4=yi2p(z,m,b2,c,d)
        z5=yi1(z,m,b1)
        z6=yi2(z,m,b2,c,d)
        z7=zi12p(z,aa2,c,d,n,a1,m,b1,w,c1,d1)
        z8=zii12(z,aa2,c,d,n,a1,m,b1,w,c1,d1)
        z9=zii12p(z,aa2,c,d,n,a1,m,b1,w,c1,d1)
        z10=zi21p(z,aa1,c,d,n,a2,m,b2,w,c2,d2)
        z11=zii21(z,aa1,c,d,n,a2,m,b2,w,c2,d2)
        z12=zii21p(z,aa1,c,d,n,a2,m,b2,w,c2,d2)
        z13=yii1p(z,m,d1)
        z14=zii1p(z,n,c1)
        z15=zii1(z,n,c1)
        z16=yii2p(z,m,d2,c,d)
        z17=zii2p(z,n,c2,c,d)
        z18=zii2(z,n,c2,c,d)
```

```
      d=y*aimag(z1)+y*aimag(z3)-real(z5)+y*aimag(z13)+y*aimag(z14)
+    -real(z15)+g*aimag(z2)+g*aimag(z4)-real(z6)+g*aimag(z16)
+    +g*aimag(z17)-real(z18)+g*aimag(z7)+g*aimag(z9)-real(z8)
+    +y*aimag(z10)+y*aimag(z12)-real(z11)

      t=-y*real(z1)-y*real(z3)-aimag(z4)-y*real(z13)-y*real(z14)
+    -aimag(z15)-g*real(z2)-g*real(z4)-aimag(z6)-g*real(z16)
+    -g*real(z17)-aimag(z18)-g*real(z7)-g*real(z9)-aimag(z8)
+    -y*real(z10)-y*real(z12)-aimag(z11)
      End

      function zi1(z,n,a1)
       Complex zi1,z
       Real a1(8)
       Integer i,n
            zi1=(0.0,0.0)
       Do 200, i=1,n
            zi1=zi1+a1(i)*(sqrt(z))**(2*i-3)
200       Continue
      End

      function zi1p(z,n,a1)
       Complex zi1p,z
       Real a1(8)
       Integer i,n
            zi1p=(0.0,0.0)
            Do 210, i=1,n
              zi1p=zi1p+(i-1.5)*a1(i)*(sqrt(z))**(2*i-5)
210         Continue
      End

      function zii1(z,n,c1)
       Complex zii1,z
       Real c1(8)
```

```
      Integer i,n
      zii1=(0.0,0.0)
            Do 200, i=1,n
              zii1=zii1+c1(i)*(sqrt(z))**(2*i-3)
200         Continue
      zii1=zii1*cmplx(0.0,-1.0)
     end

     function zii1p(z,n,c1)
      Comple x zii1p,z
      Real c1(8)
      Integer i,n
      zii1p=(0.0,0.0)
      Do 200, i=1,n
            zii1p=zii1p+(i-1.5)*c1(i)*(sqrt(z))**(2*i-5)
200     Continue
      zii1p=zii1p*cmplx(0.0,-1.0)
     end


     function yi1(z,m,b1)
      Complex yi1,z
      Real b1(8)
      Integer i,m
      yi1=(0.0,0.0)
        Do 220, i=1,m
            yi1=yi1+b1(i)*z**(i-1)
220     Continue
   End

     function yi1p(z,m,b1)
      Complex yi1p,z
      Real b1(8)
      Integer i,m
      yi1p=(0.0,0.0)
```

```
            Do 230, i=1,m
                yi1p=yi1p+(i-1)*b1(i)*z**(i-2)
230         Continue
          End

          function yii1(z,m,d1)
            Complex yii1,z
            Real d1(8)
            Integer i,m
            yii1=(0.0,0.0)
          Do 220, i=1,m
                yii1=yii1+d1(i)*z**(i-1)
220         Continue
            yii1=yii1*cmplx(0.0,-1.0)
          End

          function yii1p(z,m,d1)
            Complex yii1p,z
            Real d1(8)
        Integer i,m
            yii1p=(0.0,0.0)
           Do 220, i=1,m
                 yii1p=yii1p+(i-1)*d1(i)*z**(i-2)
220              Continue
            yii1p=yii1p*cmplx(0.0,-1.0)
          End

          function zi2(z,n,a2,c,d)
            Complex zi2,z,h,zi1
            Real a2(8),c,d
            Integer n
            zi2=(0.0,0.0)
            h=cmplx(d,-c)
            zi2=zi1(z+h,n,a2)
          end
```

```
      function zi2p(z,n,a2,c,d)
        Complex zi2p,z,h,g,zi1p
        Real a2(8),c,d
        Integer n
        zi2p=(0.0,0.0)
        h=cmplx(d,-c)
        zi2p=zi1p(z+h,n,a2)
      end

      function zii2(z,n,c2,c,d)
        Complex zii2,z,h,zii1
        Real c2(8),c,d
        Integer n
        zii2=(0.0,0.0)
        h=cmplx(d,-c)
        zii2=zii1(z+h,n,c2)
      end

      function zii2p(z,n,c2,c,d)
        Complex zii2p,z,h,zii1p
        Real c2(8),c
        Integer n
        zii2p=(0.0,0.0)
        h=cmplx(d,-c)
        zii2p=zii1p(z+h,n,c2)
      end

      function yi2(z,m,b2,c,d)
        Complex yi2,z,h,g,yi1
        Real b2(8),c,d
        Integer m
        yi2=(0.0,0.0)
        h=cmplx(d,-c)
    yi2=yi1(z+h,m,b2)
```

```
      end

      function yi2p(z,m,b2,c,d)
        Complex yi2p,z,h,yi1p
        Real b2(8),c,d
        Integer m
        yi2p=(0.0,0.0)
        h=cmplx(d,-c)
     yi2p=yi1p(z+h,m,b2)
      end

      function yii2(z,m,d2,c,d)
        Complex yii2,z,h,g,yii1
        Real d2(8),c,d
        Integer m
        yii2=(0.0,0.0)
        h=cmplx(d,-c)
        yii2=yii1(z+h,m,d2)
      end

      function yii2p(z,m,d2,c,d)
        Complex yii2p,z,h,g,yii1p
        Real d2(8),c,d
        Integer m
        yii2p=(0.0,0.0)
        h=cmplx(d,-c)
        yii2p=yii1p(z+h,m,d2)
      end

      function zi12(z,aa2,c,d,n,a1,m,b1,w,c1,d1)
     Complex zi12,z,h,g,p,zi1,zi1p,yi1p,u,CATAN,q,yii1,
     +          yii1p,zii1p
     External CATAN
        Real x1,x2,dx,a1(8),b1(8),c1(8),d1(8),c,d,aa1,pi
        Integer i,n,m,w
```

```
      zi12=(0.0,0.0)
      pi=3.1415926536
      dx=aa2/w
      x1=-aa2
      q=z+cmplx(d,-c)
        Do 300, i=1,w
            x2=x1+dx
            g=cmplx(-x1/q)
            p=cmplx(-x2/q)
            h=cmplx((x1+x2)/2,c)
     zi12=zi12+2/pi*(real(zi1(h,n,a1))+c*aimag(zi1p(h,n,a1))
    +  +c*aimag(yi1p(h,m,b1))+real(yii1(h,m,d1))
    +  +c*aimag(yii1p(h,m,d1))+c*aimag(zii1p(h,n,c1)))*(-sqrt(p)
    +  +CATAN(sqrt(p))+sqrt(g)-CATAN(sqrt(g)))
       x1=x2
300     Continue
      end

      function zi12p(z,aa2,c,d,n,a1,m,b1,w,c1,d1)
        Complex zi12p,z,g,p,h,q,zi1,zi1p,yi1p,yii1,yii1p,zii1p
        Real a1(8),b1(8),c1(8),d1(8),aa2,c,d,pi,dx,x1,x2
        Integer i,n,m,w
        zi12p=(0.0,0.0)
        pi=3.1415926536
        dx=aa2/w
        x1=-aa2
        q=z+cmplx(d,-c)
          Do 310, i=1,w
            x2=x1+dx
            g=cmplx(-x1)
            p=cmplx(-x2)
            h=cmplx((x1+x2)/2,c)
            zi12p=zi12p+1/(pi*(sqrt(q))**3)*(real(zi1(h,n,a1))
    +     +c*aimag(zi1p(h,n,a1))+c*aimag(yi1p(h,m,b1))
    +     +real(yii1(h,m,d1))+c*aimag(yii1p(h,m,d1))
```

```
     +            +c*aimag(zii1p(h,n,c1)))*(sqrt(p)**3/(q+p)
     +            -sqrt(g)**3/(q+g))
                      x1=x2
310             Continue
          end

          function zii12(z,aa2,c,d,n,a1,m,b1,w,c1,d1)
        Complex zii12,z,h,g,p,zi1p,yi1p,yi1,u,CATAN,q,yii1p,zii1p,zii1
        External CATAN
        Real x1,x2,dx,aa2,c,d,a1(8),b1(8),c1(8),d1(8),pi
        Integer i,n,m,w
             zii12=(0.0,0.0)
             pi=3.1415926536
             dx=aa2/w
             x1=-aa2
             q=z+cmplx(d,-c)
         Do 320, i=1,w
         x2=x1+dx
         g=cmplx(-x1/q)
         p=cmplx(-x2/q)
         h=cmplx((x1+x2)/2,c)
         zii12=zii12-2/pi*(c*real(zi1p(h,n,a1))+c*real(yi1p(h,m,b1))
     +     +aimag(yi1(h,m,b1))+c*real(yii1p(h,m,d1))
     +     +c*real(zii1p(h,n,c1))+aimag(zii1(h,n,c1)))*(-sqrt(p)
     +     +CATAN(sqrt(p))+sqrt(g)-CATAN(sqrt(g)))
                      x1=x2
320          Continue
               zii12=zii12*cmplx(0.0,-1.0)
       END

       Function zii12p(z,aa2,c,d,n,a1,m,b1,w,c1,d1)
               Complex zii12p,z,q,g,h,p,zi1p,yi1p,yi1,yii1p,zii1p,zii1
               Real aa2,c,d,a1(8),b1(8),c1(8),d1(8),pi,dx,x1,x2
               Integer i,n,m,w
               zii12p=(0.0,0.0)
```

```
            pi=3.1415926536
            dx=aa2/w
            x1=-aa2
            q=z+cmplx(d,-c)
              Do 420, i=1,w
                    x2=x1+dx
                    g=cmplx(-x1)
                    p=cmplx(-x2)
                    h=cmplx((x1+x2)/2,c)
                    zii12p=zii12p-1/(pi*(sqrt(q))**3)*(c*real(zi1p(h,n,a1))
     +      +c*real(yi1p(h,m,b1))+aimag(yi1(h,m,b1))
     +      +c*real(yii1p(h,m,d1))+c*real(zii1p(h,n,c1))
     +      +aimag(zii1(h,n,c1)))*(sqrt(p)**3/(q+p)-sqrt(g)**3/(q+g))
                    x1=x2
420           Continue
              zii12p=zii12p*cmplx(0.0,-1.0)
           end

           function zi21(z,aa1,c,d,n,a2,m,b2,w,c2,d2)
         Complex zi21,z,h,g,zi2,zi2p,yi2p,u,p,CATAN,yii2,yii2p,zii2p
              Real x1,x2,dx,aa1,c,d,a2(8),b2(8),c2(8),d2(8),pi
              Integer i,n,m,w
         External CATAN
              zi21=(0.0,0.0)
              pi=3.1415926536
              dx=aa1/w
              x1=-aa1
                Do 320, i=1,w
                    x2=x1+dx
                    g=cmplx(-x1/z)
                    p=cmplx(-x2/z)
                    h=cmplx((x1+x2)/2,0.0)
       zi21=zi21+2/pi*(real(zi2(h,n,a2,c,d))-c*aimag(zi2p(h,n,a2,c,d))
     +  -c*aimag(yi2p(h,m,b2,c,d))+real(yii2(h,m,d2,c,d))
     +  -c*aimag(yii2p(h,m,d2,c,d))-c*aimag(zii2p(h,n,c2,c,d)))
```

```
     +  *(-sqrt(p)+CATAN(sqrt(p))+sqrt(g)-CATAN(sqrt(g)))
              x1=x2
  320          Continue
             end

             function zi21p(z,aa1,c,d,n,a2,m,b2,w,c2,d2)
               Complex zi21p,z,g,h,p,zi2,zi2p,yi2p,yii2,yii2p,zii2p
               Real aa1,c,d,a2(8),b2(8),c2(8),d2(8),pi,dx,x1,x2
               Integer i,n,m,w
               zi21p=(0.0,0.0)
            pi=3.1415926536
               dx=aa1/w
               x1=-aa1
                 Do 440, i=1,w
                       x2=x1+dx
                       g=cmplx(-x1)
                       p=cmplx(-x2)
                       h=cmplx((x1+x2)/2,0.0)
                       zi21p=zi21p+1/(pi*(sqrt(z))**3)*(real(zi2(h,n,a2,c,d))
     +        -c*aimag(zi2p(h,n,a2,c,d))-c*aimag(yi2p(h,m,b2,c,d))
     +        +real(yii2(h,m,d2,c,d))-c*aimag(yii2p(h,m,d2,c,d))
     +        -c*aimag(zii2p(h,n,c2,c,d)))*(sqrt(p)**3/(z+p)
     +        -sqrt(g)**3/(z+g))
                       x1=x2
  440          Continue
             end

             function zii21(z,aa1,c,d,n,a2,m,b2,w,c2,d2)
            Complex zii21,z,h,g,zi2p,yi2,yi2p,u,p,CATAN,yii2p,zii2p,zii2
            External CATAN
                Real x1,x2,dx,aa1,c,d,a2(8),b2(8),c2(8),d2(8),pi
               Integer i,n,m,w
               zii21=(0.0,0.0)
               pi=3.1415926536
               dx=aa1/w
```

```
      x1=-aa1
        Do 330, i=1,w
            x2=x1+dx
            g=cmplx(-x1/z)
            p=cmplx(-x2/z)
            h=cmplx((x1+x2)/2,0.0)
     zii21=zii21+2/pi*(c*real(zi2p(h,n,a2,c,d))
    +    +c*real(yi2p(h,m,b2,c,d))-aimag(yi2(h,m,b2,c,d))
    +    +c*real(yii2p(h,m,d2,c,d))+c*real(zii2p(h,n,c2,c,d))
    +    -aimag(zii2(h,n,c2,c,d)))*(-sqrt(p)+CATAN(sqrt(p))
    +    +sqrt(g)-CATAN(sqrt(g)))
            x1=x2
330       Continue
        zii21=zii21*cmplx(0.0,-1.0)
      end

      function zii21p(z,aa1,c,d,n,a2,m,b2,w,c2,d2)
        Complex zii21p,z,g,h,p,zi2p,yi2p,yi2,yii2p,zii2p,zii2
        Real aa1,c,d,a2(8),b2(8),c2(8),d2(8),dx,x1,x2,pi
        Integer i,n,m,w
        zii21p=(0.0,0.0)
        pi=3.1415926536
        dx=aa1/w
        x1=-aa1
          Do 460, i=1,w
            x2=x1+dx
            g=cmplx(-x1)
            p=cmplx(-x2)
            h=cmplx((x1+x2)/2,0.0)
      zii21=zii21p+1/(pi*(sqrt(z))**3)*(c*real(zi2p(h,n,a2,c,d))
    +    +c*real(yi2p(h,m,b2,c,d))-aimag(yi2(h,m,b2,c,d))
    +    +c*real(yii2p(h,m,d2,c,d))+c*real(zii2p(h,n,c2,c,d))
    +    -aimag(zii2(h,n,c2,c,d)))
    +    *(sqrt(p)**3/(z+p)-sqrt(g)**3/(z+g))
        x1=x2
```

```
460         Continue
            zii21p=zii21p*cmplx(0.0,-1.0)
          end
```

```
      PROGRAM SIF

* Calculates the Open and Shear Mode Stress Intensity Factors
* for both cracks



       REAL X,Y,FSIGMA,H
       Real L,M,IO,K,SIGMAX,SIGMAY,TAUXY,C,AA1,AA2,PI,X1,X2,X3,DX
       REAL A1(8),B1(8),C1(8),D1(8),A2(8),B2(8),C2(8),D2(8),
     +  KI1,KII1,KI2,KII2
       INTEGER W,I,J,N1,N2,N3

* N = NUMBER OF PLOTS
* FSIGMA = MATERIA L FRINGE CONSTANT
* H = SPECIMEN THICKNESS
* W = NUMBER OF DIVISONS ALONG CRACK 1 AND 2
* C = DISTANCE BETWEEN THE CRACKS
* AA1,AA2 = LENGTH OF CRACK 1 AND 2, RESPECTIVELY
       PI=3.141592654
       OPEN (UNIT=5, FILE='PLOTDATA', STATUS='OLD')
       OPEN (UNIT=6, FILE='SIFS.dat', STATUS='NEW')
       READ (5,*) FSIGMA,H
       READ (5,*) W,C,AA1,AA2

* ZERO OUT COEFFICENTS
       DO 6,K1=1,8
         A1(K1)=0.0
         B1(K1)=0.0
         C1(K1)=0.0
         D1(K1)=0.0
         A2(K1)=0.0
         B2(K1)=0.0
         C2(K1)=0.0
         D2(K1)=0.0
6      CONTINUE
```

```
      KI1=0.0
      KII1=0.0
      KI2=0.0
      KII2=0.0

* READ IN COEFFICIENTS
* LABEL(I),I=1,80 = HEADING LABEL TO BE PRINTED AT THE TOP OF THE PLOT
* N1 = 0 DARK FIELD (COSINE SQUARED) ; N1 = 1 FOR LIGHT FIELD
* N2 = NUMBER OF OPEN MODE PARAMETERS TO BE READ
* N3 = NUMBER OF SHEAR MODE PARAMETERS TO BE READ
* A(I),I=1,N2 = COEFFICENTS OF MODE I SOLUTION STARTING AT A(1).
* B(I),I=1,N3 = COEFFICENTS OF MODE I SOULT ION STARTING AT B(1).
* W/Symm case A1=A2, B1=B2, C1=C2, D1=D2

      READ (5,*) N2,N3
          Do 10,I=1,N2
      READ(5,*) A1(I)
10        Continue
          I=0
          Do 11,I=1,N2
      READ(5,*) C1(I)
11        Continue
          I=0
          Do 12,I=1,N2
      READ(5,*) B1(I)
12        Continue
          I=0
          Do 13,I=1,N2
      READ(5,*) D1(I)
13        Continue
            I=0
          Do 14,I=1,N3
      READ(5,*) A2(I)
14        Continue
          I=0
```

```
          Do 15,I=1,N3
       READ(5,*) C2(I)
15        Continue
          I=0
          Do 16,I=1,N3
       READ(5,*) B2(I)
16        Continue
          I=0
          Do 17,I=1,N3
       READ(5,*) D2(I)
17        Continue
          I=0




       WRITE (6,*)
       WRITE (6,*)
       WRITE (6,*) (N2+N3),' PARAMETER SOLUTION A1=',AA1,' A2=',AA2
            WRITE(6,*) 'C=',C

      WRITE (6,*)

      WRITE(6,1002) A1(1),A1(2),A1(3),A1(4),A1(5),A1(6)
      WRITE(6,1003) B1(1),B1(2),B1(3),B1(4),B1(5),B1(6)
      WRITE(6,1004) C1(1),C1(2),C1(3),C1(4),C1(5),C1(6)
      WRITE(6,1005) D1(1),D1(2),D1(3),D1(4),D1(5),D1(6)
      WRITE(6,1006) A2(1),A2(2),A2(3),A2(4),A2(5),A2(6)
      WRITE(6,1007) B2(1),B2(2),B2(3),B2(4),B2(5),B2(6)
      WRITE(6,1008) C2(1),C2(2),C2(3),C2(4),C2(5),C2(6)
      WRITE(6,1009) D2(1),D2(2),D2(3),D2(4),D2(5),D2(6)

1002    FORMAT (2X,'AO-1=',F10.2,5X,'A1-1=',F10.2,5X,'A2-1=',F10.2,5X,
     +  'A3-1=',F10.2,5X,'A4-1=',F10.2,5X,'A5-1=',F10.2)
1003    FORMAT (2X,'BO-1=',F10.2,5X,'B1-1=',F10.2,5X,'B2-1=',F10.2,5X,
```

```
     +  'B3-1=',F10.2,5X,'B4-1=',F10.2,5X,'B5-1=',F10.2)
1004    FORMAT (2X,'CO-1=',F10.2,5X,'C1-1=',F10.2,5X,'C2-1=',F10.2,5X,
     +  'C3-1=',F10.2,5X,'C4-1=',F10.2,5X,'C5-1=',F10.2)
1005    FORMAT (2X,'DO-1=',F10.2,5X,'D1-1=',F10.2,5X,'D2-1=',F10.2,5X,
     +  'D3-1=',F10.2,5X,'D4-1=',F10.2,5X,'D5-1=',F10.2)
1006    FORMAT (2X,'AO-2=',F10.2,5X,'A1-2=',F10.2,5X,'A2-2=',F10.2,5X,
     +  'A3-2=',F10.2,5X,'A4-2=',F10.2,5X,'A5-2=',F10.2)
1007    FORMAT (2X,'BO-2=',F10.2,5X,'B1-2=',F10.2,5X,'B2-2=',F10.2,5X,
     +  'B3-2=',F10.2,5X,'B4-2=',F10.2,5X,'B5-1=',F10.2)
1008    FORMAT (2X,'CO-2=',F10.2,5X,'C1-2=',F10.2,5X,'C2-2=',F10.2,5X,
     +  'C3-2=',F10.2,5X,'C4-2=',F10.2,5X,'C5-1=',F10.2)
1009    FORMAT (2X,'DO-2=',F10.2,5X,'D1-2=',F10.2,5X,'D2-2=',F10.2,5X,
     +  'D3-2=',F10.2,5X,'D4-2=',F10.2,5X,'D5-2=',F10.2)

*    CALCULATE STRESS INTENSITY FACTORS
*    KI1 = OPEN MODE FOR CRACK 1
*    KII1 = SHEAR MODE FOR CRACK 1
*    KI2 = OPEN MODE FOR CRACK 2
*    KII2 = SHEAR MODE FOR CRACK 2

       KI1=A1(1)*SQRT(2*PI)
       KII1=C1(1)*SQRT(2*PI)
       KI2=A2(1)*SQRT(2*PI)
       KII2=C2(1)*SQRT(2*PI)
       DX=AA1/W
       X1=-AA1
       Y=0.0
       DO 2000,J=1,W
        X2=X1+DX
        X3=(X1+X2)/2
        CALL DOUBLE(SY1,SY2,TXY1,TXY2,X3,Y,C,AA1,AA2,N2,N3,
     +   A1,B1,C1,D1,A2,B2,C2,D2,W)
        KI1=KI1-(2*SQRT(2/PI))*(SY2)*(-SQRT(ABS(X1))+SQRT(ABS(X2)))
        KII1=KII1-2*SQRT(2/PI)*TXY2*(-SQRT(ABS(X1))+SQRT(ABS(X2)))
        X1=X2
```

```
2000    CONTINUE

        DX=AA2/W
        X1=-AA2
        Y=C
        DO 2010,J=1,W
         X2=X1+DX
         X3=(X1+X2)/2
         CALL DOUBLE(SY1,SY2,TXY1,TXY2,X3,Y,C,AA1,AA2,N2,N3,
     +   A1,B1,C1,D1,A2,B2,C2,D2,W)
         KI2=KI2-2*SQRT(2/PI)*SY1*(-SQRT(ABS(X1))+SQRT(ABS(X2)))
         KII2=KII2-2*SQRT(2/PI)*TXY1*(-SQRT(ABS(X1))+SQRT(ABS(X2)))
         X1=X2
2010    CONTINUE

        WRITE (6,*)
        WRITE (6,1011) KI1,KII1
1011    FORMAT (2X,'KI-1=',F10.2,5X,'KII-1=',
     +  F10.2,5X)

        CLOSE (5)
        CLOSE (6)
        STOP
        END
*END OF MAIN PROGRAM


* SUBROUTINE TO GENERATE STRESS COMPONENTS AT EACH PARTICULAR PLOT POINT

      SUBROUTINE DOUBLE(SY1,SY2,TXY1,TXY2,X,Y,C,AA1,AA2,N,M,
     +  A1,B1,C1,D1,A2,B2,C2,D2,W)

       COMPLEX z,z1,z2,z3,z4,z5,z6,z7,z8,z9,z10,z11,z12,
     + zi1,zi1p,yi1,yi1p,zi2,zi2p,yi2,yi2p,zi12,zi12p,zii12,zii12p,
     + zi21,zi21p,zii21,zii21p,zii1,zii1p,yii1,yii1p,zii2,zii2p,
```

```
     + yii2,yii2p,z13,z14,z15,z16,z17,z18,z19,z20,z21,z22,z23,z24

       REAL p(32),a1(8),b1(8),c1(8),d1(8),a2(8),b2(8),c2(8),d2(8),
     + aa1,c,d,t,g,aa2,sigmax,sigmay,tauxy,x,y

       INTEGER i,j,n,m,w

       g=y-c
       d=aa1-aa2
       z=cmp lx(x,y)

       z1=zi1p(z,n,a1)
       z2=zi2p(z,n,a2,c,d)
       z3=yi1p(z,m,b1)
       z4=yi2p(z,m,b2,c,d)
       z5=yi1(z,m,b1)
       z6=yi2(z,m,b2,c,d)
       z13=yii1p(z,m,d1)
       z14=zii1p(z,n,c1)
       z15=zii1(z,n,c1)
       z16=yii2p(z,m,d2,c,d)
       z17=zii2p(z,n,c2,c,d)
       z18=zii2(z,n,c2,c,d)
       z19=zi1(z,n,a1)
       z20=zi2(z,n,a2,c,d)
       z23=yii1(z,m,d1)
       z24=yii2(z,m,d2,c,d)

       sy1=real(z19+z23)+y*aimag(z1+z3+z13+z14)
       sy2=real(z20+z24)+g*aimag(z2+z4+z16+z17)

       txy1=-y*real(z1+z3+z13+z14)-aimag(z5+z15)
       txy2=-g*real(z2+z4+z16+z17)-aimag(z6+z18)
       END
*END OF DOUBLE SUBROUTINE
```

```
*START OF FUNCTION SECTION
      function zi1(z,n,a1)
       Complex zi1,z
       Real a1(8)
       Integer i,n
            zi1=(0.0,0.0)
       Do 200, i=1,n
            zi1=zi1+a1(i)*(sqrt(z))**(2*i-3)
200         Continue
      End

      function zi1p(z,n,a1)
       Complex zi1p,z
       Real a1(8)
       Integer i,n
            zi1p=(0.0,0.0)
            Do 210, i=1,n
              zi1p=zi1p+(i-1.5)*a1(i)*(sqrt(z))**(2* i-5)
210         Continue
      End

      function zii1(z,n,c1)
       Complex zii1,z
       Real c1(8)
       Integer i,n
       zii1=(0.0,0.0)
            Do 200, i=1,n
              zii1=zii1+c1(i)*(sqrt(z))**(2*i-3)
200         Continue
       zii1=zii1*cmplx(0.0,-1.0)
      end

      function zii1p(z,n,c1)
        Complex zii1p,z
```

```
      Real c1(8)
      Integer i,n
      zii1p=(0.0,0.0)
      Do 200, i=1,n
            zii1p=zii1p+(i-1.5)*c1(i)*(sqrt(z))**(2*i-5)
200   Continue
      zii1p=zii1p*cmplx(0.0,-1.0)
    end


    function yi1(z,m,b1)
      Complex yi1,z
      Real b1(8)
      Integer i,m
      yi1=(0.0,0.0)
        Do 220, i=1,m
            yi1=yi1+b1(i)*z**(i-1)
220     Continue
  End

    function yi1p(z,m,b1)
      Complex yi1p,z
      Real b1(8)
      Integer i,m
      yi1p=(0.0,0.0)
        Do 230, i=1,m
            yi1p=yi1p+(i-1)*b1(i)*z**(i-2)
230     Continue
    End

    function yii1(z,m,d1)
      Complex yii1,z
      Real d1(8)
      Integer i,m
      yii1=(0.0,0.0)
```

```
      Do 220, i=1,m
              yii1=yii1+d1(i)*z**(i-1)
220        Continue
        yii1=yii1*cmplx(0.0,-1.0)
      End

      function yii1p(z,m,d1)
        Complex yii1p,z
        Real d1(8)
      Integer i,m
        yii1p=(0,0)
       Do 220, i=1,m
              yii1p=yii1p+(i-1)*d1(i)*z**(i-2)
220           Continue
        yii1p=yii1p*cmplx(0.0,-1.0)
      End

      function zi2(z,n,a2,c,d)
        Complex zi2,z,h,zi1
        Real a2(8),c,d
        Integer n
        zi2=(0.0,0.0)
        h=cmplx(d,-c)
        zi2=zi1(z+h,n,a2)
      end

      function zi2p(z,n,a2,c,d)
        Complex zi2p,z,h,g,zi1p
        Real a2(8),c,d
        Integer n
        zi2p=(0.0,0.0)
        h=cmplx(d,-c)
        zi2p=zi1p(z+h,n,a2)
      end
```

```
    function zii2(z,n,c2,c,d)
      Complex zii2,z,h,zii1
      Real c2(8),c,d
      Integer n
      zii2=(0.0,0.0)
      h=cmplx(d,-c)
      zii2=zii1(z+h,n,c2)
    end

    function zii2p(z,n,c2,c,d)
      Complex zii2p,z,h,zii1p
      Real c2(8),c
      Integer n
      zii2p=(0.0,0.0)
      h=cmplx(d,-c)
      zii2p=zii1p(z+h,n,c2)
    end

    function yi2(z,m,b2,c,d)
      Complex yi2,z,h,g,yi1
      Real b2(8),c,d
      Integer m
      yi2=(0.0,0.0)
      h=cmplx(d,-c)
  yi2=yi1(z+h,m,b2)
    end

    function yi2p(z,m,b2,c,d)
      Complex yi2p,z,h,yi1p
      Real b2(8),c,d
      Integer m
      yi2p=(0.0,0.0)
      h=cmplx(d,-c)
  yi2p=yi1p(z+h,m,b2)
    end
```

```
function yii2(z,m,d2,c,d)
  Complex yii2,z,h,g,yii1
  Real d2(8),c,d
  Integer m
  yii2=(0.0,0.0)
  h=cmplx(d,-c)
  yii2=yii1(z+h,m,d2)
end

function yii2p(z,m,d2,c,d)
  Complex yii2p,z,h,g,yii1p
  Real d2(8),c,d
  Integer m
  yii2p=(0.0,0.0)
  h=cmplx(d,-c)
  yii2p=yii1p(z+h,m,d2)
end
```

APPENDIX B
RANDOM NUMBER STUDY

A study to determine if the number of random points from the finite element generated stress field would significantly change the coefficients obtained in the analysis. This study was needed to determine if the number of points used in previous research of smaller separation would adequate for this analysis. The leading coefficients for model 5.3 were calculated using a range of random number values. Figure 5.1 doesn't show much variation for the first 6 order coefficient calculations. The only difference was seen in the higher order parameters, which was still small. The values in Figure 5.2 varied the most through out the orders studied. This was expected since this was the coefficient responsible for the shear stress data, which was very small in model 5.3. The conclusion of the study was that taking 229 random points, as Hardin[1] did would be adequate for the study even with the increased field size.

Table B.1 – Ao Results from Random Number Study

Ao	Points					
Order	100	229	300	400	500	600
2	647.73	655.82	678.20	667.68	678.04	675.81
3	1078.24	1093.92	1112.51	1099.31	1094.89	1092.20
4	1097.57	1092.91	1113.07	1100.65	1097.08	1093.05
5	1381.58	1359.43	1381.94	1372.17	1371.76	1371.90
6	1339.92	1364.93	1351.01	1345.48	1355.71	1351.40
7	1297.79	1303.47	1306.21	1306.10	1314.17	1311.20
8	1291.44	1343.45	1319.26	1324.51	1329.81	1327.08
9	1262.50	1333.19	1258.26	1270.24	1278.60	1269.88
10	1336.05	1364.31	1267.06	1251.72	1242.38	1213.92

Table B.2 – Co Results from Random Number Study

Co	Points					
Order	100	229	300	400	500	600
2	-65.56	-56.62	-86.95	-85.17	-85.42	-85.43
3	-10.92	6.01	6.90	7.29	9.09	10.52
4	-35.98	11.07	-20.42	-15.06	-5.05	-15.74
5	-0.62	-1.98	0.84	0.57	5.52	7.19
6	-155.90	-64.80	-131.36	-135.46	-138.45	-132.77
7	-113.43	-72.20	-123.49	-129.40	-138.00	-128.25
8	4.12	-38.38	-20.15	-33.09	-37.87	-33.96
9	-9.44	-42.77	-30.63	-39.92	-49.85	-44.08
10	1.37	-40.84	-39.50	-49.15	-57.81	-48.63

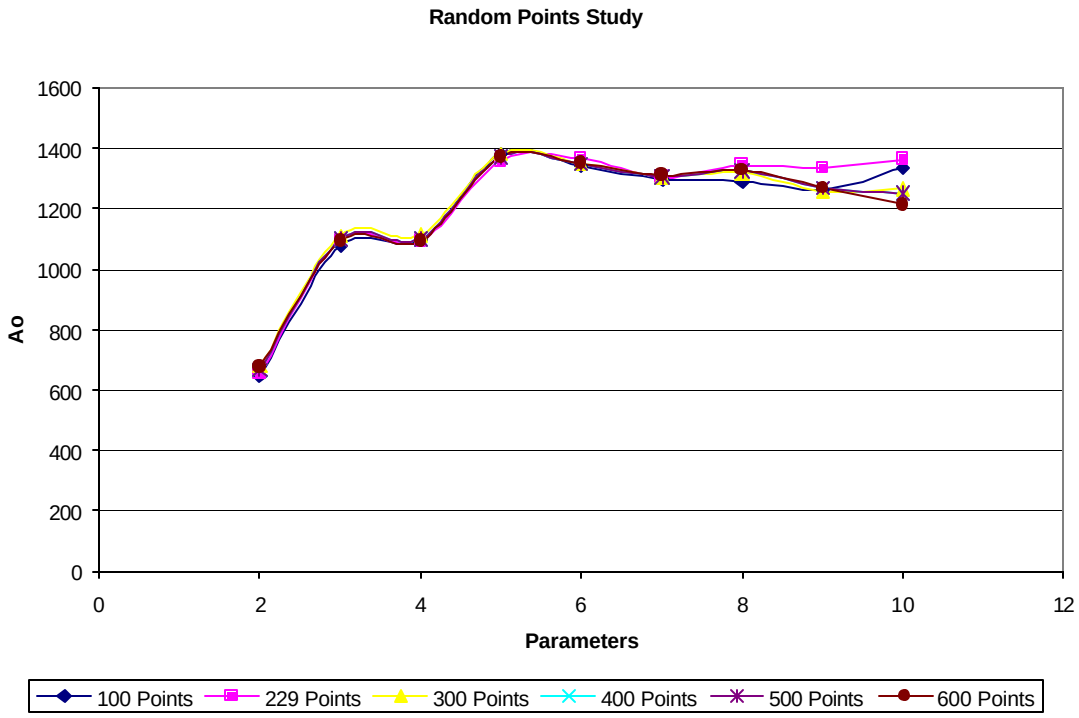

Figure B.1 – Leading Coefficient (Ao) versus Number of Random Points

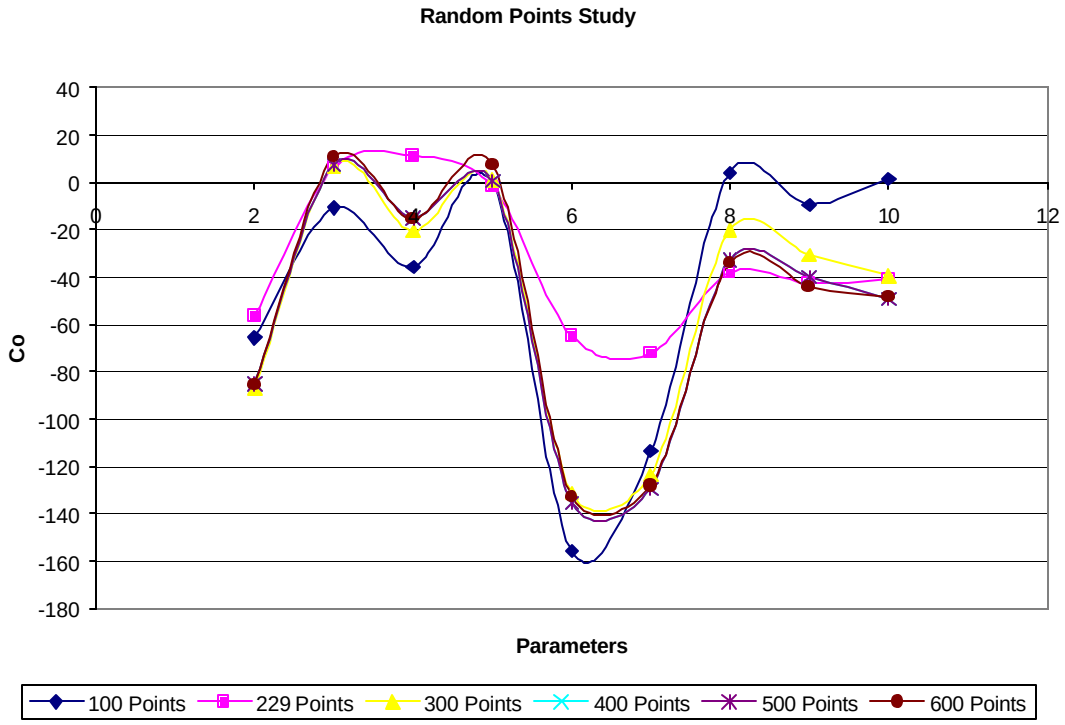

Figure B.2 Leading Coefficient (Co) versus Number of Random Points

APPENDIX C
PURE OPEN MODE STRESS INTENSITY CALCULATION

A value to which to compare the open mode stress intensity factor for the mix mode stress field was needed to determine interacting effects in the stress field. This comparative value was determined using an estimating equation from Reference 5. The equation was used to obtain an estimate of the stress intensity factor for a single crack in a pure bending situation.

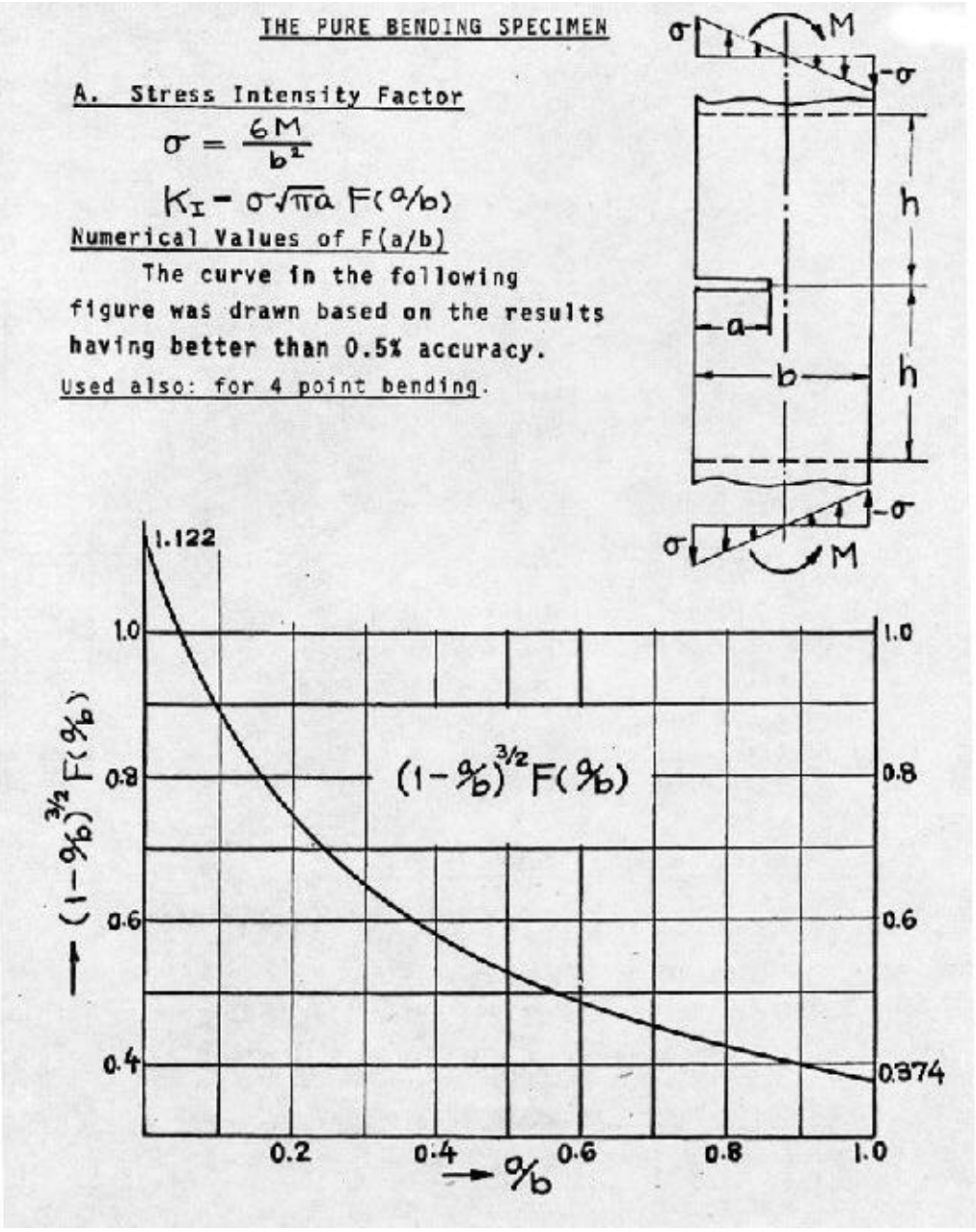

Figure C.1 – Equation and Chart for Pure Open Mode SIF Calculations

$M := 1000\,lbf \cdot in$ Bending Moment $b := 2\,in$ Specimen Width

Open Mode Stress Intensity Factor for 1 inch Crack

$a := 1\,in$ Crack Length

$$F\left(\frac{a}{b}\right) = \frac{.525}{\left(1 - \frac{1}{2}\right)^{\frac{3}{2}}} = 1.48$$

$$K_I := \frac{6 \cdot M \cdot \sqrt{\pi \cdot a}}{b^2} \cdot (1.48) \qquad K_I = 3934.85\ psi \cdot in^{.5}$$ Stress Intensity Factor

Open Mode Stress Intensity Factor for 0.75 inch Crack

$a := .75\,in$ Crack Length

$$F\left(\frac{a}{b}\right) = \frac{.61}{\left(1 - \frac{.75}{2}\right)^{\frac{3}{2}}} = 1.23$$

$$K_I := \frac{6 \cdot M \cdot \sqrt{\pi \cdot a}}{b^2} \cdot (1.23) \qquad K_I = 2832.06\ psi \cdot in^{.5}$$ Stress Intensity Factor

Open Mode Stress Intensity Factor for 0.5 inch Crack

$a := .5\ \ in$ Crack Length

$$F\left(\frac{a}{b}\right) = \frac{.7}{\left(1 - \frac{.5}{2}\right)^{\frac{3}{2}}} = 1.07$$

$$K_I := \frac{6 \cdot M \cdot \sqrt{\pi \cdot a}}{b^2} \cdot (1.07) \qquad K_I = 2011.57\ psi \cdot in^{.5}$$ Stress Intensity Factor

VITA

Justin Patrick Gilman was born in Little Rock, Arkansas on June 5, 1979. After graduating from Warren Central High School in Vicksburg Mississippi in May 1997, he attended Mississippi State University and majored in mechanical engineering. He received his B.S. in mechanical engineering in May 2002. Fall 2002 he enrolled in the master's program at Texas A&M University also majoring in mechanical engineering. During his time in graduate school he worked as a teaching and research assistant in the Mechanical Engineering Department.

Justin Patrick Gilman's permanent address is: 2626 Porters Chapel Rd, Vicksburg, Ms 39180